

"ULTIMATE STRENGTH OF MEMBERS OF REINFORCED  
CONCRETE FRAMES IN COMBINED  
BENDING AND TORSION"

Thesis submitted for the degree of

Doctor of Philosophy

of the

University of Edinburgh

by

N. Saw Kulh, B.S.C.E. (Arizona)

April, 1969



## ACKNOWLEDGEMENTS

First, I should like to acknowledge my gratitude to Professor A.W. Hendry for giving me the opportunity to undertake the research work in the department of Civil Engineering and Building Science.

I am greatly indebted to Dr. D.R. Fairbairn whose close supervision and encouragement throughout the duration of the research directed my attention to the problems.

I should also like to acknowledge my gratitude to Mr. R.S. Elder and the technical staff for their co-operation.

To Miss Betty Turner and Mr. Ross MacKenzie goes my appreciation for the fine photographic work.

The excellent typing and form of the thesis is due entirely to Miss Elizabeth Spinks, to whom the author is most grateful.

Thanks are due to all my colleagues and co-workers for help in the solution of many problems both technical and personal.

To Dr. Hla Mon, M.B., B.S. (Rgn) and Mr. Chris. Chambers, B.Sc.(Eng) goes my acknowledgement for help in the tracing of the graphs and figures.

Finally, the financial help of the Colombo Plan must be mentioned without which this research work would not have been possible.

<u>CONTENTS</u>	(i) <u>Page Nos.</u>
Contents	(i) to (iii)
Notations	(iv) to (v)
Synopsis	(iv)
1. <u>Introduction</u>	1 - 6
2. <u>Brief Review of Previous Works</u>	7
2.1    Introductions	7
2.2    General background	7 - 9
2.3    Inclination of the angle of crack	9 - 11
2.4    Inclination of the compression zone	11 - 13
2.5    Depth of the compression block	13 - 14
2.6    Transverse binders crossed by the cracks	14
2.7    Summary and Conclusions	14 - 15
3. <u>Ultimate Moment in Combined Bending and           Torsion</u>	
3.1    General Introduction	16
3.2    Basis of the equation	16
(1)   The angle of crack	17 - 19
(2)   The assumptions	19
(3)   The modified "k" ratio	19 - 20
3.3    Derivation of the ultimate moment equation	20 - 25
3.4    Significance of the coefficient $C_1$	25 - 27
3.5    Significance of the coefficient $C_2$	27 - 29
3.6    Torsional Resistance of longitudinal reinforcement	29 - 31
3.7    Proposed minimum compressive reinforcement	31 - 32

	<u>Page Nos.</u>
3.8 Depth of the compression zone	32 - 37
3.9 Significance of $M_o$	37 - 38
3.10 Presentation of design charts	38 - 44
3.11 Limiting conditions for validity of the equation	44 - 45
3.12 Correlation of theoretical and experimental results	45 - 46
3.13 Sample solutions	46 - 47
(1) Method of using equation (3.14)	47 - 48
(2) Method of using equation (3.15)	48
3.14 Summary and Conclusions	49 - 50
4. <u>Optimum Reinforcement</u>	
4.1 Introduction	51
4.2 Proposal for balanced longitudinal steel $p_{bc}$	51 - 55
4.3 Provision for torsional shear reinforcement	55 - 57
4.4 Force Intensity method	57 - 61
4.5 Internal Couple method	61 - 65
4.6 Comparison of proposed ratios with existing recommendations	65
(1) Pure torsion	66
(2) Combined bending and torsion	68
4.7 Summary and Conclusions.	69

5.	<u>Experimental Investigation</u>	
5.1	Introduction	70
5.2	Object and scope of investigation	71
5.3	Description of test specimens	70
5.4	Description of torsion bracket	71 - 72
5.5	Materials and Fabrication of specimen	72
5.6	Test arrangement and procedure	73 - 75
5.7	Experimental results	75
5.8	Analysis and discussion of results	75
5.8.1	Development of cracks	75 - 79
5.8.2	Mechanism of failure	79 - 83
5.9	Deformations	83 - 85
5.10	Ultimate strength	85 - 87
5.11	Summary and Conclusions	87 - 88
6.	<u>Conclusions and Recommendations</u>	
6.1	Conclusions	89 - 90
6.2	Recommendations for future research	90 - 91
	<u>Acknowledgements</u>	92
	<u>References</u>	92 - 98
	<u>Appendix A</u> Calculation for beam K11 tested at $\phi = 2.1$	99
	<u>Appendix B</u> Calculation for $M_{bt}$ for beam K11 tested at $\phi = 2.1$	100

NOTATIONS

The following symbols are not defined within the text:

- $A_L$  = cross-sectional area of tensile steel  
 $A_{Lc}$  = cross-sectional area of steel at the compression zone.  
 $A_T$  = cross-sectional area of one leg of transverse steel.  
 $b$  = width of beam  
 $b'$  = width of the reinforcing cage  
 $C_u$  = cube strength of concrete  
 $C_1$  = efficiency coefficient of longitudinal steel  
 $C_2$  = efficiency coefficient of transverse steel  
 $d$  = effective depth of beam  
 $d'$  = depth of the reinforcing cage  
 $f$  = compressive bending stress of the concrete at the compression zone for combined bending and torsion  
 $f_c$  = compressive bending stress of concrete for pure bending  
 $f'_c$  = cylinder strength of concrete  
 $f_L$  = yield strength of the longitudinal steel  
 $f_s$  = yield strength of the longitudinal steel in the compression zone  
 $f_t$  = allowable tensile strength of concrete  
 $h$  = over-all depth of beam

- $K$  = coefficient of concrete bending stress  
 $k$  = ratio of depth to width of the reinforcing cage  
 $M_u$  = ultimate flexural capacity of the section  
 $M_{bt}$  = applied torsional moment  
 $M_{bu}$  = applied bending moment  
 $M_{buL}$  = bending moment contributed by the longitudinal steel  
 $M_{buT}$  = bending moment contributed by the transverse steel  
 $n$  = depth of neutral axis of beam in combined bending and torsion  
 $n_b$  = depth of neutral axis of beam in pure bending  
 $p$  = ratio of longitudinal steel to concrete area in beams  
 $p_b$  = ratio of balanced longitudinal steel for pure bending  
 $p_{bc}$  = ratio of balanced longitudinal steel in combined bending and torsion  
 $r$  = torsional shear reinforcement ratio  
 $r_o$  = optimum torsional shear reinforcement ratio  
 $r_u$  = maximum torsional shear reinforcement ratio  
 $s$  = spacing of transverse binders  
 $\alpha$  = angle of crack  
 $\beta$  = inclination of angle of inclined compression zone with respect to the longitudinal axis  
 $\phi$  = ratio of applied bending moment to applied torsional moment

SYNOPSIS

Based on the equilibrium of external and internal loads acting normal to the inclined compression zone of the failure surface proposed by previous investigators for reinforced concrete beams subjected to combined bending and torsion, a simplified ultimate moment equation was developed by using the ultimate equilibrium method suggested by the Russian researchers.

The ultimate moment is shown to consist of the contributions of longitudinal and transverse reinforcement.

Analysis of forty-three beams tested by previous investigators and fifteen beams tested by the author showed that the equation predicts the ultimate moment with good accuracy.

A method for computing the position of the neutral axis was developed and used in the analysis of the above beams to obtain the lever arms of the internal moments.

The equation was extended to evolve design charts which are equally good for analytical purposes.

Finally, proposals were presented to restrict the quantity of the reinforcement for the validity of the equation.



INTRODUCTION

Torsion occurs in structural members due to the monolithic characteristics of reinforced concrete members, and wherever there is asymmetry of loading of beams and slabs. Some examples of members with torsion may be listed as follows:-

- (1) spandrel beams
  - (2) secondary beams framing into a primary beam.
  - (3) bow girders
  - (4) interconnected girders
  - (5) space frames
- and (6) free-standing spiral staircases.

Critical examination of past practice in structural design reveals that in the absence of methods of design for torsion, three approaches are generally resorted to: first, the structural frames are arranged in such a way that the effect of torsion is minimised; second, the dimensions of the structural members are chosen so that the sizes are much larger than actually calculated, hoping by so doing to cater for the torsional stresses developed in the members; the third resort is to use an ample amount of transverse reinforcement to resist the torsional shearing stresses. In addition, the accepted methods of

design of concrete structures have been based on the elastic theory, the use of which has been found to result in concrete sections larger than necessary and thus the extra strength obtained supposed to resist the torsional stresses. Fortunately, no catastrophic failure of structures due to torsion seemed to have been recorded.

Recently, there has been a tremendous upsurge in the structural design of concrete. A new method of design, the ultimate-load method, has been advocated strongly by research scientists and advanced thinking engineers. This led to the publication of a report by the Institution of Civil Engineers<sup>(1)\*</sup>. The ultimate-load method consists of calculating accurately the ultimate load imposed on the structural member so that, unlike the elastic method where the actual factor of safety is not known, the ultimate-load method can forecast the true margin of safety of the structure, and is thus a more realistic method of design. In addition, the new method can make full use of the potential strength of the materials and is thus conducive to economy.

Due to the more realistic assessment of the load factor made possible by the use of this new method, together with the more effective employment of the materials, the resulting design sections are more slender. The possibility of catering for torsional stresses by the

\* The superscript numbers refer to the list of references.

extra strength due to large margin of safety inherent in the elastic method no longer applies. If these stresses are to be provided for, then definite design formulae must be evolved. Further, the formulae must be based on the ultimate-load method in keeping with developments in other aspects of structural design. It is thus necessary to investigate the effect of torsional stresses on the behaviour and strength of concrete members.

In general, torsional moments rarely exist by themselves but act in conjunction with bending and shear. Some published works<sup>(2,3,4,5)</sup> are available where investigations have been made of the behaviour of beams in combined bending, shear and torsion. The results are however erratic and inconclusive and more research is still necessary. The complication in this type of combined action arises from lack of knowledge of the behaviour of beams in combined bending and shear. It is felt that until this aspect is resolved, the nature of combined bending, shear and torsion cannot be properly investigated. This is particularly true if the proportioning of flexural shear reinforcement is to be considered in conjunction with the torsional reinforcement as advocated by Cowan<sup>(6,7)</sup>. It is therefore considered that the combined effect should be studied first by establishing the action of bending and torsion. With this in mind, the author feels justified in tackling this problem.

A review of works already carried out for combined bending and torsion at the ultimate level indicates that most of the investigators have used the ultimate equilibrium method developed by the Russian Engineers<sup>(8)</sup>. The method consists of obtaining the ultimate load (in this case the ultimate moment) at the failure stage when the reinforcement has yielded. The method is complicated and the equations obtained are far from simple. Attempts have been made to simplify the equation but so far there seems to have been no success. The complication arises mainly from the three dimensional aspect of the combined action, resulting in a complicated failure surface. There seems to be difficulty in obtaining the correct angles of crack at the sides, and subsequently, the inclination of the compression zone about which the beam rotates at the failure stage. This problem has been resolved by Evans and Sarkar<sup>(9)</sup> and more recently by Fairbairn<sup>(10,11)</sup>. But still, the resulting equations are not simple and are not suitable for use in a design office.

The author after careful examination of most of the works feels that further simplifications and modifications may be achieved. An analytical investigation is thus made, employing these simplifications to develop a formula for computing the ultimate bending moment. The

results obtained are again employed to ascertain the contribution of the reinforcement to bending of the beam. In this way, the net contribution of reinforcement, both longitudinal and transverse, is obtained. From this, the actual function of the transverse binders is isolated, together with the effect of torsion on the bending capacity, thereby also obtaining the contribution of the longitudinal steel to the torsional resistance. Finally, a method of obtaining the position of the neutral axis is proposed.

Further investigation is then carried out to estimate the balanced reinforcement for combined bending and torsion by comparing the balanced longitudinal reinforcement to that for pure bending. Two methods are then used to calculate the minimum and maximum transverse torsional reinforcement for the yielding of the steel to occur, namely: (1) the intensity of force method, in which the distribution of the reinforcement at yielding is studied using a hypothetical failure mechanism, and (2) the internal couple method in which the mechanism of the action of the reinforcement in resisting the internal torsional stresses is studied using a similar hypothesis. The results obtained from the two methods are compared, first with each other and then with the recommendations put forward by other investigators and the Russian Code of Practice. Finally, a design equation is developed for calculating the reinforced concrete sections required

for combined bending and torsion.

The experimental investigation consists of justifying the assumptions made in the theoretical study and comparing the calculated ultimate bending moments with the experimental results observed. The mode of propagation of the cracks are particularly observed, especially at the compression zone on the top surface. The results are given in the form of tables and graphs.

The author feels that the theoretical formulae obtained can only be justified within the limitations of the experimental studies, and thus further experimental evidence will be necessary to fully justify the acceptance of the formulae. With this in mind, the last part of the thesis is devoted to this aspect of the problem, with further recommendations for theoretical investigations and experimental observations.

CHAPTER 2BRIEF REVIEW OF PREVIOUS WORKS2.1 Introduction

The main object of this chapter is to review briefly the existing works on combined bending and torsion of reinforced concrete beams, with a view to using the findings to develop an ultimate moment equation. The discussions will be confined to works on under-reinforced beams with both longitudinal and transverse reinforcement.

2.2 General background

When reinforced concrete beams are subjected to combined bending and torsion, the geometry of the surface formed by the failure of the beams has been observed by previous investigators to be related to definite crack patterns. The works of Evans and Sarkar<sup>(9)</sup>, Fairbairn<sup>(10,11)</sup>, Chinenkov<sup>(12)</sup>, Lessig<sup>(13)</sup>, Gesund et al<sup>(15)</sup>, Yudin<sup>(27)</sup>, Goode and Helmy<sup>(35)</sup>, and other investigators showed that, for specimens with moderate to high ratios of bending to torque, the cracks develop first on the side of the beam where flexural tension occurs and extend later to the vertical sides. On the fourth side, a compression zone is formed. For beams with predominant torsion, cracks have been observed to form first on the vertical side, extending later to the horizontal faces, and culminating in the formation of the compression zone in the vertical plane.

It was further observed that, for under-reinforced beams, failure of the beam is preceded by yielding of the reinforcement intercepted by the cracks, and the rotation of the beam about the compression zone.

On the basis of the observed behaviour of these beams and the crack patterns formed, a failure surface has been developed. This failure surface consists of intercepts on the three sides of the beam, whose inclination to the axis of twist is equal, and a compression zone on the fourth side.

The ultimate moment equation is developed by considering the equilibrium of the internal and external forces and moments acting normal to the compression zone. The equation thus obtained can be used to calculate the bending moment of any rectangular beam section under a known bending to torque ratio and the results obtained, when compared with the experimental values, generally have close agreement. However, these equations are far too complicated for use in a design office.

Yudin<sup>(27)</sup> and Goode and Helmy<sup>(35)</sup> have attempted to simplify the equation by also considering the equilibrium of moments and forces transverse to the failure surface, thus obtaining two simultaneous equations. The magnitude of the bending moment  $M_b$  and the torque  $M_t$  obtained from the process of elimination did not agree with the experimental results.



The main complication in the ultimate moment equation arises due to the following:

- (1) variation in the angle of inclination of cracks.
- (2) variation of the angle of inclination of the compression zone with the horizontal axis.
- (3) the magnitude of the depth of the compression block.
- and (4) the number of transverse binders crossed by the vertical and horizontal cracks.

### 2.3 Inclination of the angle of cracks

It is generally agreed that the inclination of the crack on the faces of the beam due to the action of combined bending and torsion varies between 45 degrees for pure torsion and 90 degrees for pure bending with values close to the former for predominant torsion and approaching the later where bending is predominant. However, due to the complex stress-strain relationship for concrete in tension, together with the general difficulty of obtaining the true stress distribution in combined bending and torsion, no previous studies have given recommendation for calculating the magnitude of the angle.

Examination of published works on combined bending and torsion shows that only two experimental studies are available which consider the variation of this angle. Evans and Sarkar<sup>(9)</sup> in 1964 developed a formula for calculating the magnitude of this angle based on two assumptions, namely that concrete behaves plastically in

torsion, and semi-plastically in tension. Their formula expresses the angle of crack in terms of the shape of the beam and the bending to torque ratio. They also reported that the values obtained from experiments agree with the calculated values. An ultimate moment equation was developed by them, incorporating their formula for the angle of crack. The resulting general agreement of the theoretical and experimental values indicates that the formula is acceptable.

In 1967, Fairbairn<sup>(10)</sup> suggested that the formula of Evans and Sarkar could be modified into three simple formulae, considering three conditions of bending and torsion, namely (1) predominant torsion case, (2) combined bending and torsion, and (3) predominant bending. The advantage of his formulae lies in their simplicity of directly relating the angle of crack to the bending to torque ratio. Comparisons with the original formula shows that the results obtained are justifiable.

The author firmly believes that for an accurate determination of the ultimate bending moment, the equation must take into account the variation of this angle directly. The importance of this rises from the fact that, both the intercept of the transverse binders and the inclination of the compression fulcrum are directly related to this angle. It is felt that the formulae developed for calculating this angle of crack though not absolutely correct may enable a more accurate evaluation of the ultimate moment. With this in mind, it is proposed

to develop the ultimate moment equation incorporating the formulae of Fairbairn with other simplifications.

#### 2.4 Inclination of the compression zone

It has been briefly mentioned that the ultimate moment equation is generally developed by equating the external and internal moments about the compression zone normal to this plane. Thus, the correct evaluation of the bending moment is directly related to this angle.

It was further shown that the angle of crack also affects this inclination because of the formation of the compression zone as a result of the connecting up of the vertical cracks on the upper face.

The approach made in evaluating this angle of inclination by previous investigators consisted of one of the following:

- (1) The assumption of a constant angle for the inclination.
- (2) The assumption of 45 degree crack angles on the sides, thus obtaining the projected length on the horizontal axis.
- and (3) By obtaining the projected length on the horizontal axis with consideration for its variation with the crack angle.

Evans and Sarkar<sup>(9)</sup> assumed this angle of inclination to be 45 degrees, at the same time using their formula for the crack angle. They showed that the use of the 45 degree inclination resulted in predicting the ultimate bending moment which is close to the experimental value.

The works of the Russian investigators seem to be based on the assumption of 45 degrees for the angle of crack. This is indicated by the analysis of works of Lyalin<sup>(3)</sup>, Chinenkov<sup>(12)</sup>, Lessig<sup>(13)</sup> and Yudin<sup>(27)</sup>. Their method of approach is to consider the projected length of the crack on the horizontal axis and to restrict this length to a specified value. They mention at the same time that the value of the projected length is influenced by the tensile strength of concrete, the bending to torque ratio and the spacing of the transverse reinforcement. The equation evolved by them is however far from simple.

Goode and Helmy<sup>(35)</sup> introduced certain simplifications regarding the inclination of the compression zone by relating it as a function of the projected length of the vertical intercepts on the horizontal axis and the breadth of the beam. In particular, it is interesting to note that they also introduce the concept of using the dimensions of the reinforcing cage instead of the usual over-all dimensions. The equations they obtained for calculating the bending moment and torque are simple, but unfortunately, the results did not agree with the experimental values obtained.

Finally, Fairbairn<sup>(9)</sup> uses his formulae for the angle of crack to determine the intercept of the crack on the horizontal axis and expresses the inclination of the compression zone as a function of the angle of crack and the depth to breadth ratio of the beam.

Thus, he is the first to consider the effect of the variation of angle of cracks on the inclination of the compression zone. He further incorporates this angle to develop ultimate moment equations which are far too complicated for use in a design office. The author feels that these equations can be modified by introducing certain simplifications. For instance, it seems that the length of the lever arm is over-conservative.

On consideration of the various approaches made by the above investigators, the author feels that the approach used by both Goode and Helmy<sup>(35)</sup> and Fairbairn<sup>(10)</sup> offer the best method available for determining the inclination of the compression zone, and in particular, simplification can be achieved combining the two methods to produce a modified formula for the angle of inclination of the compression zone.

## 2.5 Depth of the compression block

Of the several works available, the method used for obtaining the depth of the compression block is by considering the resolution of the forces normal to the compression zone. The equation obtained relates the longitudinal and transverse reinforcement with the strength of the concrete in compressive bending.

An examination of the approach used by the above authors to evolve the formula for calculating the compression block reveals that they have not considered the equilibrium of forces transverse to the failure zone. The author feels that if this is introduced,

the formula can be simplified considerably.

## 2.6 Transverse binders crossed by the cracks

The derivation of the ultimate moment equation includes the effect of the transverse binders in contributing to the bending capacity of the beam. It is thus imperative that the actual number of binders crossed by the cracks is known.

The cracks at the tension zone crossed the face of the beam completely and thus it is simple to estimate the number of binders crossed by the cracks. This is not true for the vertical face since the crack is assumed only to reach the neutral axis, and thus the equations are derived with the number of binders calculated on this basis. This method has been adopted by most of the research workers and tends to make the equation very complicated.

If the neutral axis plane is considered located at about the level of the compression steel, then the term relating the number of transverse binders intercepted by the crack on the vertical side is considerably simplified, enabling further simplification in the ultimate equation. Goode and Helmy<sup>(35)</sup> showed that the path traversed by the crack can be approximated by the projection of the depth of the reinforcing cage on the horizontal axis so that the resulting equation is much simpler.

## 2.7 Summary and Conclusions

The previous studies examined in this chapter are concerned with the development of the original ultimate bending moment

15.  
equation. The summary of the discussions is given below, together with the conclusions arrived at by the author. It is felt that these discussions have yielded considerable data for the author's proposed investigation. The following points have been discussed:

- (1) the evolution of the failure surface of reinforced concrete beams in combined bending and torsion.
- (2) the concept of deriving the ultimate bending moment equations using the above failure surface as a base.
- (3) the formulating of an ultimate equation arising from the following: (a) the use of Fairbairn's angle of crack, (b) the use of a new formula for the inclination of the compression zone, (c) the derivation of a new formula for calculating the depth of the neutral axis, and (d) an expression for the number of transverse binders crossed by the crack on the vertical sides.

The author has concluded that in developing the ultimate moment equation, the following additional simplifications should be introduced:-

- (1) the use of the angle of crack proposed by Fairbairn.
  - (2) a modification of Fairbairn's expression for the angle of inclination of the compression zone.
  - (3) a simplification of the formula for obtaining the position of the neutral axis.
- and (4) the use of the reinforcing cage dimensions as a basis for estimating the quantity of the transverse binders crossing the failure zone.

CHAPTER 3ULTIMATE MOMENT IN COMBINED BENDING AND TORSION3.1 General Introduction

The author proposes to derive an equation for calculating the ultimate bending moment of reinforced concrete beams of rectangular section containing both longitudinal and transverse reinforcement, subjected to combined bending and torsion. The ultimate equilibrium method proposed by the Russian investigators Gvozdez<sup>(8)</sup>, Chinenkov<sup>(12)</sup>, Lessig<sup>(13)</sup>, Yudin<sup>(27)</sup> and Lyalin<sup>(36)</sup> will be used together with certain modifying assumptions. The angle of crack as proposed by Fairbairn<sup>(10)</sup> will be adopted. It is proposed to analyse several research works using the new equation in order to demonstrate its accuracy.

3.2 Basis of the equation

The ultimate equilibrium method has been adopted by several research workers<sup>(9,10,14,35)</sup> and their general conclusion is that the method is applicable to the analysis of reinforced concrete structures at the ultimate stage. The method is based on a consideration of the equilibrium of the external loads with the internal resistance of the structural members. In particular, for reinforced concrete members, the resistance is offered by the stresses in the reinforcement



and the torsional and compressive stresses of the concrete in the compression zone.

A critical review of works on rectangular sections subjected to combined bending and torsion in Chapter 2 has shown that differences in the existing theories lie mainly in the following categories:-

- (1) the inclination of the angle of crack.
  - (2) the position of the neutral axis.
  - (3) the number of equilibrium conditions to be considered.
- and (4) the distribution and magnitude of the internal stresses.

It will be shown in the following paragraphs that the author has considered his study on the basis of the following:-

- (1) the adoption of the angle of crack proposed by Fairbairn.
- (2) by introduction of certain assumptions thus simplifying the problem.
- (3) the adoption of a new ratio of "k".\*

(1) The angle of crack

Evans and Sarkar<sup>(9)</sup> have suggested that the angle of crack may be completely determined once the concrete properties,

\* see notations

the beam dimensions, and the applied bending moment and torque are known. Their expression for the angle of crack was derived by assuming that the concrete stress distribution in flexure is semi-plastic and fully plastic in torsion, as suggested by Cowan<sup>(28)</sup>. Fairbairn<sup>(10)</sup> modified the expression into a very simple form by introducing three ranges of loading, namely: (a) predominant torsion, (b) combined bending and torsion, and (c) predominant bending. The angle of crack as given by him is

$$\text{For } \phi < 2, \text{ Cot } \alpha = \frac{0.63}{\phi^2} \dots\dots\dots (3.1)$$

$$2 \leq \phi \leq 8, \text{ Cot } \alpha = \frac{0.80}{\phi} \dots\dots\dots (3.2)$$

$$\phi > 8, \text{ Cot } \alpha = 0.10 \dots\dots\dots (3.3)$$

The angle of crack was found to be applicable to hollow as well as solid sections. The validity of this fact enables the author to analyse the beams tested by Evans and Sarkar<sup>(9)</sup> and the correlation of the calculated  $M_{bu}$  with the experimental values shown in Table 3.4 indicates the applicability of Fairbairn's proposal.

The author intends to use the above angle of crack in deriving the ultimate moment equation with certain simplifying assumptions, together with a modified k value for the

beam dimensions.

(2) The assumptions

The following assumptions are adopted to simplify the derivation of the ultimate bending moment equation:-

- (a) the concrete has no tensile strength
- (b) the beam is under-reinforced
- (c) the transverse binders are uniformly distributed within the failure zone
- (d) the contribution of the compressive reinforcement is negligible
- (e) the reinforcement crossed by the cracks reach the yield stress
- (f) the neutral axis lies in a plane on the horizontal section
- (g) the centroid of the compression block is at the mid-depth of the compression zone
- (h) the vertical deviation of the angle of crack beyond the neutral axis is negligible, and therefore, the compressive zone is rectangular.
- (i) the concrete compressive stress block is rectangular with an average stress value of  $\frac{2}{3}c$

(3) The modified "k" ratio

Most of the existing theories for the behaviour and strength of reinforced concrete sections, subjected to pure torsion, relate the strength as a function of a coefficient which depends on the over-all ratio of k. It was generally considered

satisfactory to extend this concept to the case of combined bending and torsion.

The author analysed several experimental data available and found that, for reinforced concrete beams with both longitudinal and transverse reinforcement, subjected to combined bending and torsion, the ratio  $k$  should be based on the dimensions of the reinforcing cage. The new ratio is thus

$$k = \frac{d'}{b'} \dots\dots\dots (3.4)$$

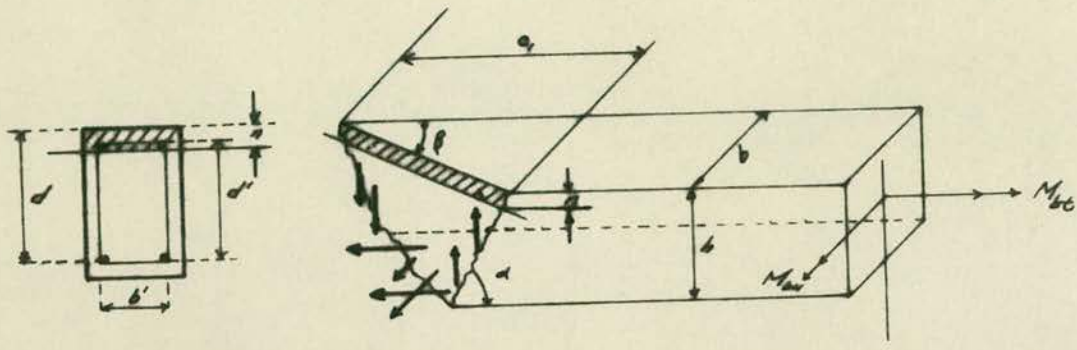
The use of the new ratio results in a higher value for  $k$  as compared to the original ratio, and therefore, the strength of designed sections is generally under estimated.

The new ratio is restricted to  $1 \leq k \leq 2.5$ .

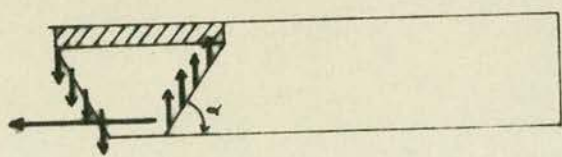
### 3.3 Derivation of the ultimate moment equation

When a reinforced concrete beam is subjected to combined bending and torsion, the resulting failure surface is as shown in Fig. 3.1(a). This is based on the assumption that the beam fails by formation of a compression zone across the horizontal face. The inclination of the angle of crack is the same throughout the two vertical sides, and the horizontal face as shown in Figs. 3.1 (b) and 3.1 (c).

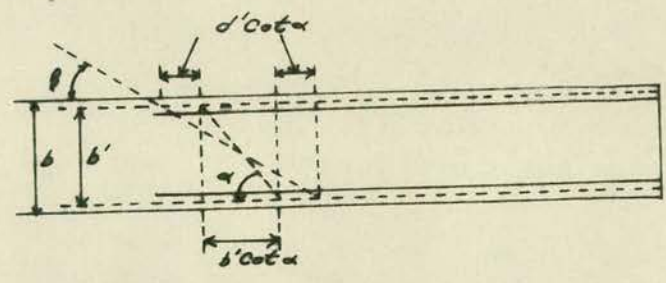
In order to solve the internal forces, it is necessary to estimate the number of transverse binders intercepted by the



(a) Failure surface



(b) Elevation



(c) Plan view

FIG 3.1- Failure conditions of reinforced concrete beams under combined bending and torsion

cracks, both on the horizontal and vertical faces. By considering that the reinforcement is confined within the reinforcing cage, considerable simplification is achieved. In addition to this, the intercepts crossed by the cracks can now be obtained accurately. In order to simplify the calculation of the number of binders on the vertical side, it will be assumed that the neutral axis plane lies at the level of the top reinforcement. This is fully justified because experiments have shown that the depth of the compression block is generally very small and lies in the order of the depth to the top layer of the reinforcement measured from the top compression face. No further complexity is introduced by the intercepts on the horizontal crack.

Using the above assumptions, the ultimate moment equation will now be derived. To do that, the equilibrium of the internal and external loads will be first considered.

Using the above assumptions, the ultimate moment equation will now be derived. To do that, the equilibrium of the internal and external loads will be first considered.

The internal forces acting across the failure surface, normal to the compression zone are

(a) longitudinal steel .....  $A_L f_L \sin \beta$

(b) transverse binders

intercepted by the

vertical cracks .....  $\frac{A_T f_T d'}{s} \cot \alpha \sin \beta$

- (c) transverse binders  
intercepted by the  
horizontal cracks .....  $\frac{A_T f_T b'}{s} \cot \alpha \cos \beta$

The above internal forces generate the following internal moments by rotating about the centroid of the compression zone, i.e.

- (d) due to force (a) .....  $A_L f_L \sin \beta (d - \frac{n}{2})$   
 (e) due to force (b) .....  $\frac{A_T f_T d'}{s} \cot^2 \alpha \sin \beta (d - \frac{n}{2})$   
 (f) due to force (c) .....  $\frac{A_T f_T b'}{s} \cot \alpha \cos \beta (d - \frac{n}{2})$

The total internal moment is obtained by summation of the moments given by (d), (e) and (f), as

$$M_{Bi} = A_L f_L \sin \beta (d - \frac{n}{2}) + \frac{A_T f_T b'}{s} (d - \frac{n}{2}) \left[ \left( \frac{d'}{b'} \right) \cot \alpha \sin \beta + \cos \beta \cot \alpha \right] \dots (3.5)$$

The internal moment given by expression (3.5) is balanced by the external moment  $M_{bu}$  and torsional moment  $M_{tu}$ . The total external moment is obtained by resolving normal to the failure plane, i.e.

$$M_{Be} = M_{bu} \sin \beta + M_{tu} \cos \beta \dots (3.6)$$

For equilibrium, the external and internal moments must balance each other, and therefore, the moment given by expression (3.6) must be balanced by the moment given by expression (3.5), i.e.

$$M_{bu} \sin \beta + M_{bt} \cos \beta = A_L f_L \sin \beta \left( d - \frac{n}{2} \right) + \frac{A_T f_T b'}{s} \left( d - \frac{n}{2} \right) \left[ \left( \frac{d'}{b'} \right) \cot \alpha \sin \beta + \cos \beta \cot \alpha \right] \dots (3.7)$$

Dividing the above expression throughout by  $\sin \beta$  and introducing the ratio  $\phi = \frac{M_{bu}}{M_{bt}}$ , the equation is simplified to

$$M_{bu} \left( 1 + \frac{\cot \beta}{\phi} \right) = A_L f_L \left( d - \frac{n}{2} \right) + \frac{A_T f_T b'}{s} \left( d - \frac{n}{2} \right) \left[ \left( \frac{d'}{b'} \right) \cot \alpha + \cot \beta \right] \cot \alpha \dots (3.8)$$

From Fig. 3.1(c), the expression for the inclination of the compression zone can be obtained as

$$\cot \beta = \frac{(b' + 2d') \cot \alpha}{b'} \dots (3.9)$$

$$= (1 + 2k) \cot \alpha \dots (3.10)$$

If the expression for  $\cot \beta$  obtained above is substituted in equation (3.8), and the resulting equation rearranged, the ultimate moment equation is given as



$$M_{bu} = A_L f_L (d - \frac{n}{2}) (\frac{\phi}{\phi + (1 + 2k) \cot \alpha})$$

$$+ \frac{A_T f_T b'}{s} (d - \frac{n}{2}) (\frac{\phi(1 + 3k) \cot^2 \alpha}{\phi + (1 + 2k) \cot \alpha}) \dots\dots\dots (3.11)$$

For a particular beam section, the reinforcement is generally known or obtainable from the known conditions of loading. The unknowns left in the above expression are the value of n and the terms in the bracket. The author intends to present a method of calculating the first in Section 3.8, while the terms in the bracket may be replaced by coefficients C<sub>1</sub> and C<sub>2</sub> which are given as

$$\frac{\phi}{\phi + (1+2k) \cot \alpha} = C_1 \dots\dots\dots (3.12)$$

$$\frac{\phi(1 + 3k) \cot^2 \alpha}{\phi + (1 + 2k) \cot \alpha} = C_2 \dots\dots\dots (3.13)$$

For a particular beam with given φ, the value of the angle of crack is obtained from expression (3.1), (3.2) or (3.3) and therefore, the values of C<sub>1</sub> and C<sub>2</sub> are found to be constant.

The author has obtained the coefficients C<sub>1</sub> and C<sub>2</sub> for variations of φ from 0 to 12 with k = 1.0, 1.5, 2.0 and 2.5, using a computer program. The results are plotted graphically in, Figs. 3.2, 3.3 and 3.4. The graphs of Figs. 3.3 and 3.4 give the values of the coefficient C<sub>2</sub> for pre-dominant torsion and combined bending and torsion to predominant

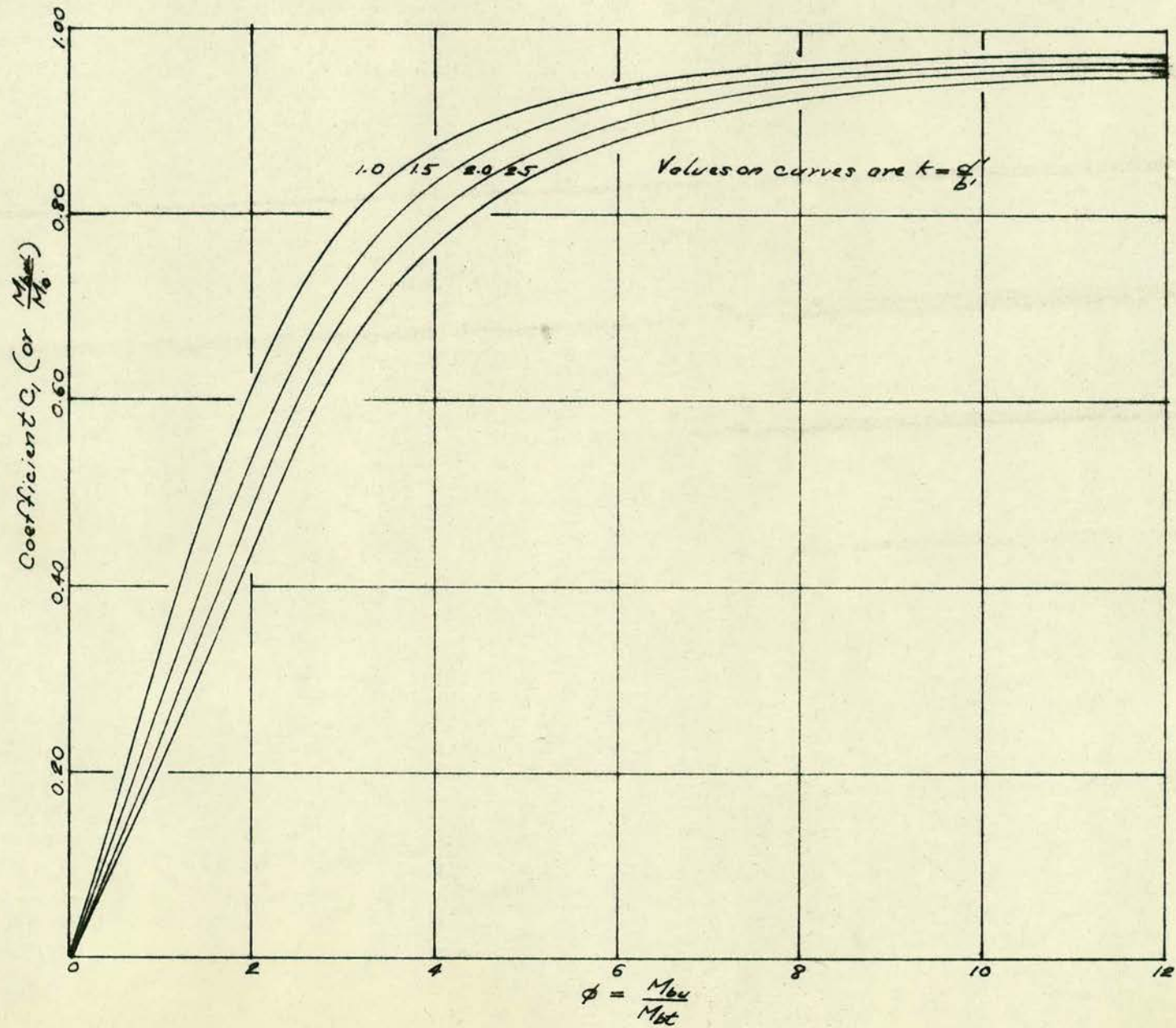


FIG 3.2- Variation of coefficient  $C_1$  with  $\phi$

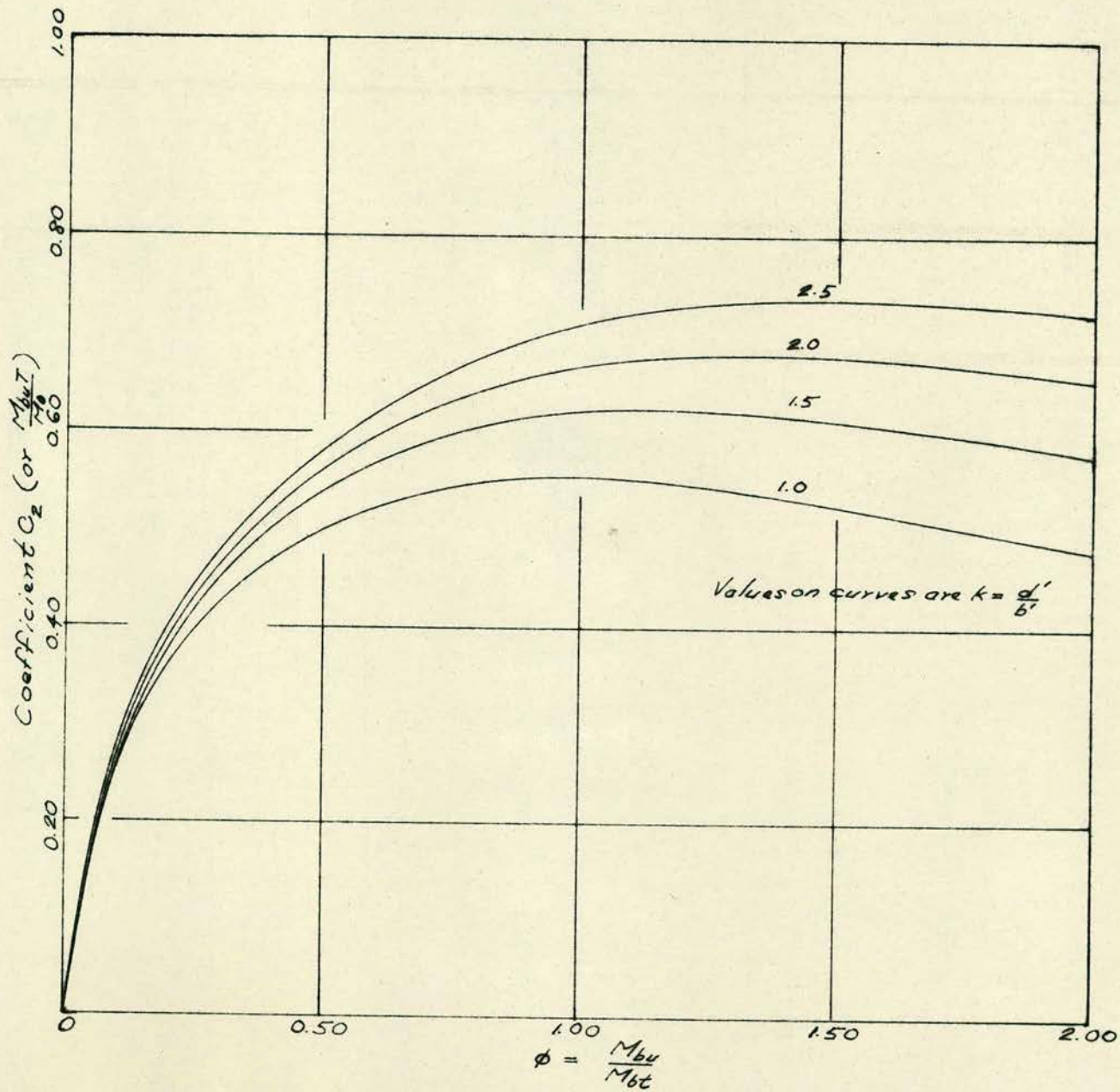


FIG 3.3- Variation of coefficient  $C_2$  with  $\phi$

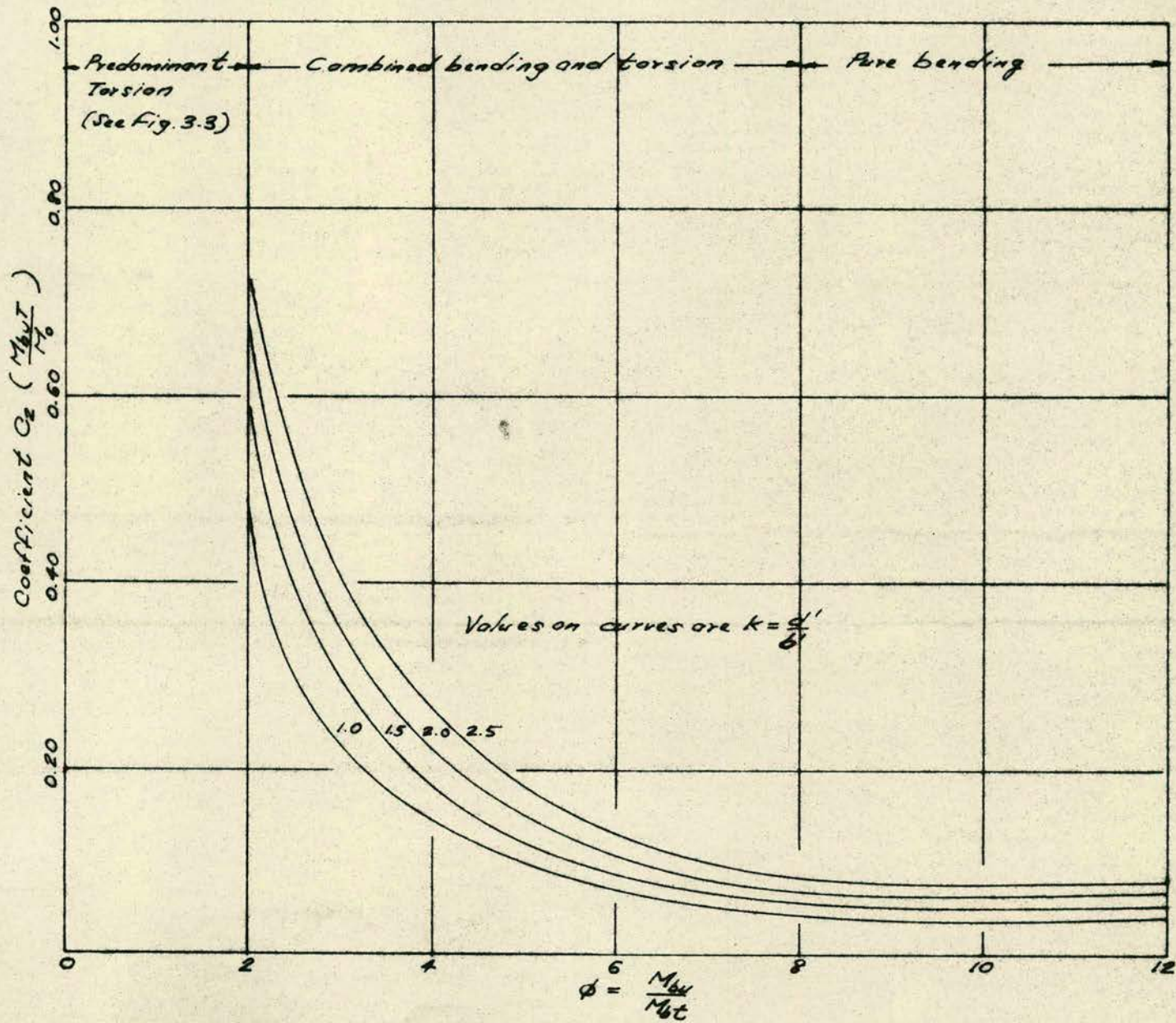


FIG 3.4- Variation of coefficient  $C_2$  with  $\phi$

bending conditions respectively.

Once the coefficients  $C_1$  and  $C_2$  are obtained, either by direct calculation using the formulae (3.12) and (3.13), or from the graphs of Figs. 3.2, 3.3 and 3.4, the ultimate bending moment  $M_{bu}$  can be calculated at once by the use of equation (3.14) given as

$$M_{bu} = A_L f_L \left(d - \frac{n}{2}\right) C_1 + \frac{A_T f_T b'}{s} \left(d - \frac{n}{2}\right) C_2 \dots\dots\dots (3.14)$$

It is necessary to establish the conditions under which the above equation is valid. The author proposes to deal with this in chapter 4.

#### 3.4 Significance of the coefficient $C_1$

It can be deduced by inspection of equation (3.14) that, the first term on the right hand side expresses the contribution of the longitudinal reinforcement, and the second term, the contribution of the transverse binders. The ultimate moment  $M_{bu}$  can be thus considered as consisting of the bending moments contributed by the longitudinal steel and the transverse binders, and may be represented by

$$M_{bu} = M_{buL} + M_{buT} \dots\dots\dots(3.15)$$

where  $M_{buL} = A_L f_L \left(d - \frac{n}{2}\right) C_1 \dots\dots\dots(3.16)$

and  $M_{buT} = \frac{A_T f_T b'}{s} \left(d - \frac{n}{2}\right) C_2 \dots\dots\dots(3.17)$

It is proposed to consider the implications of equation (3.16) to find the significance of  $C_1$ . From Fig. 3.2, it can be observed that as  $\phi$  increases, the value of  $C_1$  increases also and vice versa. The values are also higher for higher ratio of  $k$ . By rearranging equation (3.16), the coefficient  $C_1$  can be expressed as a function of the relative reduction factor in bending capacity of the beam under consideration, namely:

$$C_1 = \frac{M_{buL}}{A_L f_L (d - \frac{n}{2})} \dots\dots\dots (3.18)$$

Letting  $M_o = A_L f_L (d - \frac{n}{2}) \dots\dots\dots (3.19)$

Then  $C_1 = \frac{M_{buL}}{M_o} \dots\dots\dots (3.20)$

It will be shown in Section 3.8 that the magnitude of  $n$  is very small, and therefore, for purpose of discussion  $M_o$  can be considered approximately constant. In fact, the actual value is related to  $M_u$  by the inequality as

$$\frac{M_u}{M_o} < 1 \dots\dots\dots (3.21)$$

Equation (3.20) can be represented as the abscissa

in Fig. 3.2, and therefore, the graph may be considered as showing the efficiency of the longitudinal steel in contributing to the bending moment resistance of the beam. From this consideration, the author decides to define  $C_1$  as "the efficiency coefficient of the longitudinal reinforcement".

### 3.5 Significance of the coefficient $C_2$

The ultimate bending moment has been expressed as equation (3.15), where  $M_{buL}$  represents the bending moment due to the longitudinal reinforcement, and  $M_{buT}$  due to the transverse binders. It is thus accepted that transverse binders in the case of combined bending and torsion also contribute to the bending capacity. This fact has been verified by experiments, particularly that due to Gesund et al<sup>(15)</sup>.

From equation (3.17), the contribution of the transverse binders has been given as

$$M_{buT} = \frac{A_T f_T b'}{s} \left( d - \frac{n}{2} \right) C_2$$

For a fixed quantity of transverse binders, i.e.  $\frac{A_T f_T b'}{s}$ , it appears that the coefficient  $C_2$  represents the effective contribution of that quantity to the bending moment. The author therefore proposes to define  $C_2$  as "the efficiency coefficient of the transverse reinforcement".

Gesund et al<sup>(15)</sup> has also shown that the bending moment increases with the increase in the transverse binders within a certain range. This contribution can be related to the parameter "r" which was introduced by Lessig<sup>(13)</sup>.

Introducing this parameter in equation (3.17), the form of equation is changed to

$$M_{buT} = A_L f_L \left(d - \frac{n}{2}\right) C_2 r \quad \dots\dots\dots(3.22)$$

or  $\frac{M_{buT}}{M_o} = C_2 r \quad \dots\dots\dots(3.23)$

where  $r = \frac{A_T f_T b'}{A_L f_L s} \quad \dots\dots\dots(3.24)$

For a specified beam section, subjected to known combined bending and torsional moment, the contribution of the transverse binders varies with r, and since the primary function of the transverse binders is to resist shearing stresses, the author proposes to define "r" as "the torsional shear reinforcement ratio".

The advantage of presenting equation (3.17) in the form of equation (3.23) lies in that, the later equation can be plotted graphically as shown in Figs. 3.5, 3.6, 3.7, 3.8, 3.9, 3.10, 3.11 and 3.12 for r = 0.25, 0.50, 0.75 and 1.00. From the graphs,



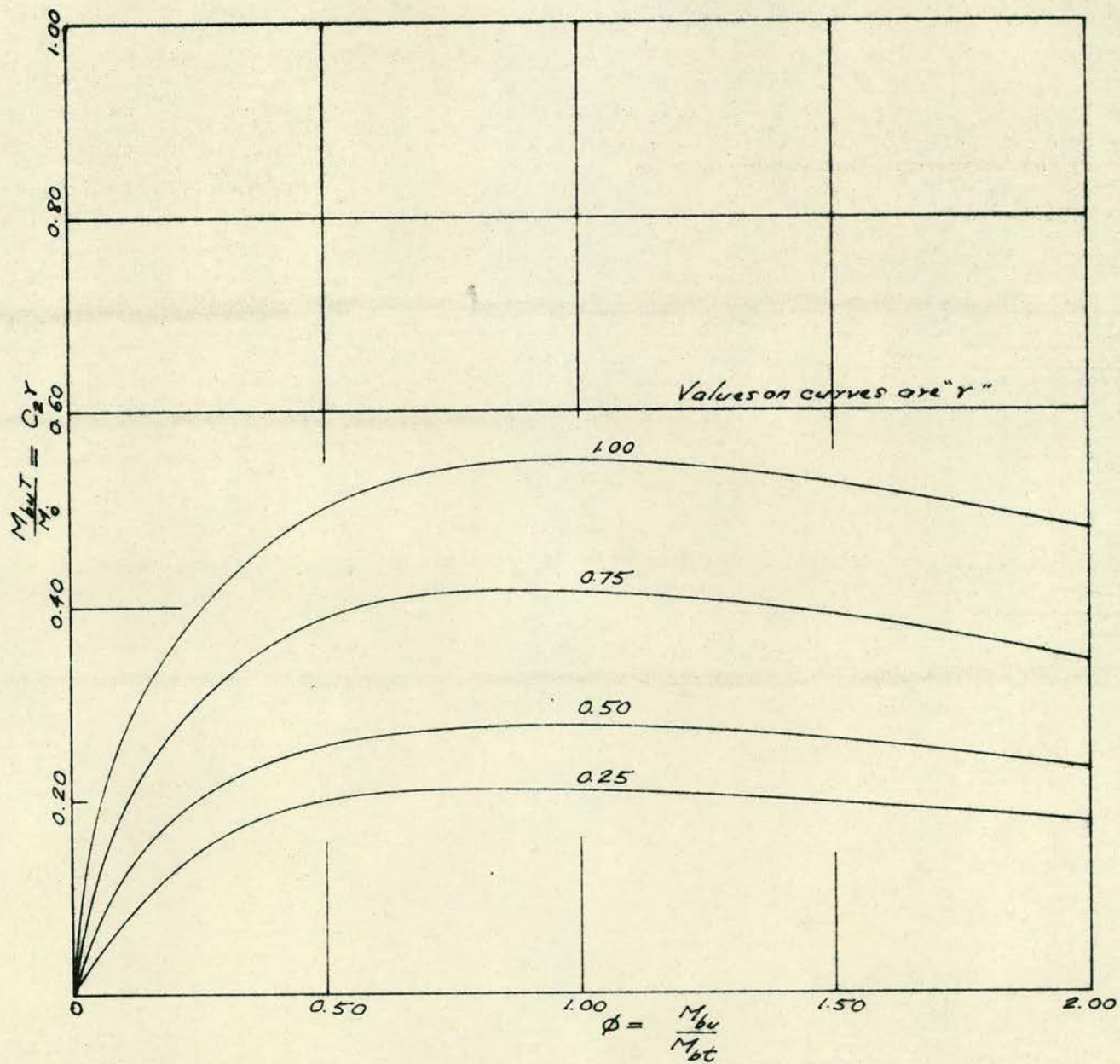


FIG 3.5 - Variation of  $\frac{M_{buT}}{M_0}$  with  $\phi$  for  $k = 1.00$

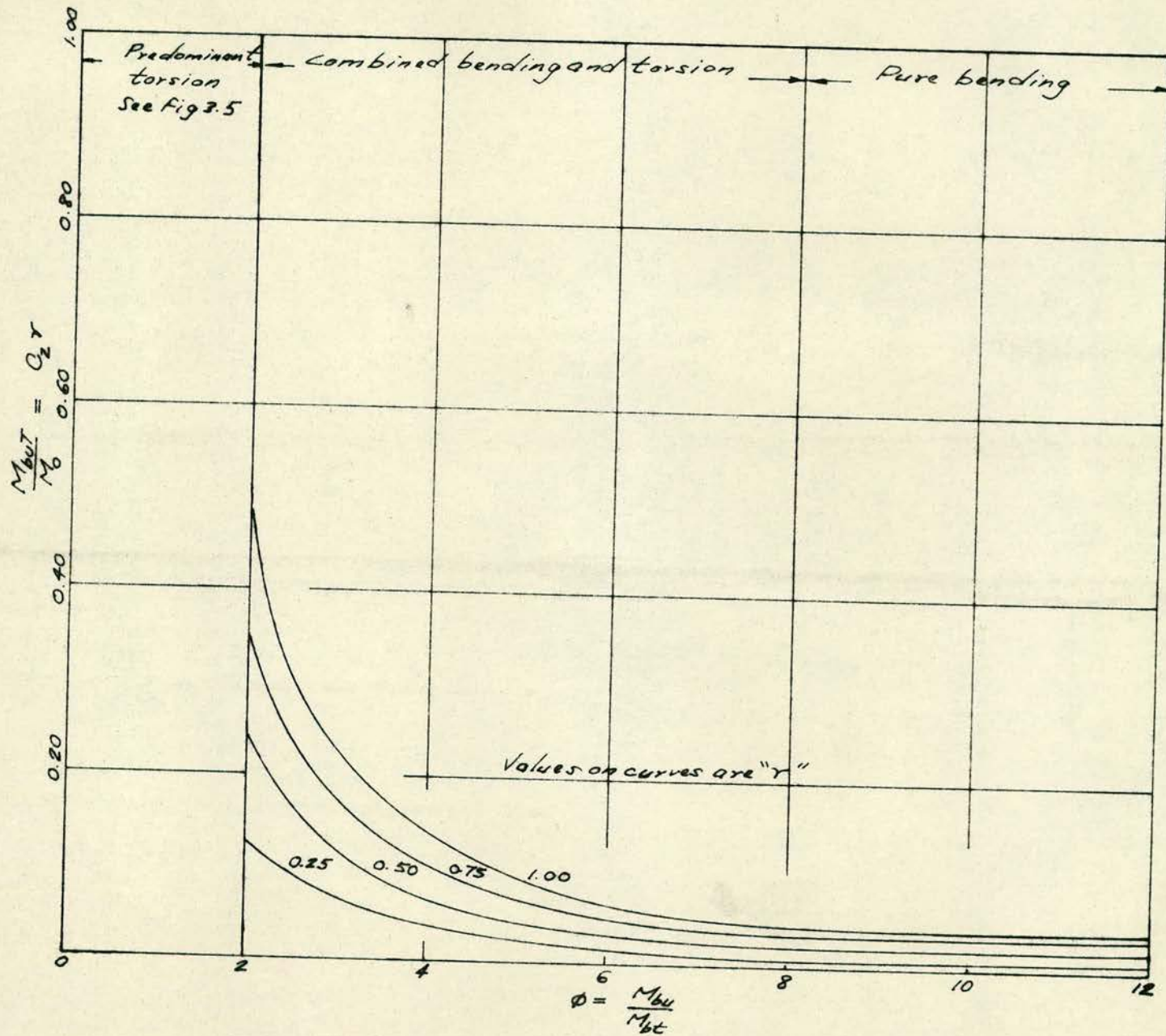


FIG 3.6 - Variation of  $\frac{M_{buT}}{M_0}$  with  $\phi$  for  $k=1.00$

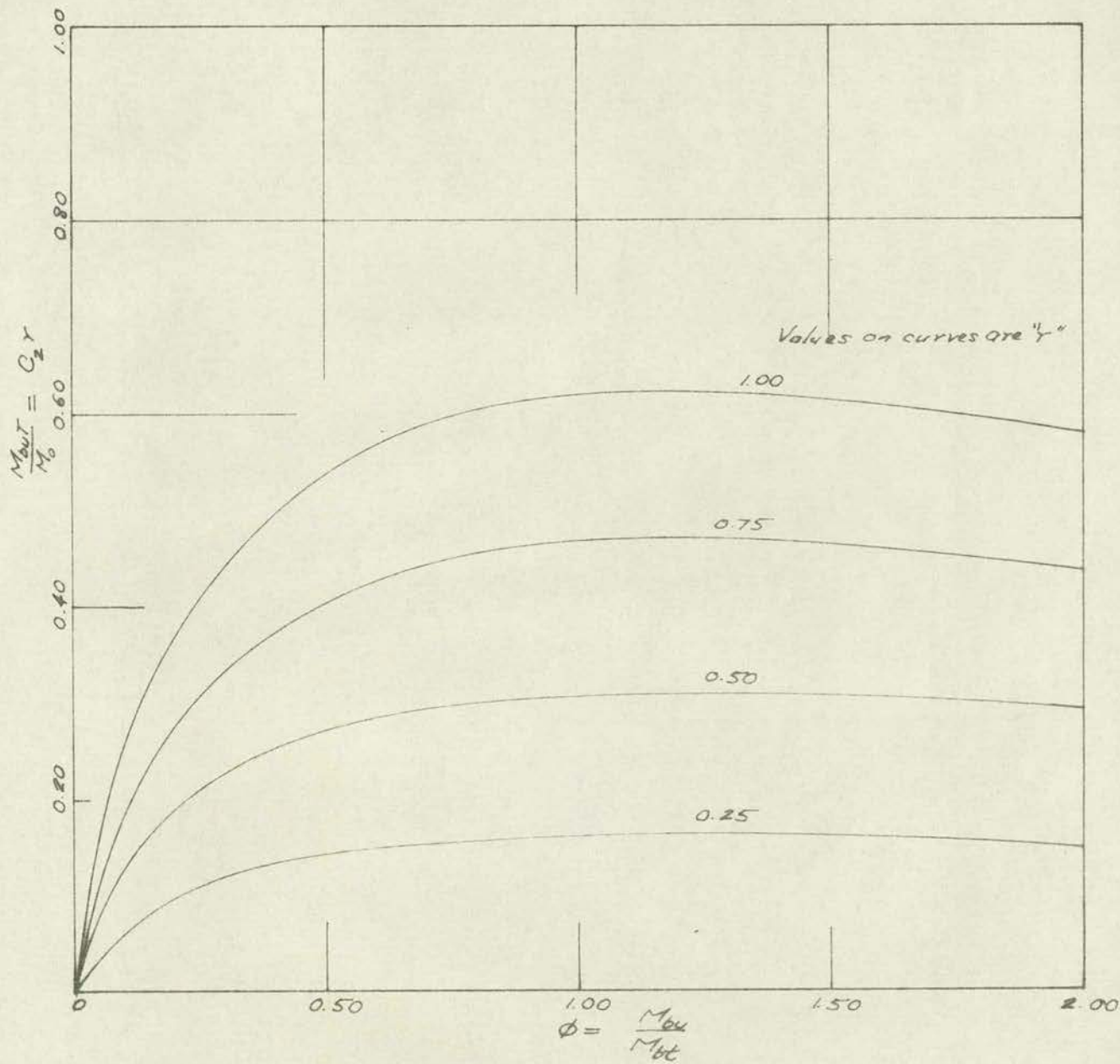


FIG 3.7- Variation of  $\frac{M_{buT}}{M_0}$  with  $\phi$  for  $k=1.50$

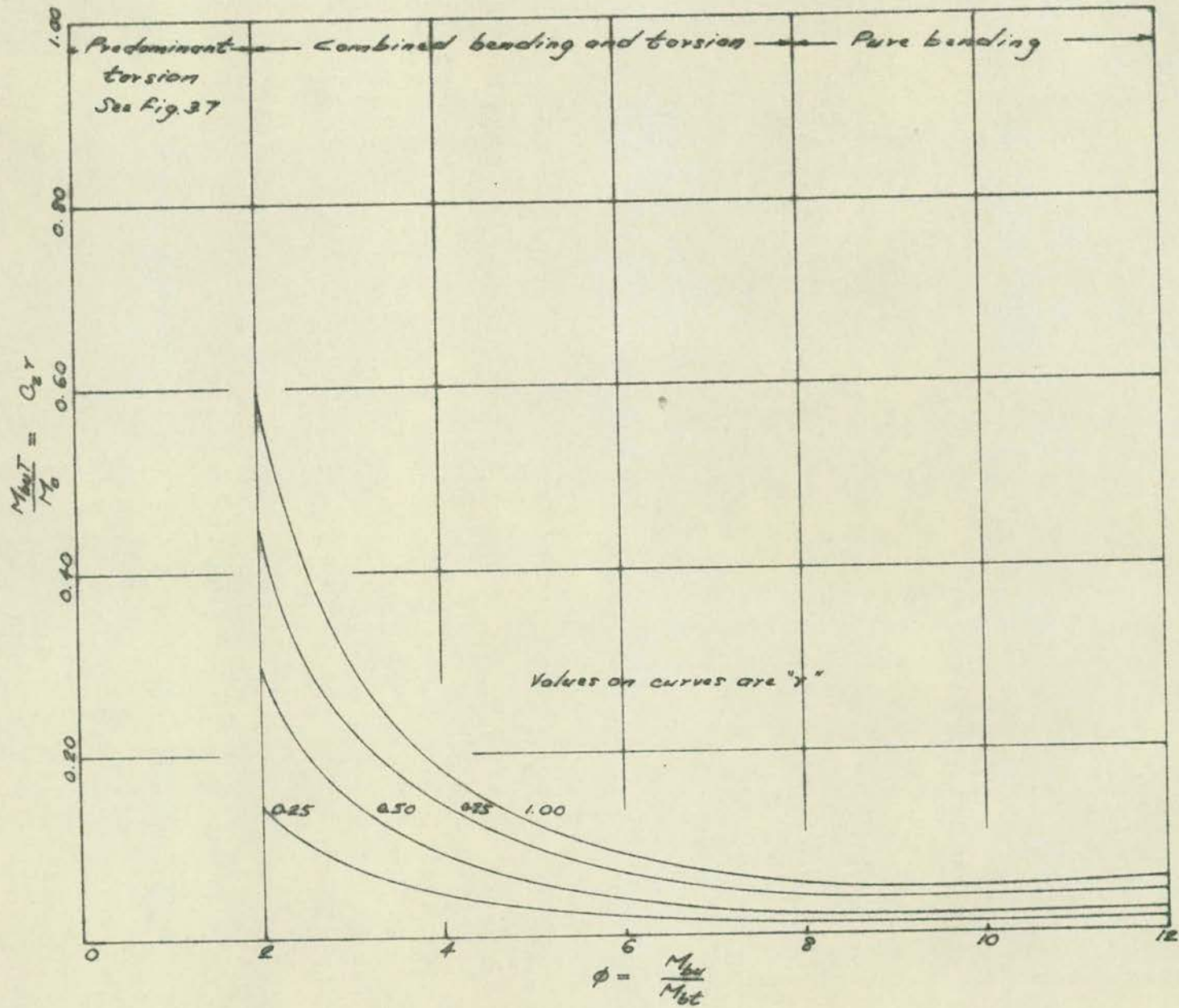


FIG 3.8 - Variation of  $\frac{M_{maxT}}{M_0}$  with  $\phi$  for  $k = 1.50$

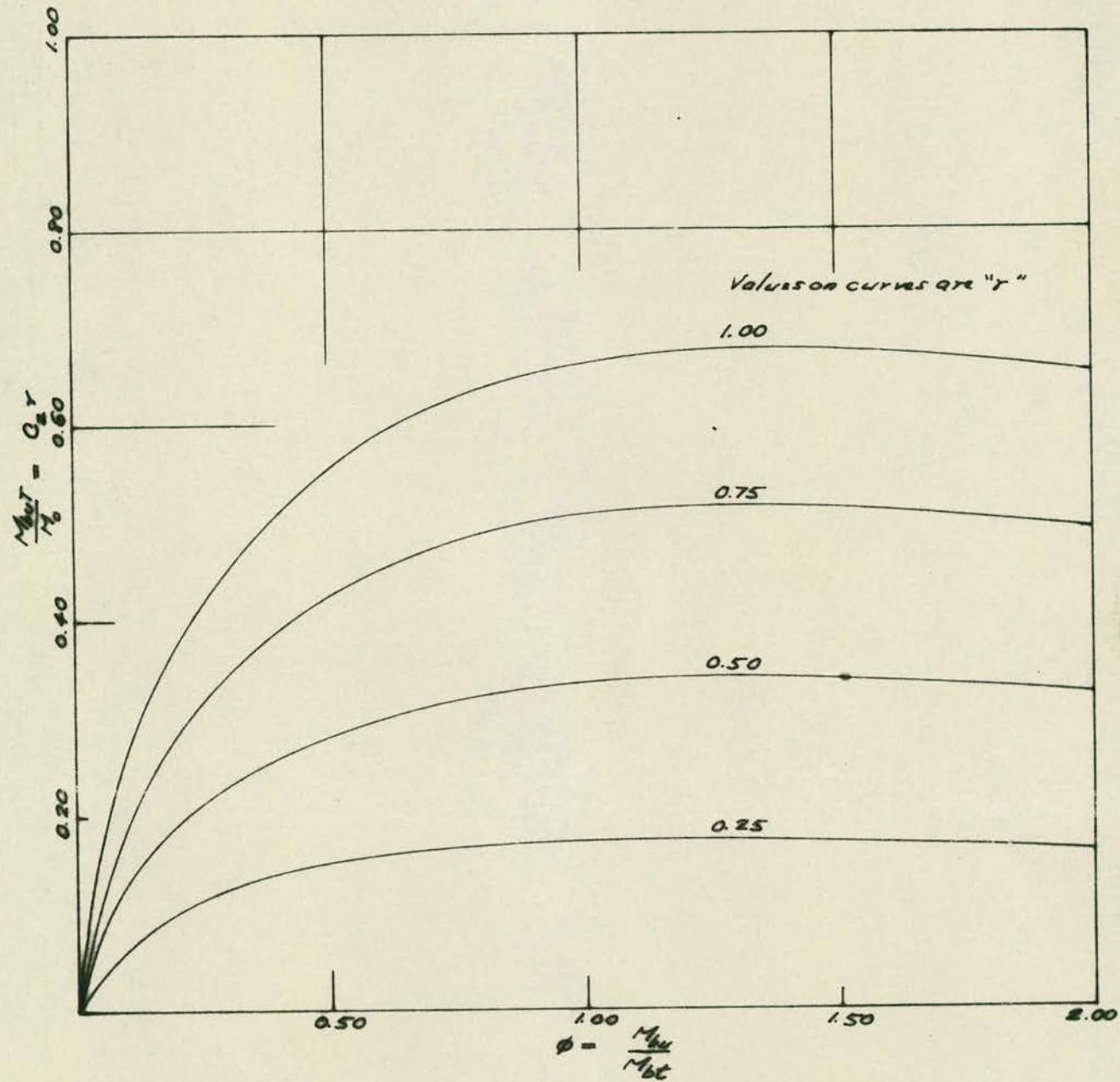


FIG 3.9 - Variation of  $\frac{M_{\max}}{M_0}$  with  $\phi$  for  $k = 2.00$

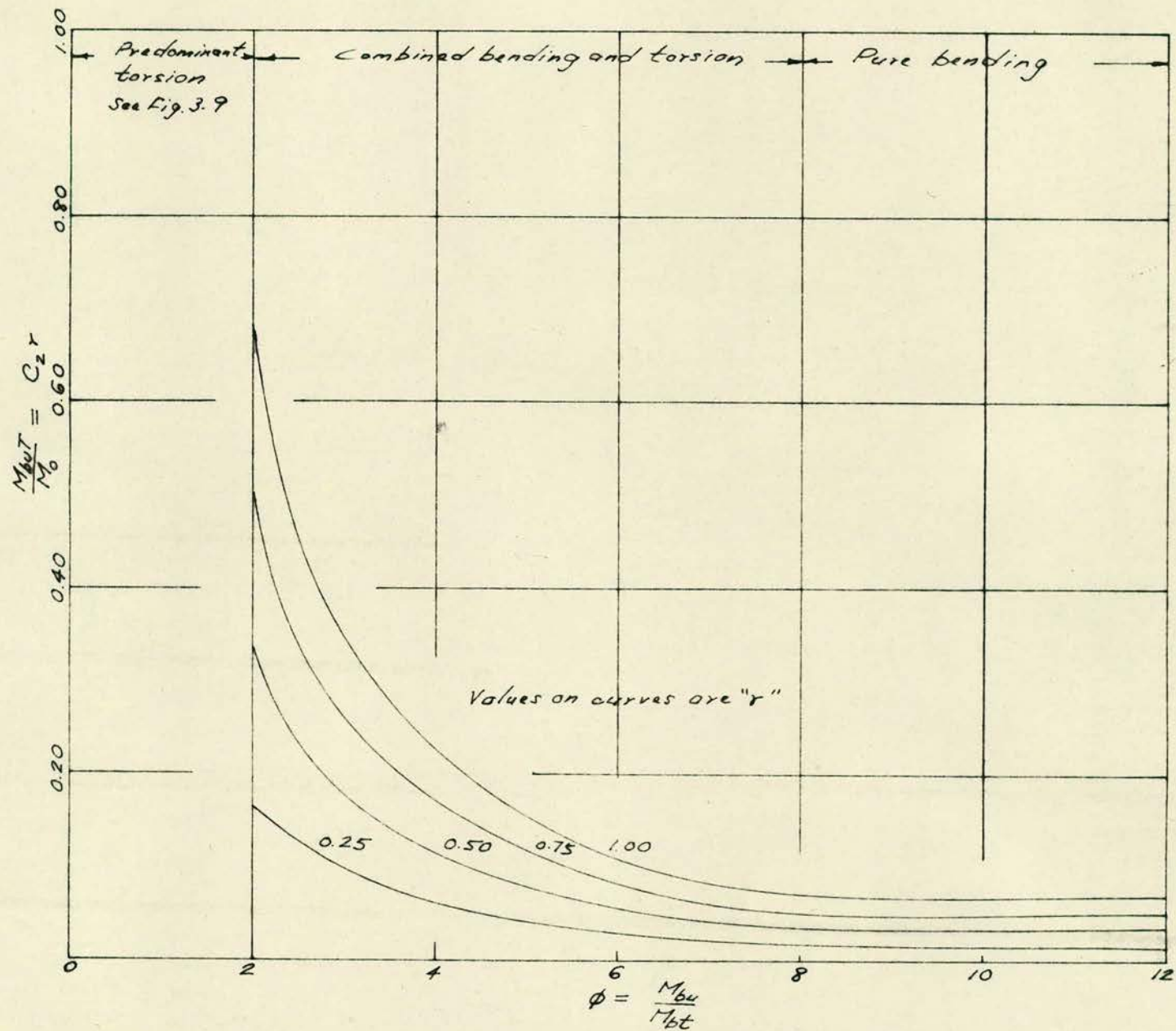


FIG 3.10 - Variation of  $\frac{M_{buT}}{M_0}$  with  $\phi$  for  $k = 2.00$

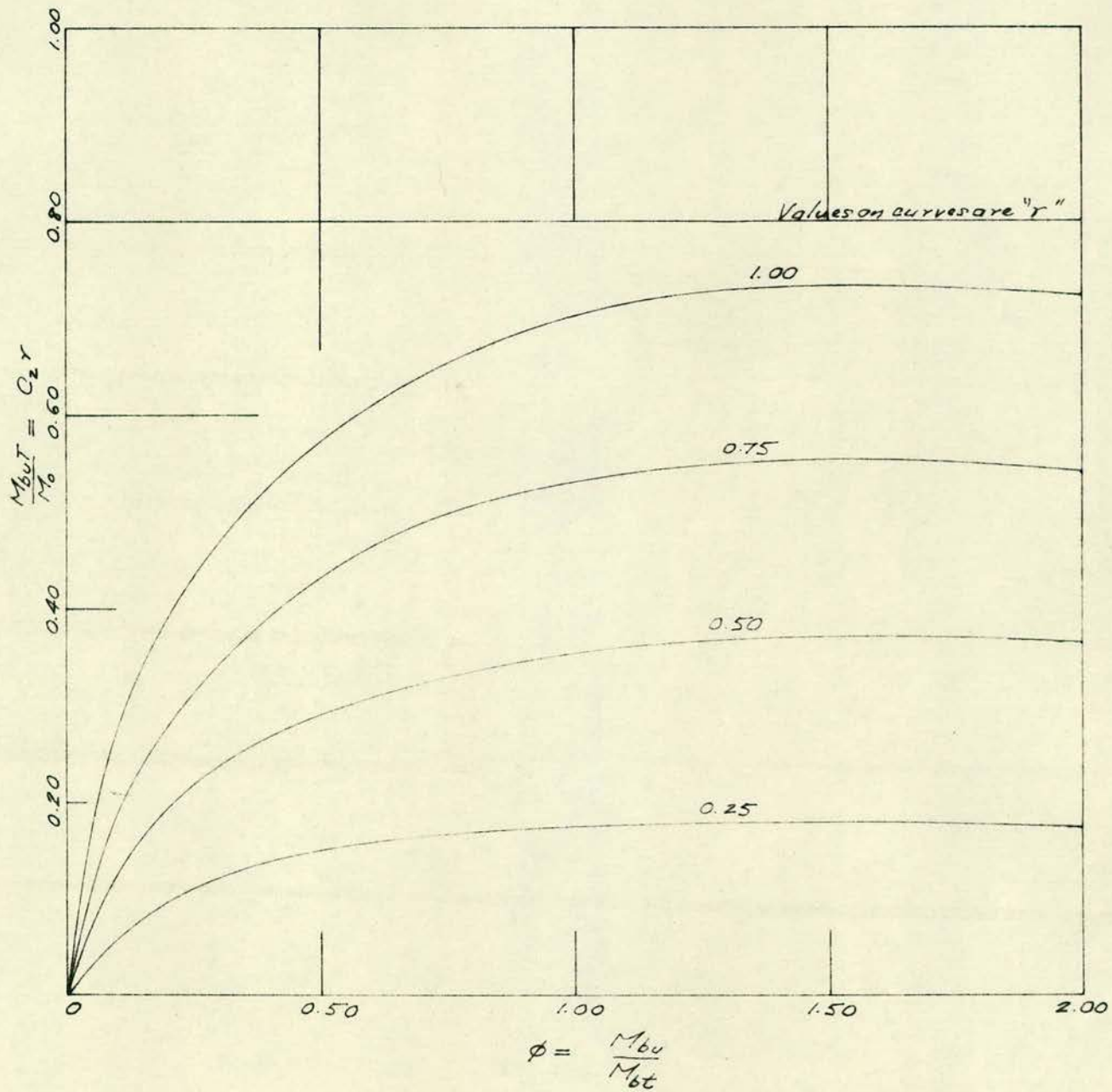


FIG 3.11 - Variation of  $\frac{M_{buT}}{M_0}$  with  $\phi$  for  $k = 2.50$

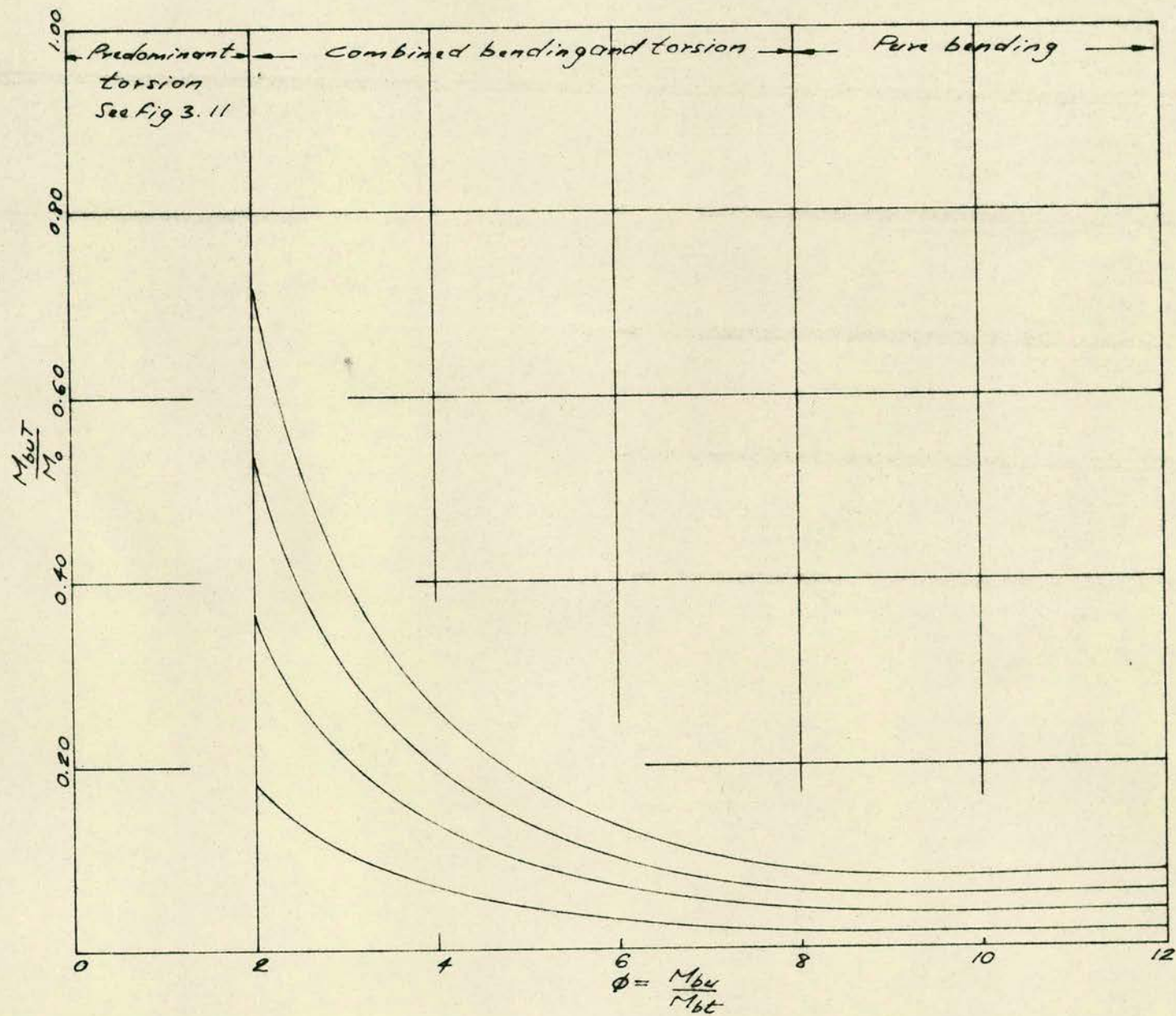


FIG 3.12- Variation of  $\frac{M_{buT}}{M_0}$  with  $\phi$  for  $k=2.50$



the contribution of the transverse binders to the bending capacity is obtained as a dimensionless ratio from which the actual amount can be easily calculated. It is of interest to mention that Figs. 3.3 and 3.4 represent the special case of plotting equation (3.23) with  $r = 1.00$ .

Another important fact which emerged from these graphs is the increase of coefficient  $C_2$  with increase in the ratio of  $k$ . This indicates that the contribution of the transverse binders increases as the relative depth of the beam increases.

### 3.6 Torsional Resistance of longitudinal reinforcement

Discussion in Section 3.4 has revealed that the coefficient  $C_1$  represents the efficient factor of the contribution of the longitudinal reinforcement to the resistance of bending moment. This indicates that, for combined bending and torsion, there is a loss of the potential resistance of the longitudinal steel. The author believes that this loss is accounted for by the resistance of torsional stresses. Since  $C_1$  represents the net contribution of the longitudinal steel to bending, the remaining force could have been used in torsional resistance.

The net force lost to the resistance of torsion may be obtained by subtracting the amount contributed to bending, i.e.

$$F_{\text{Loss}} = A_L f_L - C_1 A_L f_L = (1 - C_1) A_L f_L \dots\dots\dots(3.25)$$

Ernst<sup>(26)</sup> has shown that, for pure torsion, the longitudinal steel contributes to torsional resistance. It is believed that this concept is equally applicable to the case of combined bending and torsion. Therefore, it is decided to accept that the longitudinal reinforcement contributes to the resistance of torsion, the amount of which may be obtained from the above expression.

It is generally known that torsional stresses are distributed on the four faces of a beam when subjected to pure torsion. The distribution should be similar for combined bending and torsion. However, the distribution of bending stresses on the top and bottom section varies, the compression zone above the neutral axis, for instance takes the compressive stress while the tensile steel takes the tensile stress below the neutral axis. From this consideration, the author believes that the torsional stress resisted by the longitudinal steel in the tension zone is the longitudinal component which occurs below the neutral axis. From this, it can also be deduced that the transverse component is transferred to the vertical binders. This concept will be extended to investigate the optimum transverse reinforcement in chapter 4.

From the above discussion, it is concluded that, for

beams subjected to combined bending and torsion, the amount of tensile longitudinal force utilised for resisting the longitudinal component of the torsional stresses is given by expression (3.25).

### 3.7 Proposed minimum compressive reinforcement

Based on the concept of similar stress distribution throughout the four faces of a beam for pure torsion, it is generally accepted that the longitudinal reinforcement should be provided equally both in the top and bottom part of the beam. It is suggested that this concept should be applicable to the case of combined bending and torsion also.

From expression (3.25), longitudinal force in the tension zone for resisting torsional stresses has been suggested as

$$(1 - C_1)A_L f_L$$

In order to resist the longitudinal component of the torsional stresses which occur at the compression zone, the amount of reinforcement provided at the zone should have equal force. This force may be given as

$$F_{LC} = A_{LC} f_s \dots\dots\dots(3.26)$$

For equilibrium, the force given by expression (3.26) should be balanced by the force given by expression (3.25), i.e.

$$A_{LC} f_s = (1 - C_1) A_L f_L \dots\dots\dots(3.27)$$

$$\text{i.e. } A_{LC} = \frac{(1 - C_1) A_L f_L}{f_s} \dots\dots\dots(3.28)$$

It is proposed that the minimum compressive reinforcement should be calculated from expression (3.28).

For reinforcement with equal compressive and tensile stress, the reinforcement reduced to

$$A_{LC} = (1 - C_1) A_L \dots\dots\dots(3.29)$$

3.8 Depth of the compression zone

In this section, the author proposes to present a method of obtaining the depth of the compression zone "n", using the following points which emerged from the preceeding sections:

- (a) the net longitudinal force contributing to the ultimate bending moment  $M_{bu}$  is  $C_1 A_L f_L$
- (b) the remaining steel  $(1 - C_1) A_L$  generates a force  $(1 - C_1) A_L f_L$  to resist the longitudinal component of torsional stresses.
- and(c) transverse binders contributes to the bending capacity of the beam.

The effect of the longitudinal steel resisting torsional stresses as given by (b) will be ignored as the author believed that it is neutralised by the action of transverse binders on the vertical side. Only the horizontal intercept of the binders will be considered.

Therefore, it is proposed that the depth of the compression zone is primarily influenced by the longitudinal steel and the concrete strength. The net effect can now be shown in Fig. 3.13 which is plan view of the failure surface.

The compressive force acting normal to the inclined compression zone is

$$f_c b d \cos \beta \dots\dots\dots(3.29)$$

The tensile force acting normal to the failure zone contributed by the longitudinal steel is

$$C_1 A_{sL} f_L \sin \beta \dots\dots\dots(3.30)$$

Finally, transverse binders intercepted on the horizontal face contribute tensile force normal to the failure zone amounting to

$$\frac{A_T f_T b'}{s} \cot \alpha \cos \beta \dots\dots\dots(3.31)$$

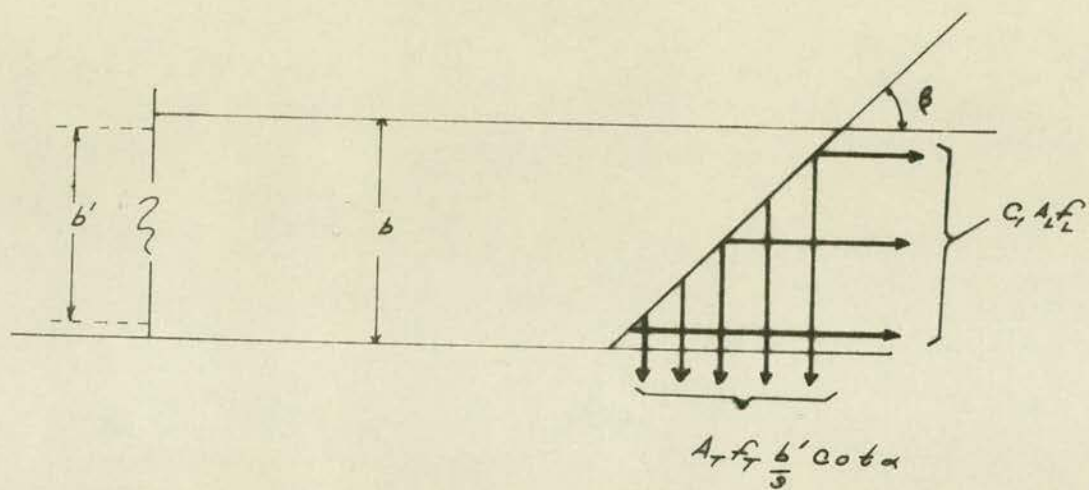


FIG 3.13 - Plan view of failure surface

For equilibrium, the force given by expression (3.29) is balanced by the summation of the forces given by expression (3.30) and (3.31), i.e.,

$$f_n b \operatorname{Cosec} \beta = C_1 A_L f_L \sin \beta + \frac{A_T f_T b'}{s} \cot \alpha \cos \beta \dots (3.32)$$

The above equation can be simplified by considering the equilibrium of the tensile forces acting transverse to the failure zone. Thus

$$\frac{A_T f_T b'}{s} \cot \alpha \sin \beta = C_1 A_L f_L \cos \beta \dots (3.33)$$

or

$$\frac{A_T f_T b'}{s} \cot \alpha = C_1 A_L f_L \cot \beta \dots (3.34)$$

Solving the two simultaneous equations (3.32) and (3.34) equation (3.32) reduces to

$$f_n b \operatorname{Cosec} \beta = C_1 A_L f_L \sin \beta + C_1 A_L \cot \alpha \cos \beta \dots (3.35)$$

$$= C_1 A_L f_L \sin \beta (1 + \cot^2 \beta) \dots (3.36)$$

$$\text{i.e. } n = \frac{C_1 A_L f_L}{f_b} \dots (3.37)$$

The author contends that, the depth of the compression zone is given by equation (3.37).

However, difficulty arises due to lack of knowledge regarding the actual value of the compressive stress to be used for combined bending and torsion. Available data<sup>(14,17,37,38,39)</sup> indicate that the magnitude is related to the ratio of compressive stress to shear stress. Under this circumstance, it was decided to use the compressive stress for pure bending. Thus

$$f = \frac{2}{3} C_u \dots\dots\dots (3.38)$$

Substituting this value in equation (3.37) results in the magnitude of  $n$  to be

$$n = \frac{C_1 A_L f_L}{\frac{2}{3} C_u b} \dots\dots\dots (3.39)$$

The depth of compression block for pure bending is given as

$$n_b = \frac{A_L f_L}{\frac{2}{3} C_u b} \dots\dots\dots (3.40)$$

From this, the depth of compression zone for combined bending and torsion may be related to that of pure bending as

$$n = C_1 n_b \dots\dots\dots (3.41)$$

The author has used the above formula for analysing works of previous investigators which are given in Tables 3.1,



3.2, 3.3, and 3.4. The close correlation of the calculated moments with the observed values seems to indicate that the formula for  $n$  is acceptable.

It is proposed to study the influence of variation of  $\phi$  on the formula. In order to do this, the formula is rearranged by expressing the coefficient as

$$C_1 = \frac{\phi}{\phi + (1 + 2k)\text{Cot } \beta} \dots\dots\dots \text{from (3.12)}$$

$$\text{or} \quad = \left( \frac{\phi}{\phi + \text{Cot } \beta} \right) \dots\dots\dots (3.42)$$

Dividing throughout by  $\phi$ , the formula reduces to

$$C_1 = \frac{1}{\left( 1 + \frac{\text{Cot } \beta}{\phi} \right)} \dots\dots\dots (3.43)$$

$$\text{i.e.} \quad n = \frac{n_b}{\left( 1 + \frac{\text{Cot } \beta}{\phi} \right)} \dots\dots\dots (3.45)$$

Equation (3.45) shows that the magnitude of  $n$  is related to the ratio  $\frac{\text{Cot } \beta}{\phi}$ , and in particular when  $\beta = 45$  degrees as assumed by Evans and Sarkar<sup>(9)</sup>,  $n$  is obtained in a very simple form as

$$n = n_b \left( \frac{\phi}{1 + \phi} \right) \dots\dots\dots (3.46)$$

The above formula is probably applicable when the level of torsion is high. Thus, it is suggested that the formula be used for  $\phi < 2$ .

Another interesting development of the formula is that, for pure bending,  $\beta = 90$  degrees and  $\phi = \infty$ . Therefore

$$n = n_b \dots\dots\dots (3.47)$$

### 3.9 Significance of $M_o$

It is now possible to study the relation between  $M_u$  and  $M_o$  by using formula (3.41). In order to do that, the ultimate bending moment  $M_u$  in pure bending will be written as

$$M_u = A_L f_L \left( d - \frac{n_b}{2} \right) \dots\dots\dots (3.48)$$

Similarly,  $M_o$  may be written as

$$M_o = A_L f_L \left( d - \frac{n}{2} \right) \dots\dots\dots \text{from (3.19)}$$

Substituting the value of  $n$  in terms of  $n_b$  from the relation (3.41),  $M_o$  is obtained as

$$M_o = A_L f_L \left( d - \frac{c_1 n_b}{2} \right) \dots\dots\dots (3.49)$$

The relation of  $M_u$  and  $M_o$  is obtained from equations 3.48 and 3.50 as

$$\frac{M_u}{M_o} = \frac{d - \frac{n_b}{2}}{d - \frac{C_1 n_b}{2}} \dots\dots\dots (3.50)$$

The coefficient  $C_1$  is always less than unity for combined bending and torsion, and therefore by inspection

$$\frac{M_u}{M_o} < 1$$

The above relation has already been shown in Section 3.4 by equation (3.21).

The relationship between  $M_u$  and  $M_o$  is very important for practical purposes because it gives  $M_o$  in terms of  $M_u$  which in practice can be obtained for reinforced concrete beams. This will become obvious in Section 3.10 when design charts are considered.

### 3.10 Presentation of design charts

The ultimate moment equation given in the form of expression (3.11) or (3.14) is basically suitable for purpose of analysis and not for design. In this section, the author proposes to present design equations in the form of charts, but the design process can also be approached analytically. This will be explained in the following paragraphs.

From Section 3.3, the ultimate moment equation has been

shown by equation (3.14) as

$$M_{bu} = A_L f_L (d - \frac{n}{2}) C_1 + \frac{A_T f_T b'}{s} (d - \frac{n}{2}) C_2$$

where n is given by formula (3.39) developed in Section 3.9

as

$$n = \frac{C_i A_L f_L}{\frac{2}{3} C_u b}$$

If the moment equation is divided throughout by  $A_L f_L (d - \frac{n}{2})$ , the resulting expression is

$$\frac{M_{bu}}{A_L f_L (d - \frac{n}{2})} = C_1 + \frac{A_T f_T b'}{A_L f_L s} C_2 \dots\dots\dots(3.51)$$

Further simplification is achieved by introducing  $M_o$  and r from equations (3.19) and (3.24) respectively. The resulting equation is

$$\frac{M_{bu}}{M_o} = C_1 + C_2 r \dots\dots\dots(3.52)$$

The equation has been plotted graphically with  $\frac{M_{bu}}{M_o}$  as abscissa and  $\phi$  as ordinates for k = 1.0, 1.5, 2.0, and 2.5, varying r from 0 to 1.00 as shown in Figs. 3.14, 3.15, 3.16 and 3.17. It can be seen that, for beams under combined

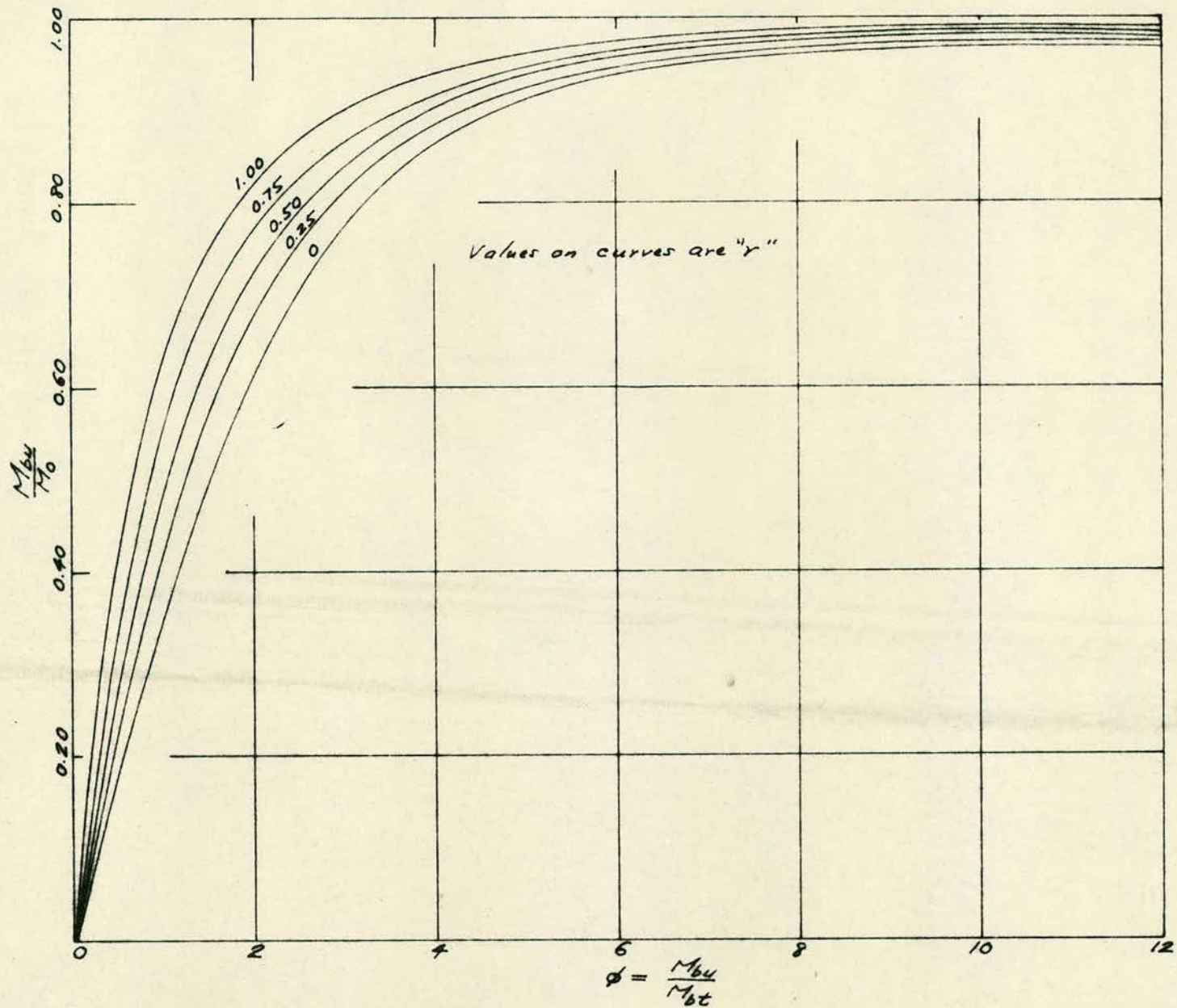


FIG 3.14 - Variation of  $\frac{M_{b4}}{M_0}$  with  $\phi$  for  $k=1.00$

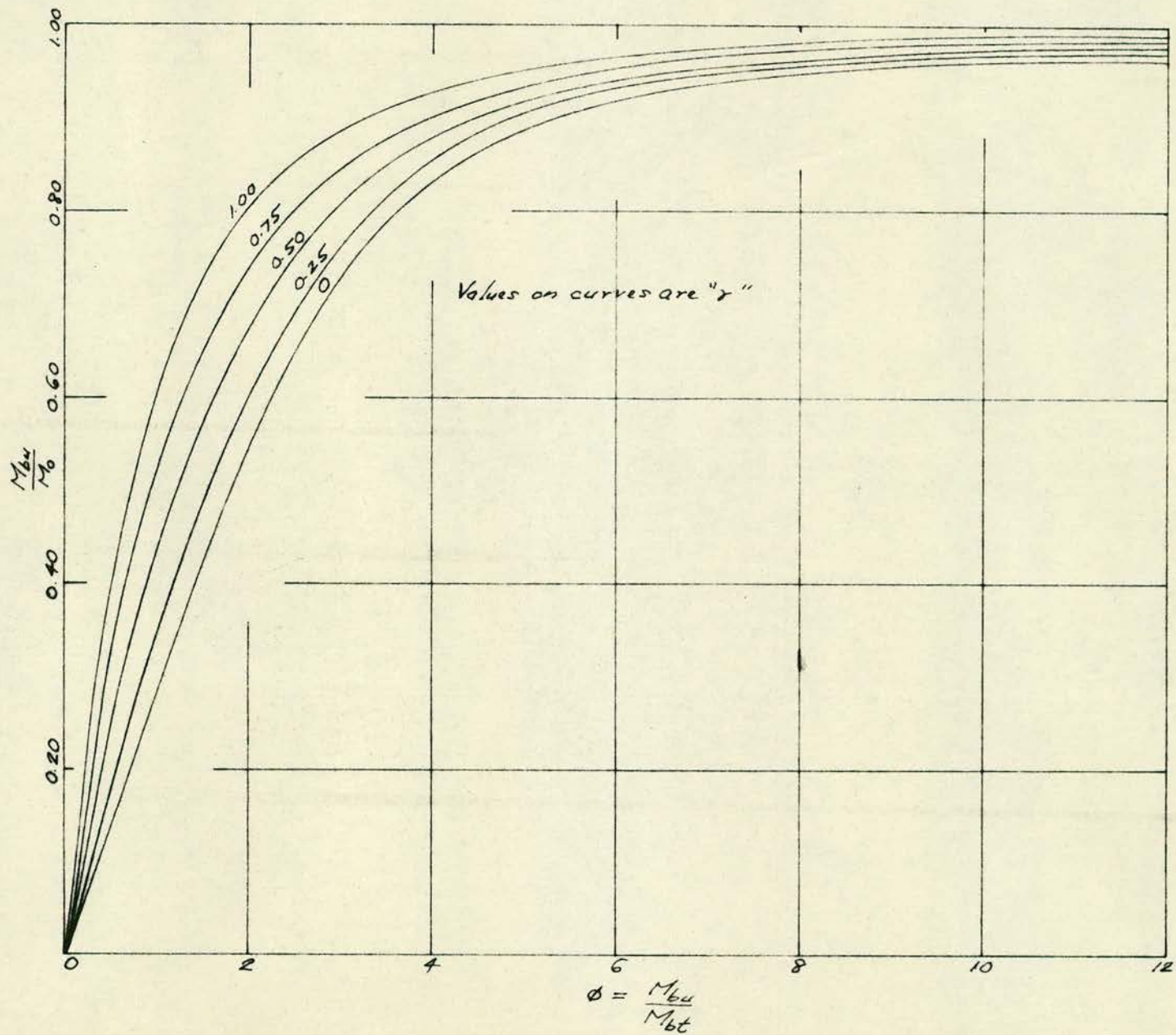


FIG 3.15- Variation of  $\frac{M_{bu}}{M_0}$  with  $\phi$  for  $k=1.50$

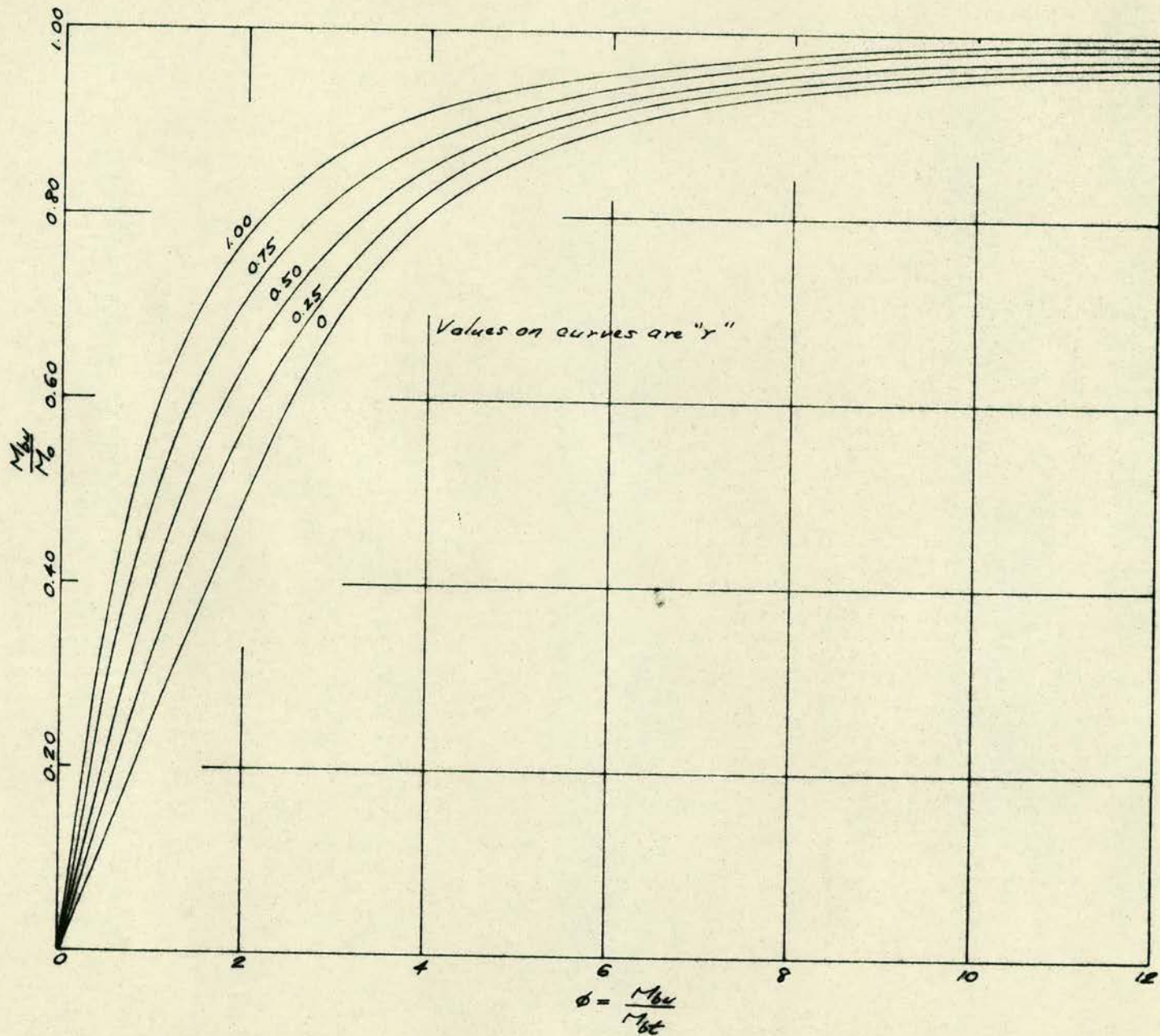


FIG 3.16 - Variation of  $\frac{M_{bu}}{M_0}$  with  $\phi$  for  $k = 2.00$

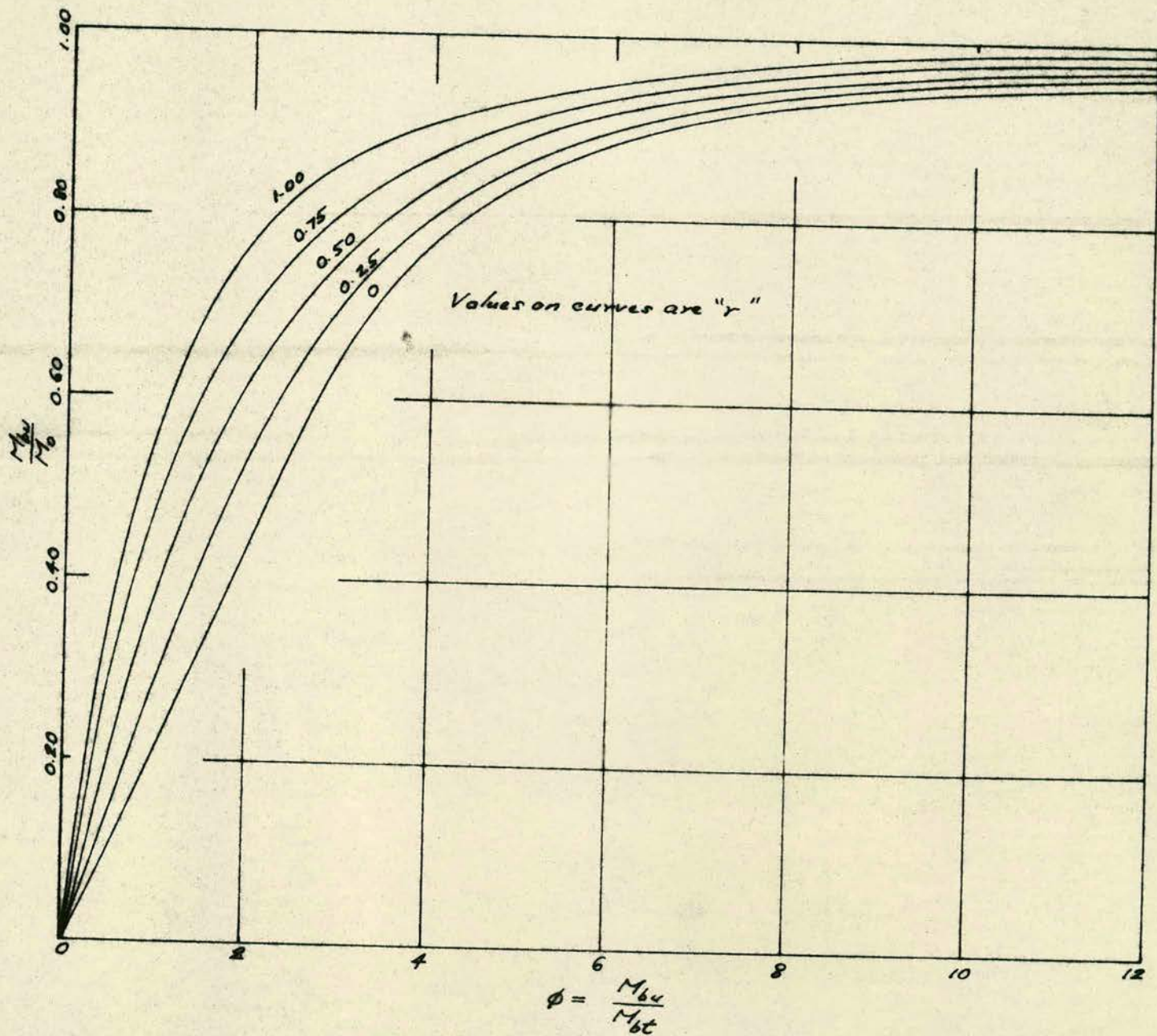


FIG 3.17- Variation of  $\frac{M_{bL}}{M_0}$  with  $\phi$  for  $k=2.50$



bending and torsion, the graphs can be used for analysing any beam fulfilling the conditions valid for the applicability of the ultimate moment equation. The process of analysis is outlined as follows:-

- (a) From the given beam section, calculate the ratio of k
- (b) Compute the ratio of r.
- (c) Using equation (3.39), calculate the value of n
- (d) Calculate  $M_o$  by using equation (3.19)
- (e) Knowing the value of  $\phi$ , k and r, use the graph to obtain the corresponding ratio for  $\frac{M_{bu}}{M_o}$

finally (f) Obtain the value of  $M_{bu}$  from the result of (e)

The process of design is not as straightforward as the process of analysis. The difficulty arises from the fact that  $M_o$  has no practical significance. However, its relation with  $M_u$  can be exploited to obtain the required beam section and the reinforcement. It is also necessary to modify the allowable compressive stress in bending. The author proposes to use the recommendation of the British Code of Practice<sup>(21)</sup> and thus,  $f = \frac{4}{9} C_u$  and the value of  $n_b$  as given in equation (3.40) is now transformed to

$$n_b = \frac{A_L f_L}{\frac{4}{9} c_u b} \dots\dots\dots (3.53)$$

Subsequently, the value of n changed to

$$n = \frac{C_1 A_L f_L}{\frac{4}{9} C_u b} \dots\dots\dots (3.54)$$

The above two formulae will be modified by introducing the following parameter

$$q = p \frac{f_L}{C_u} \dots\dots\dots (3.55)$$

where  $p = \frac{A_L}{bd} \dots\dots\dots (3.56)$

Substituting the value of q in equation(3.53), the formula reduced to

$$n_b = \frac{9}{4} qd \dots\dots\dots (3.57)$$

It is now possible to transform the relation of  $M_u$  and  $M_o$  from equation (3.50) as

$$\frac{M_u}{M_o} = \frac{1 - \frac{9}{8}q}{1 - \frac{9}{8}C_1q} \dots\dots\dots (3.58)$$

In designing reinforced concrete beams in pure bending

or in combined bending and shear, the usual procedure consists of obtaining the beam dimensions from the ultimate bending strength of the concrete given as

$$M_u = Kbd^2C_u \dots\dots\dots (3.59)$$

where  $K = \frac{1}{4}$  to  $\frac{1}{6}$   $\dots\dots\dots (3.60)$

Jones<sup>(40)</sup> has suggested the use of  $K = \frac{1}{6}$  for balanced condition when  $q = \frac{2}{9}$ . However, the value for combined bending is probably greater than this value as can be seen from equation (3.21). Thus

$$M_o > \frac{1}{6} bd^2C_u \dots\dots\dots (3.61)$$

The exact value can be obtained from equation 3.58 as

$$M_o = \frac{1 - \frac{9}{8} C_1 q}{1 - \frac{9}{8} q} \left( \frac{1}{6} bd^2 C_u \right) \dots\dots\dots (3.62)$$

From the relation of  $M_o$  and  $M_u$ , it is now possible to proceed with the design of beams in combined bending and torsion. In order to do this, it is suggested that the value of  $K = \frac{1}{4}$  be used. Therefore, the ultimate bending strength of the concrete is

$$M_o = \frac{1}{4} bd^2C_u \dots\dots\dots (3.63)$$

The process of design is as follows:

- (a) From the assumed loading conditions, the value of  $M_{bu}$  and  $M_{bt}$  can be obtained and the ratio  $\phi$  can be calculated.
  - (b) Choose an "appropriate" ratio for  $k$  and  $r$  (from Chapter 4).
  - (c) From the graphs, the ratio of  $\frac{M_{bu}}{M_o}$  can be obtained.
  - (d) Since  $M_{bu}$  is already known,  $M_o$  can be calculated
  - (e) Use equation 3.63 to obtain the approximate beam dimensions of  $b$  and  $d$ , keeping in mind the ratio  $k$  chosen
  - (f) Calculate the position of the neutral axis from equation 3.54.
  - (g) Calculate the longitudinal steel from equation (3.19)
  - (h) Use the ratio  $r$  selected in (b) to compute the transverse binders required
- Finally (i) Check the design as shown for analysis in preceding paragraphs.

After the design process is completed, the value of  $K$  to be used can be checked from equation (3.62) if desired.

In choosing the reinforcements, it is necessary to restrict the amount of reinforcement. This will be discussed briefly in Section 3.11 and in detail in Chapter 4.

### 3.11 Limiting conditions for validity of the equation

In deriving equation (3.11), it was assumed that failure of the beam occurs due to yielding of the reinforcement without considering the conditions under which this will occur. The application of the equation is therefore restricted to situations under which the following conditions are fulfilled:

- (1) the longitudinal reinforcement ratio  $p$  should be restricted to a value less than  $p_{bc}$  where  $p_{bc}$  represents the balanced ratio
- (2) the ratio  $r$  should lie in the range between  $r_o$  and  $r_u$  where  $r_o$  and  $r_u$  are the minimum and maximum ratio for the torsional shear reinforcement ratio
- (3) the amount of longitudinal reinforcement in the compression zone should be at least equal to that obtained by equation (3.28)
- (4) the limits for the spacing of transverse binders is proposed as

$$\text{For } \phi < 2, \quad s \leq b' \quad \dots \dots \dots (3.64)$$

$$\text{For } \phi > 2, \quad s \leq d' \quad \dots \dots \dots (3.65)$$

- (5) the applied moment  $M_{bu}$  should not be less than  
the applied torsional moment  $M_{bt}$   
and (6)  $k \geq 2.5$

The above points will be discussed in detail in  
chapter 4.

### 3.12 Correlation of theoretical and experimental results

The author has analysed experimental data available  
in order to examine the range of accuracy obtained by comparing  
the observed results with the retical values obtained from  
using the derived equation.

From the data available, the works of the following  
authors were chosen as they conform to the conditions laid down  
for the validity of the equation:-

- (1) Cowan
  - (2) Gesund and Colleagues
  - (3) Chinenkov
- and (4) Evans and Sarkar

The comparison of the results are shown in Tables 3.1,  
3.2, 3.3 and 3.4. It can be seen that, the correlation of  
experimental and calculated values is good, and therefore, the  
author feels justified that the equation may be used within the

Table 3.1 - Beams tested by Cowan

Beam No.	$\phi$	Ultimate Moment (in kip-in)		Ratio of $\frac{\text{Expt.}}{\text{Calc.}}$
		Expt.	Calc.	
R5	1	75	66	1.14
R2	2	158	120	1.32
R1	6	258	210	1.23
S1	2.5	207	152	1.36
S2	4	241	197	1.22
			Average	1.25

Table 3.2 - Beams tested by Gesund and Colleagues

Beam No.	$\phi$	Ultimate Moment (in kip-in)		Ratio of
		Expt.	Calc.	$\frac{\text{Expt.}}{\text{Calc.}}$
1	1	79	87	0.91
2	1	102	120	0.85
3	2	122	128	0.95
4	2	134	154	0.87
5	3	147	146	1.00
6	3	168	158	1.06
7	4	173	159	1.09
8	4	176	168	1.05
9	2	120	136	0.88
10	4	176	212	0.83
11	2	138	152	0.91
12	4	213	218	0.98
Average				0.95



Table 3.3 - Beams tested by Chinenkov

Beam No.	$\phi$	Ultimate Moment (in ton-meters)		Ratio of
		Expt.	Calc.	$\frac{\text{Expt.}}{\text{Calc.}}$
B-2-8-0.1	10	5.6	4.3	1.30
B-2-9-0.1a	10	5.4	4.5	1.20
B-2-8-0.2	5	4.8	4.0	1.20
B-2-8-0.2a	5	4.8	4.1	1.17
B-2-8-0.4b	3.5	4.0	3.7	1.08
B-2-8-0.4	2.5	4.2	4.1	1.02
B-2-8-0.4a	2.5	4.0	3.8	1.05
B-2-8-0.4b	2.5	4.2	4.0	1.05
B-2-8-0.4c	2.5	4.4	4.5	0.98
B-2-8-0.4d	2.5	3.6	3.9	0.92
B-2-8-0.4e	2.5	3.8	4.0	0.95
B-2-8-0.4f	2.5	4.0	3.8	1.05
B-2-8-0.4g	4.5	5.0	4.7	1.06
Average				1.17

Table 3.4 - Beams tested by Evans and Sarkar

Beam No.	$\phi$	Ultimate Moment (in kip-in)		Ratio of
		Expt.	Calc.	$\frac{\text{Expt.}}{\text{Calc.}}$
HB/2	1.9	67	64	1.05
HB/3	3.5	75	75	1.00
HB/4	4.7	82	79	1.00
HB/5	6.6	82	81	1.01
HB/6	8.0	85	84	1.01
HB/8	3.6	80	84	0.95
HB/9	4.4	85	96	0.89
HB/10	5.0	91	98	0.93
HB/11	7.0	94	100	0.94
HB/14	1.9	82	105	0.80
HB/15	3.2	111	119	0.93
HB/16	5.5	129	131	0.99
HB/17	6.9	137	138	<u>0.99</u>
			Average	0.96

accuracy required for reinforced concrete design.

Some examples of computation of  $M_{bu}$  using equations (3.14) and (3.52) and the procedure to be followed are given in Section 3.13.

### 3.13 Sample calculations

The procedure to be followed in using equation 3.52 is:-

- (1) Calculate the ratio of  $k$  from the given beam sections.
- (2) Compute the ratio  $r$  using equation (3.24).
- (3) Use formula (3.1) or (3.2) or (3.3) to obtain the magnitude of  $\text{Cot } \alpha$ .
- (4) Using  $\phi$ ,  $k$  and  $\text{Cot } \alpha$ , calculate the coefficients  $C_1$  and  $C_2$ .
- (5) Calculate  $n$  by using equation 3.39.
- (6) Use equation (3.19) to obtain the value of  $M_o$ .

- (7) The bending moment  $M_{bu}$  is now obtainable from equation (3.52).

It is also possible to compute  $M_{bu}$  directly by the use of equation (3.11) or (3.14). The method depends on personal choice.

The author will demonstrate the use of equation (3.14) and (3.52) in the following paragraph by using beam No.5 tested by Gesund and Colleagues.

(1) Method of using equation (3.14)

From the given data, the following are obtained:

$$b = 8", h = 8", d = 6.5", A_L = 0.59 \text{ sq.in.}, f_L = 51 \text{ ksi},$$

$$A_T = 0.11 \text{ sq.in.}, f_T = 50 \text{ ksi}, s = 5" \text{ c/c}, f'_c = 4.24 \text{ ksi},$$

$$\phi = 3.0.$$

The calculated reinforcing cage is 5.9 by 5.9 in.

Step (1):  $k = \frac{5.9}{5.9} = 1.00$

Step (2): Using formula (3.2), calculate  $\text{Cot } \alpha$

$$\text{i.e. } \text{Cot } \alpha = \frac{0.80}{3} = 0.27$$

Step (3): Use formula (3.12) to obtain coefficient  $C_1$

$$\text{i.e. } C_1 = \frac{3}{3 + (1 + 2)(0.27)} = 0.79$$

Step (4): Use equation (3.13) to obtain coefficient  $C_2$

$$\text{i.e. } C_2 = \frac{3}{3 + (1 + 2)(0.27)} (1+3)(0.27)^2 = 0.23$$

Step (5): Calculate n by using equation (3.39)

$$\text{i.e. } n = \frac{(0.59)(0.51)(0.79)}{\frac{2}{3}(0.85)(4.24)(8)} = 1.22$$

Step (6): From equation (3.14),  $M_{bu}$  is obtained as follows:

$$\begin{aligned} M_{bu} &= (0.59)(51)(6.5 - 0.61)(0.79) \\ &+ \frac{(0.11)(50)(5.9)}{5} (6.5 - 0.61)(0.23) = \underline{146} \text{ kip-in} \end{aligned}$$

(2) Method of using equation(3.52)

The given data used are already given.

Step (1)  $k = 1.00$

$$\text{Step (2) } r = \frac{(0.11)(50)(5.9)}{(0.59)(51)(5)} = 0.22$$

Step (3) as before, i.e.  $\text{Cot}\alpha = 0.27$

Step (4) as before, i.e.  $C_1 = 0.79$  and  $C_2 = 0.23$

Step (5) as before,  $n = 1.22$

Step (6)  $M_o$  is obtained from equation (3.19) as shown below:

$$M_o = (0.59)(0.51)(6.5 - 0.61) = 177 \text{ kip-in.}$$

Step (7):  $M_{bu}$  can now be obtained by direct substitution in equation (3.52)

$$\begin{aligned} M_{bu} &= M_o(C_1 + C_2 r) \\ &= 177(0.79 + 0.23 \times 0.22) \\ &= \underline{146} \text{ kip-in} \end{aligned}$$

### 3.14 Summary and Conclusions

The author has developed an ultimate moment equation for under-reinforced concrete beams subjected to combined bending and torsion.

The ultimate moment was found to consist of the contribution of longitudinal and transverse reinforcement. The equation is given as (3.11).

By introducing two coefficients,  $C_1$  and  $C_2$ , defined as the efficiency coefficients of longitudinal and transverse reinforcement, the equation was simplified to the form (3.14).

Equation (3.14) was further rearranged into the form (3.52) by introducing two parameters,  $M_o$  (see equation (3.19)) and  $r$ , the later defined as torsional shear reinforcement and thus relating the contribution of the binders to the total bending moment. The special feature of expressing the equation as (3.52) was the possibility of plotting the design charts shown in Figs. 3.14, 3.15, 3.16 and 3.17.  $M_o$  was related to  $M_u$  by the expressions (3.58) and (3.62) to simplify design of beams in combined bending and torsion similar to that for pure bending.

A method of computing the position of the neutral axis was introduced in the form of formula (3.39) and related to that for pure bending by (3.41).

Further simplification was achieved in expressing the position of the neutral axis for predominant torsion cases as (3.46).

A proposal for restricting the minimum longitudinal reinforcement in the compression zone is given by the expression (3.28) or (3.29).

Finally, the accuracy of the equation was demonstrated by the analysis of forty-three beams tested by previous investigators. The comparison of the calculated and reported ultimate moments are shown in Tables 3.1, 3.2, 3.3 and 3.4.

OPTIMUM REINFORCEMENT4.1 Introduction

In chapter 3, the author presented an ultimate moment equation for calculating the bending moment  $M_{bu}$  for beams subjected to combined bending and torsion. The application of the equation is restricted to compliance with the conditions and assumptions under which the equation was derived, and it is proposed in this chapter to discuss these conditions in detail under the following:

- (1) the establishment of the balanced longitudinal steel  $p_{bc}$  for combined bending and torsion.
- and (2) the establishment of a range of values for  $r$ .

Finally, the proposed limitations will be compared with existing design recommendations.

4.2 Proposal for balanced longitudinal steel  $p_{bc}$ 

It is proposed to establish a balanced percentage of longitudinal steel  $p_{bc}$  so that, at failure, the steel attains the yield stress and crushing of the concrete follows. This will be done by reference to the case for pure bending.

For pure bending, provided the percentage of longitudinal reinforcement does not exceed a specific value, there is evidence that failure occurs due to yielding of the reinforcement and





then crushing of the concrete in the compression zone. This value is given as

$$P_b = \frac{2C_u}{9f_L} \dots\dots\dots(4.1)$$

in which limitations are imposed by the following assumptions:

- (1) the longitudinal steel reaches the yield stress.
- (2)  $n_b = \frac{d}{2}$ , thus ensuring under-reinforcement.
- (3) the concrete compressive stress block is rectangular with an average stress value of  $\frac{4C_u}{9}$ .

The author believes that a similar approach may be made for the case of combined bending and torsion. Complications are introduced however due to insufficient data regarding the true behaviour of concrete under the action of combined bending and torsion. Attempts have been made by Bresler and Pister<sup>(37,38,41)</sup>, Goode and Helmy<sup>(17)</sup> and Reeves<sup>(39)</sup>, but their results are inconclusive. The general agreement is that the presence of torsion tends to reduce the direct stress  $f_c$  to a lower value of  $f$ .

For the case of combined bending and torsion, the author has decided to use the allowable concrete stress as shown in Section 3.10 of Chapter 3, i.e.  $f = \frac{4}{9} C_u$ . It is proposed to use this assumption in obtaining the balanced ratio  $p_{bc}$  which will be done in the following.

It has been shown by expression (3.41) that, the depth of the compression block is

$$n = C_1 n_b$$

where  $n_b = \frac{A_L f_L}{9 C_u b}$

For combined bending and torsion,  $p_{bc}$  may be written as

$$p_{bc} = \frac{A_L}{bd} \dots\dots\dots (4.2)$$

or  $A_L = p_{bc} bd \dots\dots\dots (4.3)$

Substituting  $A_L$  from (4.2) in expression for  $n_b$  shown above,  $n_b$  reduces to

$$n_b = \frac{p_{bc} f_L d}{\frac{4}{9} C_u} \dots\dots\dots (4.4)$$

$$= \frac{9 p_{bc} f_L d}{4 C_u} \dots\dots\dots (4.5)$$

Substituting the value of  $n_b$  obtained from (4.5) in the formula for  $n$ , the result is

$$n = \frac{9 p_{bc} f_L C_1}{4 C_u} \dots\dots\dots (4.6)$$

Restricting the neutral axis depth to that given by assumption (2),  $n$  is found as follows

$$n = \frac{d}{2} \dots\dots\dots (4.7)$$

$$\text{i.e. } \frac{9p_{bc} f_L C_1}{4C_u} = \frac{d}{2} \dots\dots\dots (4.8)$$

From expression (4.8), the value of  $p_{bc}$  is obtained as

$$p_{bc} = \frac{2C_u}{9f_L C_1} \dots\dots\dots (4.9)$$

The author contends that expression (4.9) gives the balanced longitudinal reinforcement for the case of combined bending and torsion for different ratios of  $\phi$  and  $k$ .

It is interesting to show that, for pure bending,  $C_1 = 1.00$ , and therefore,  $p_{bc}$  reduces to the following value, i.e.

$$p_{bc} = \frac{2C_u}{9f_L} = p_b$$

which is the same as expression (4.1).

In general, expression (4.9) shows that, as  $C_1$  decreases,  $p_{bc}$  increases. Since the magnitude of  $C_1$  decreases

for low ratios of  $\phi$  as shown in Fig. 3.2 of Chapter 3, it can be concluded that,  $p_{bc}$  is always greater than  $p_b$  for combined bending and torsion. Therefore,  $p_b$  as given by expression (4.1) represents the minimum ratio of  $p_{bc}$ .

It is proposed therefore to accept the ratio given by expression (4.9) as the ratio for proportioning the longitudinal steel to ensure yielding of the steel in the longitudinal direction.

In general, the reinforcement provided in actual practice is usually less than the calculated value so that the design requirement is fulfilled. Nevertheless, the author feels that further study will result in further modification of this value.

It is now proposed to carry out investigation to establish the minimum and maximum ratios of the transverse reinforcement.

#### 4.3 Provision for torsional shear reinforcement

It was shown in Chapter 3 that, for combined bending and torsion, the ultimate moment  $M_{bu}$  consists of the contribution of longitudinal and transverse reinforcement. In particular, the net bending moment was shown to be  $M_{buL}$  as given by expression (3.16). From this result, the net loss of internal force due to the resistance of torsional stresses was given by expression (3.25).

This is reproduced in the following as it is relevant to the discussion. Thus

$$F_{\text{loss}} = A_L f_L - C_1 A_L f_L = (1 - C_1) A_L f_L$$

that is, the net force resisting the torsional moment and is equivalent to the longitudinal component of the torsional stress.

It is contended that, in order for yielding of the longitudinal steel to occur, an equivalent amount of transverse binders should be provided to resist the transverse component of the torsional stress, thus preventing possible premature failure before yielding of the longitudinal steel. Further, it is believed that this amount of reinforcement constitutes the minimum requirement and designated by Lessig<sup>(13)</sup> as the optimum amount.

It was also shown in Chapter 3 that the bending moment  $M_{\text{buT}}$  contributed by the transverse binders is given by expression (3.22) as

$$M_{\text{buT}} = A_L f_L \left( d - \frac{n}{2} \right) C_2 r$$

This expression indicates that, for a fixed ratio

of  $P_{bc}$ , the contribution of the binders to bending can be related to the ratio  $r$ . In particular, the above equation shows that,  $M_{buT}$  increases for increase in  $r$ , a relationship which has been confirmed by experiment<sup>(15)</sup>.

In addition, the fact that the bending moment increases with increase of this ratio implies the existence of a range within which this ratio may vary for yielding of the reinforcement in both categories. The author is of the opinion that there is an upper value for  $r$  which determines the maximum amount of transverse binders.

It is proposed therefore to accept  $r$  as a basis for establishing the minimum and maximum amount of transverse binders, and develop proposals for these ratios using two methods:-

(1) Force intensity method

and (2) Internal couple method

#### 4.4 Force intensity method

This method consisted of relating the intensity of the forces in the transverse binders to that of the longitudinal steel, thus expressing "r" as follows:-

$$r = \frac{\frac{A_T f_T}{s}}{\frac{A_L f_L}{b'}} \dots \dots \dots (4.10)$$

that is, the ratio of the force intensity of the transverse binders  $\frac{A_T f_T}{s}$ , to the force intensity of the longitudinal steel  $\frac{A_L f_L}{b'}$ .

If these relations can be obtained from the equilibrium of the internal stresses of the beam yielding at failure, then it forms a basis from which the minimum and maximum ratios can be established.

Experimental evidence<sup>(23)</sup> indicates that the concrete core is not effective in resisting the torsional stresses since these stresses occur only on the outer periphery of the beam. It is assumed therefore that the stresses are distributed as follows:-

- (1) the transverse components of the torsional stresses are resisted by the transverse binders.
  - (2) the top and bottom longitudinal steel resist the longitudinal component of the torsional stresses
- and (3) the resistance of concrete is negligible.

Assumption (2) is based on a further assumption that the longitudinal steel behaves as though distributed uniformly around the periphery of the beam, so that, half the tensile longitudinal steel resists the stresses on half of the periphery,

while the remainder resist the other half. The mechanism of this action is illustrated in Fig. 4.1.

From the figure, the intensity of the longitudinal steel is given as

$$f'_L = (1 - C_1) \frac{A_L f_L}{(b' + d')} \dots\dots\dots (4.11)$$

and the intensity of the transverse binders as

$$f'_T = \frac{A_T f_T}{s} \dots\dots\dots (4.12)$$

so that, for equilibrium,

$$f'_T = f'_L \dots\dots\dots (4.13)$$

i.e.  $\frac{A_T f_T}{s} = (1 - C_1) \frac{A_L f_L}{(b' + d')} \dots\dots\dots (4.14)$

or  $r = \frac{(1 - C_1)}{1 + k} \dots\dots\dots (4.15)$

Substituting for coefficient  $C_1$  from expression (3.43) in chapter 3 gives r as

$$r = \frac{1}{(1 + k)(1 + \frac{\phi}{\text{Cot}\phi})} \dots\dots\dots (4.16)$$

For a particular beam, "r" is related to the ratio



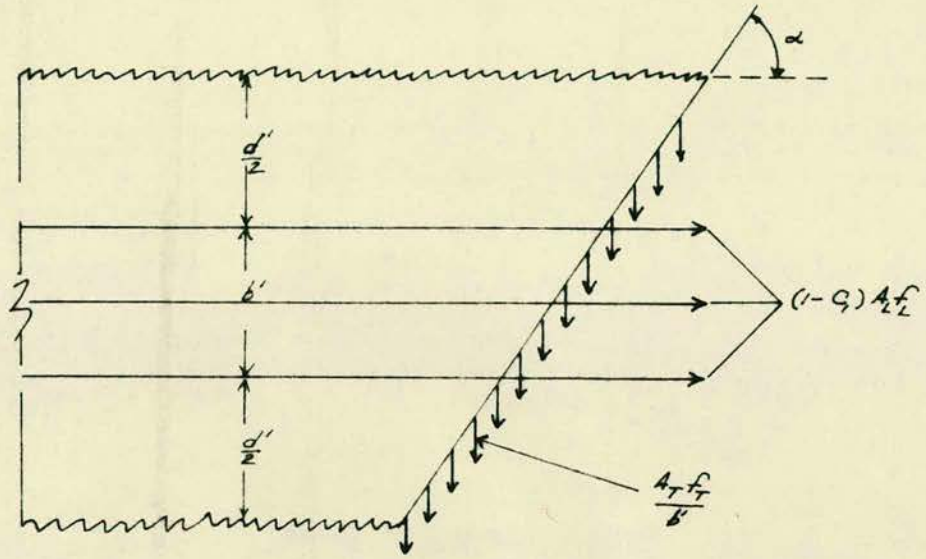


FIG 4.1- Intensity of longitudinal and transverse steel

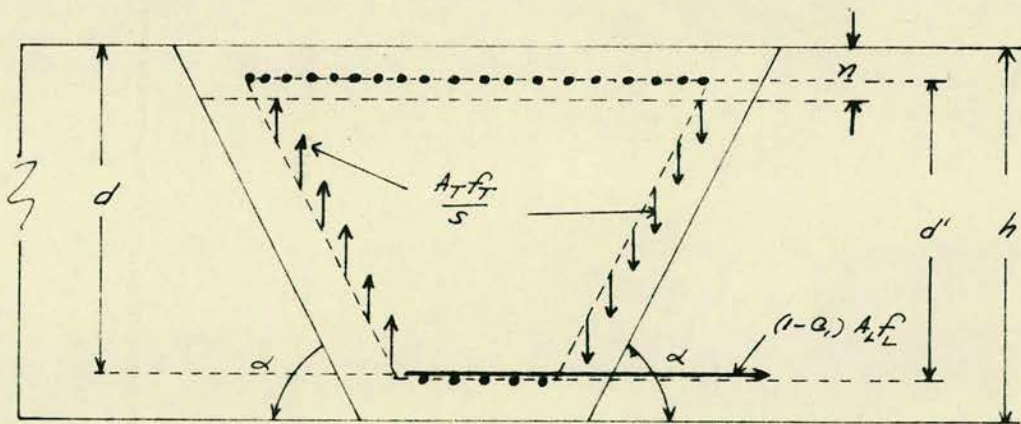


FIG 4.2- Side view of failure surface

$\frac{\phi}{\cot \beta}$ , and when  $\phi$  is fixed, the value is directly determined once the value of  $\cot \beta$  is obtained.

Chinenkov<sup>(12)</sup> found by plotting graphs of  $M_{bu}$  against  $\cot \beta$  that, the bending moment gradually decreases up to a certain value of  $\cot \beta$ , and then again increases when  $\cot \beta$  increases, and concluded that there is a minimum value for  $M_{bu}$ .

By inspection of expression (4.16),  $r$  will be a minimum when angle  $\beta$  is 45 degrees. The author proposes therefore to use this angle as a basis for fixing the minimum ratio of  $r$ . It is interesting to note that Evans and Sarkar<sup>(9)</sup> use the same angle with satisfactory results.

The optimum ratio  $r_o$  of the minimum ratio is taken as

$$r_o = \frac{1}{(1+k)(1+\phi)} \dots\dots\dots (4.17)$$

Similarly, the maximum value of  $r$  should be limited by fixing or limiting the value for the angle  $\beta$ . This consideration is supported by the fact that, Lessig<sup>(13)</sup> from experimental observation found that, for practical purposes, the intercept on the longitudinal axis can be approximated to  $(b + 2h)$ . This amounts to restricting the angle of inclination to

$$\text{Cot } \beta = \frac{b + 2h}{b} = 1 + 2k \dots\dots\dots(4.18)$$

In general, when the intercept on the longitudinal axis is about  $(b + h)$ , the structural member is badly deflected, and therefore the intercept should not be allowed to exceed this length. On the basis of this reasoning, the author decides to accept the above limitation for Cot and proposes the maximum "r" as

$$r = \frac{1}{(1 + k) \left(1 + \frac{\phi}{(1 + 2k)}\right)} \dots\dots\dots(4.19)$$

Comparisons of proposed ratios given by expression (4.17) and (4.19) with the recommendations put forward by other investigators are shown in Figs. 4.4, 4.5, 4.6 and 4.7. It may be concluded that the assumed values are both satisfactory and consistent.

Alternatively, the above formulae can be obtained by the internal couple method as described in Section 4.5.

#### 4.5 Internal couple method

This method is based on a hypothetical mechanism of the transverse and longitudinal steel as they generate internal moments. The method is simple and the author feels that it explains the internal action of the reinforcement rationally.

The effects of vertical intercepts of the transverse binders and the longitudinal steel amounting to  $(1 - C_1)A_L$  are assumed to induce the internal moments. It is assumed that the horizontal legs of the binders intercepted by the crack at the bottom do not contribute directly to bending action and the binders in the upper layer can be also ignored.

The proposed failure of the beam indicating the transverse stresses is illustrated in Fig. 4.2. The diagram is a side view of the beam at the failure stage.

The following assumptions are made:-

- (1) the lever arm of the internal moment is approximately equal to  $d'$
  - (2) the angle of inclination is as given by expression (3.10) of Chapter 3
  - (3) the effect of the tensile stress of the concrete is ignored
- and (4) all reinforcement which cross the crack reach its yield stress.

The ultimate bending moment  $M_{bu}$  and on the assumption (1) is given by equation (3.14) as

$$M_{bu} = A_L f_L \left(d - \frac{n}{2}\right) C_1 + \frac{A_T f_T b'}{s} \left(d - \frac{n}{2}\right) C_2$$

To satisfy the assumption (1) shown above, the lever arm  $(d - \frac{n}{2})$  is replaced by  $d'$  and thus, the moment  $M_{bu}$  is transformed to

$$M_{bu} = A_L f_L d' C_1 + \frac{A_T f_T b'}{s} d' C_2 \dots\dots\dots (4.20)$$

The above expression for the ultimate moment results from considering the action of internal stresses in the reinforcement as they rotate anti-clockwise about the centroid of the compression zone with a lever arm equal to  $d'$ .

From Fig. 4.2, it is observed that, the transverse binders form a couple, generating a clockwise internal moment  $M_{buTi}$  which is given as

$$M_{buTi} = \frac{A_T f_T d'}{s} (b' + d') \cot^2 \alpha \dots\dots\dots (4.21)$$

$$\text{or} \quad = \frac{A_T f_T b' d'}{s} (1 + k) \cot^2 \alpha \dots\dots\dots (4.22)$$

Similarly, the net longitudinal force  $(1 - C_1) A_L f_L$  creates an internal moment  $M_{buLi}$  in anti-clock-wise direction which is given as

$$M_{buLi} = (1 - C_1) A_L f_L d' \dots\dots\dots (4.23)$$

For equilibrium, the moments  $M_{buLi}$  and  $M_{buTi}$  must balance each other, i.e.

$$(1-C_1)A_{L f L} = \frac{A_{T f T} b' d'}{s} (1+k) \text{Cot}^2 \alpha \dots\dots\dots(4.24)$$

and simplifying,

$$\frac{A_{T f T} b'}{A_{L f L} s} = \frac{(1-C_1)}{(1+k) \text{Cot}^2 \alpha} \dots\dots\dots(4.25)$$

$$\text{i.e.} = \frac{(1-C_1)}{(1+k) \text{Cot}^2 \alpha} \dots\dots\dots(4.26)$$

For combined bending and torsion, the angle of crack may be assumed to be 45 degrees. Expression (4.26) is therefore reduced to

$$r = \frac{(1-C_1)}{1+k}$$

which is the same expression (4.15).

The process is repeated as in the case discussed in Section (4.4).

The above relation may be extended to obtain the minimum and maximum ratio of r by introducing the following range of the angle of inclination .

$$45^\circ \leq \beta \leq \text{Cot}^{-1}(1 + 2k) \dots\dots\dots(4.27)$$

Substituting the above range of  $\beta$  , the range of r is obtained as

$$\frac{1}{(1+k)(1+\phi)} \ll r \ll \frac{1}{(1+k)(1+\frac{\phi}{(1+2k)})} \dots\dots\dots (4.28)$$

It can be seen that the above range of  $r$  is the combination of expression (4.17) and (4.19).

It is proposed to compare the above limits with recommendations given by other investigators.

#### 4.6 Comparison of proposed ratios with existing recommendations

The recommendations currently available can be classified into three categories:

- (1) for torsion only
  - (2) for combined bending and torsion
- and (3) combined bending, torsion and shear.

Of these, the author intends to refer only to cases (1) and (2). Combined bending, torsion and shear is not treated in this thesis.

Comparisons will be made with recommendations suggested by the following:

- (1) Pure torsion case - Hsu<sup>(23)</sup> the Russian Code of Practice<sup>(6)</sup>, and Collins and Colleagues<sup>(4,42)</sup>.
- and (2) Combined bending and torsion - same as for torsion except recommendation of Hsu is omitted and addition of the suggestion of Lyalin<sup>(3)</sup>.

### 1. Pure torsion

Expressions (4.17), (4.19) or (4.28) require slight modification so that the ratios can be extended to the case of torsion only. This will be done by the consideration that, for pure torsion,  $\phi = 0$ , and substituting this value in expressions (4.17) and (4.19), the ratio reduces to

$$r = \frac{1}{(1+k)} \dots\dots\dots (4.29)$$

It is interesting to observe that the above expression can be obtained by slight modification of Cowan's recommendation<sup>(33)</sup>. Based on the argument that, shear reinforcement in the form of vertical stirrups must be supplemented by an equal volume of longitudinal steel uniformly distributed around the circumference to resist the horizontal component of the diagonal tension, he proposed the quantity of longitudinal steel as

$$A_L = A_T \frac{(b'+d')}{s} \dots\dots\dots (4.30)$$

The above expression is based on the assumption that, the stresses in the reinforcement in both directions are equal, and the author feels that the expression applies to this special case only.



If the difference in quality of steel used in both directions is considered, it becomes necessary to relate them by modifying the expression (4.30) as follows:-

$$A_L(f_L) = \frac{A_T(f_T)(b'+d')}{s} \dots\dots\dots (4.31)$$

$$\text{or } r = \frac{1}{(1+k)}$$

which is the same as expression (4.29).

Hsu<sup>(23)</sup> introduced a parameter "m", the value of which is given by the following and allowing for the different values of  $f_L$  and  $f_T$ ,

$$m = \frac{A_L(f_L)s}{A_T(f_T)(b' + d')} \dots\dots\dots (4.32)$$

$$= \frac{1}{r(1+k)} \dots\dots\dots (4.33)$$

The above expression is thus related to the ratio r used by the author.

The range within which this parameter may vary is given by Hsu as

$$0.7 < m < 1.5 \dots\dots\dots (4.34)$$

It is possible to use the above range to compare his

recommendation with that obtained by the author. To do this, the expression (4.33) is rearranged and the ratio  $r$  obtained as

$$r = \frac{1}{m(1+k)} \dots\dots\dots (4.35)$$

Introducing the range of expression (4.34) in the above expression, Hsu's recommendation amounts to the following:-

$$\frac{0.7}{(1+k)} < r < \frac{1.4}{(1+k)} \dots\dots\dots (4.36)$$

The above range and the proposal made in expression (4.29) are similar. In fact, expression (4.29) can be considered the mean value of expression (4.36). It is therefore felt that the author's recommendation may be considered acceptable.

Comparison of the recommendations of Hsu as in expression (4.36), the Russian Code of Practice and Collins and colleagues are plotted in Fig. 4.3. It can be observed that the author's recommendation is within the range suggested by other investigators.

## (2) Combined bending and torsion

Comparison of the author's proposal with recommendations

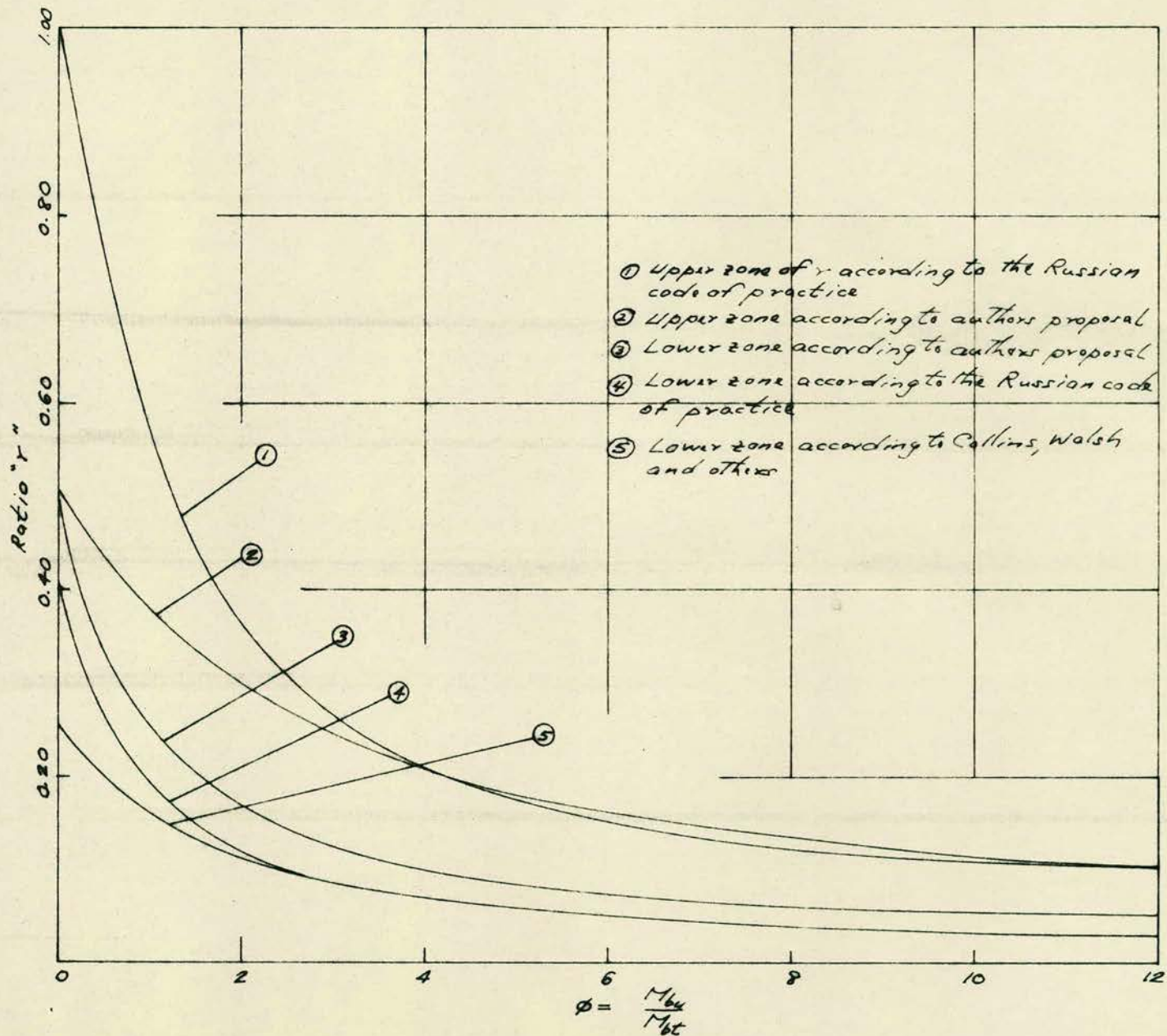


FIG 4.3- Comparison of authors  $r$  values with proposals of others for  $k=1.00$

of the Russian Code of Practice<sup>(6)</sup>, Collins and colleagues<sup>(4, 42)</sup> and Lyalin<sup>(3)</sup> are shown in Figs. 4.4, 4.5, 4.6 and 4.7 for  $\phi = 0$  to 12 with  $k = 1.0, 1.5, 2.0$  and  $2.5$ . The author's recommendation lies within the range of that suggested by other investigators and is therefore considered acceptable.

#### 4.7 Summary and conclusions

In this chapter, the author has made proposals for restricting the ratios of reinforcement for both pure torsion and combined bending and torsion.

By the use of the "force intensity method" and "internal couple method", the reinforcement may be limited as follows:-

- (1) the longitudinal steel is limited by expression (4.9) for combined bending and torsion.
  - (2) the minimum and maximum ratios of  $r$  may be given by expressions (4.17) and (4.19) respectively for combined bending and torsion.
- and
- (3) the minimum ratio  $r$  for pure torsion is given by expression (4.29).

The above proposals were compared with the existing recommendations and the close correlation shows that they may be considered acceptable for future use.

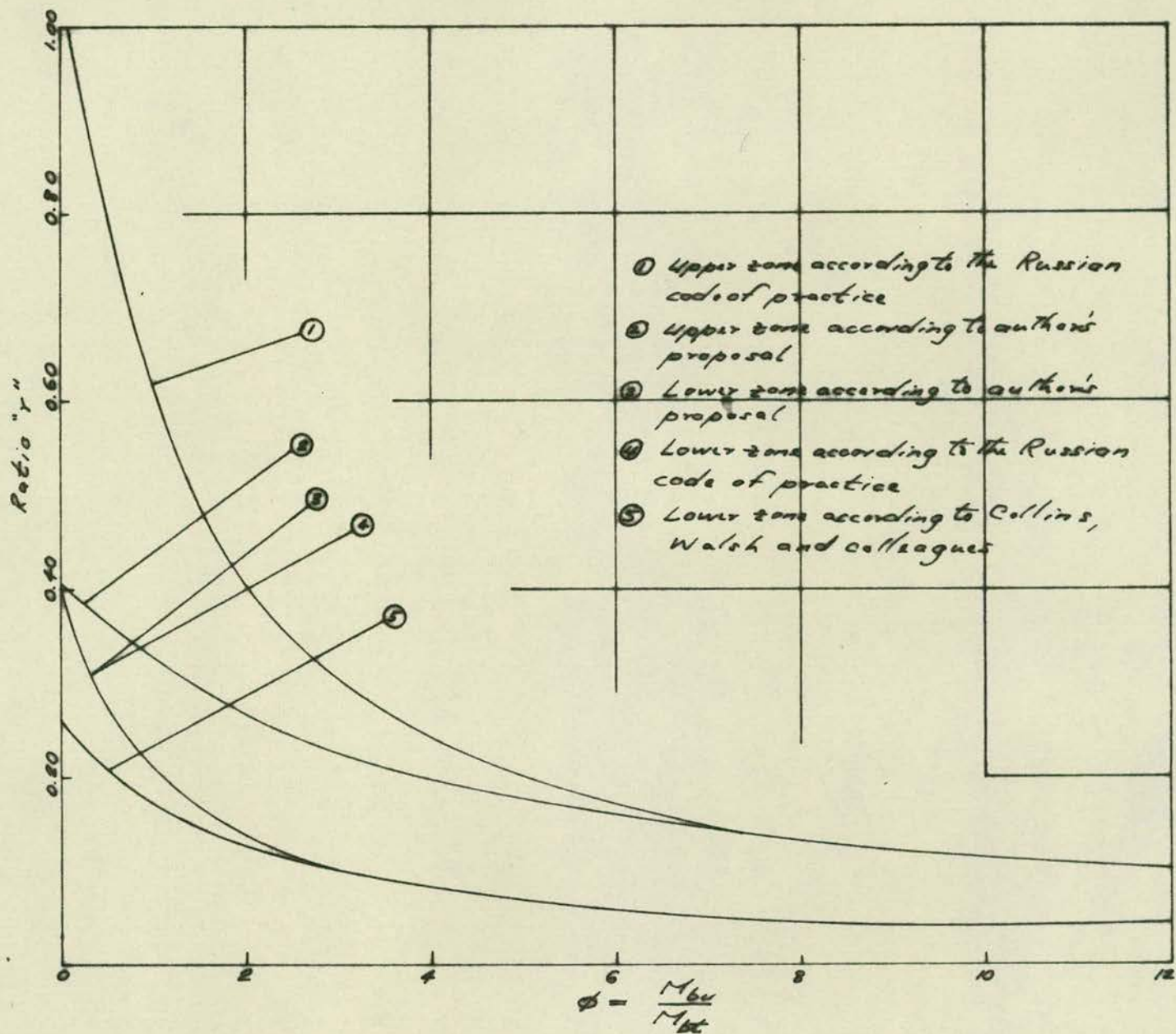


FIG. 4. 4 - Comparison of authors  $r$  values with proposals of others for  $k=1.50$

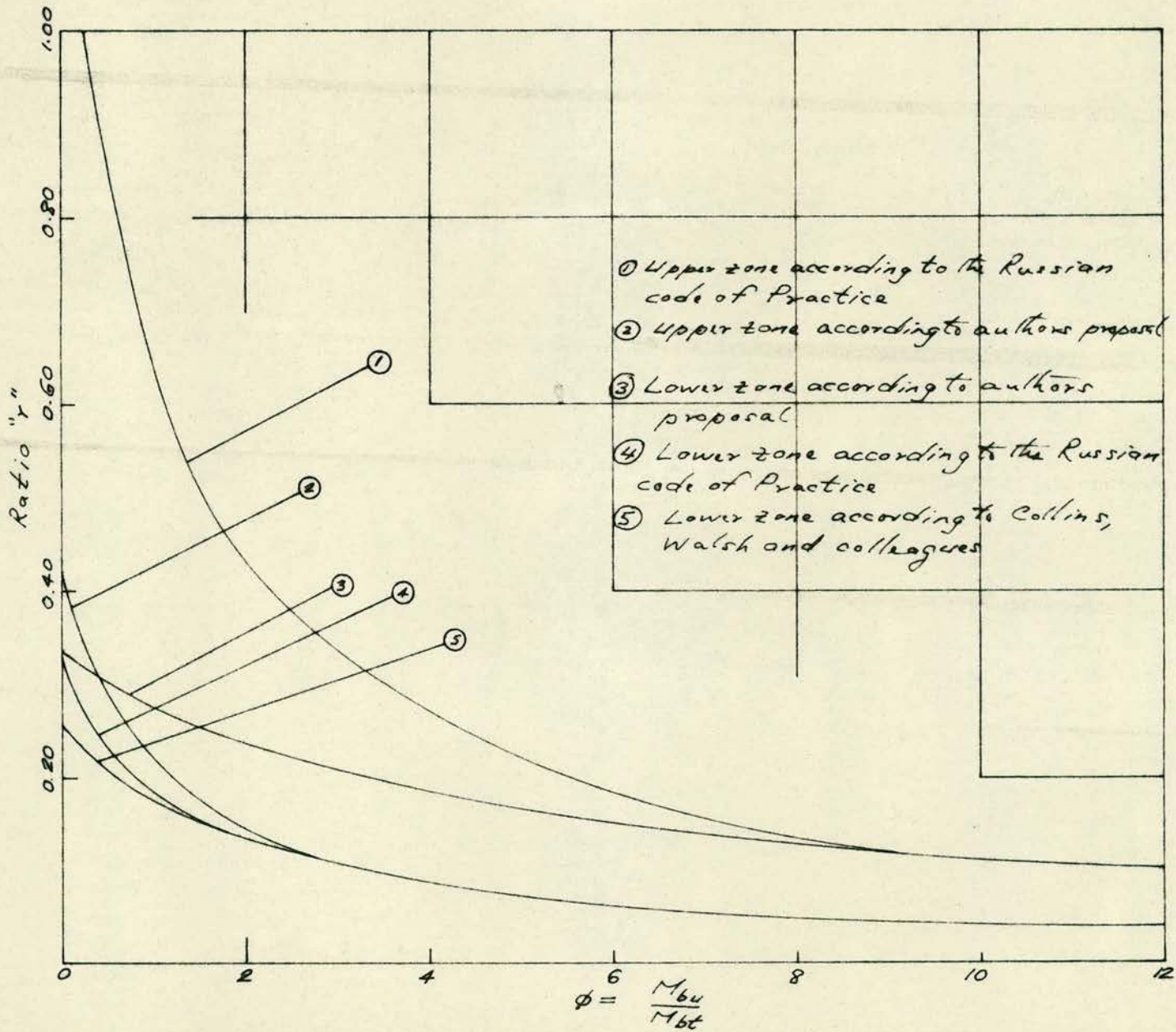


FIG 4.5- Comparison of authors' r values with proposals of others for k=2.00

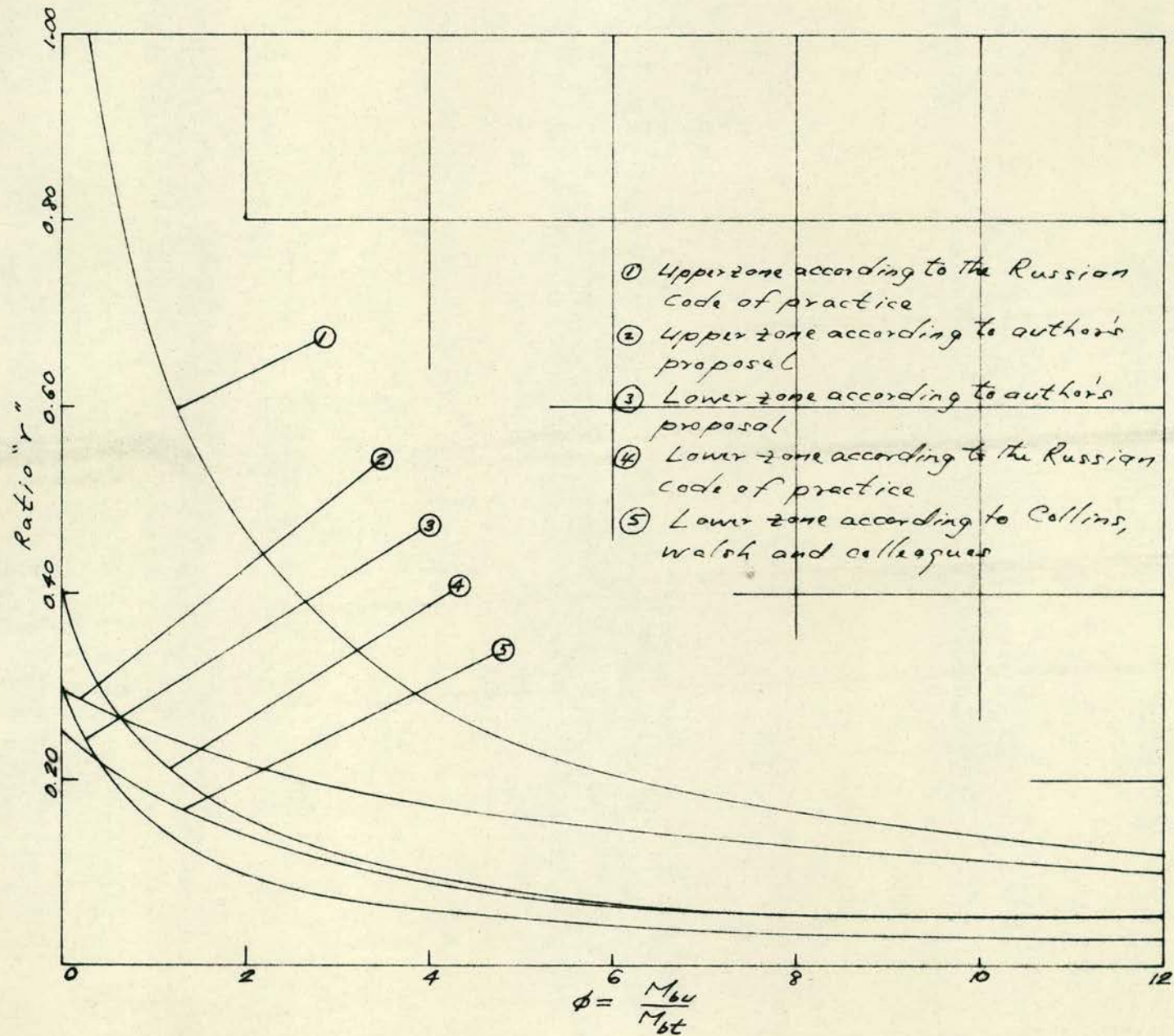


FIG 4-6 - Comparison of author's  $r$  values with proposals of others for  $k=2.50$

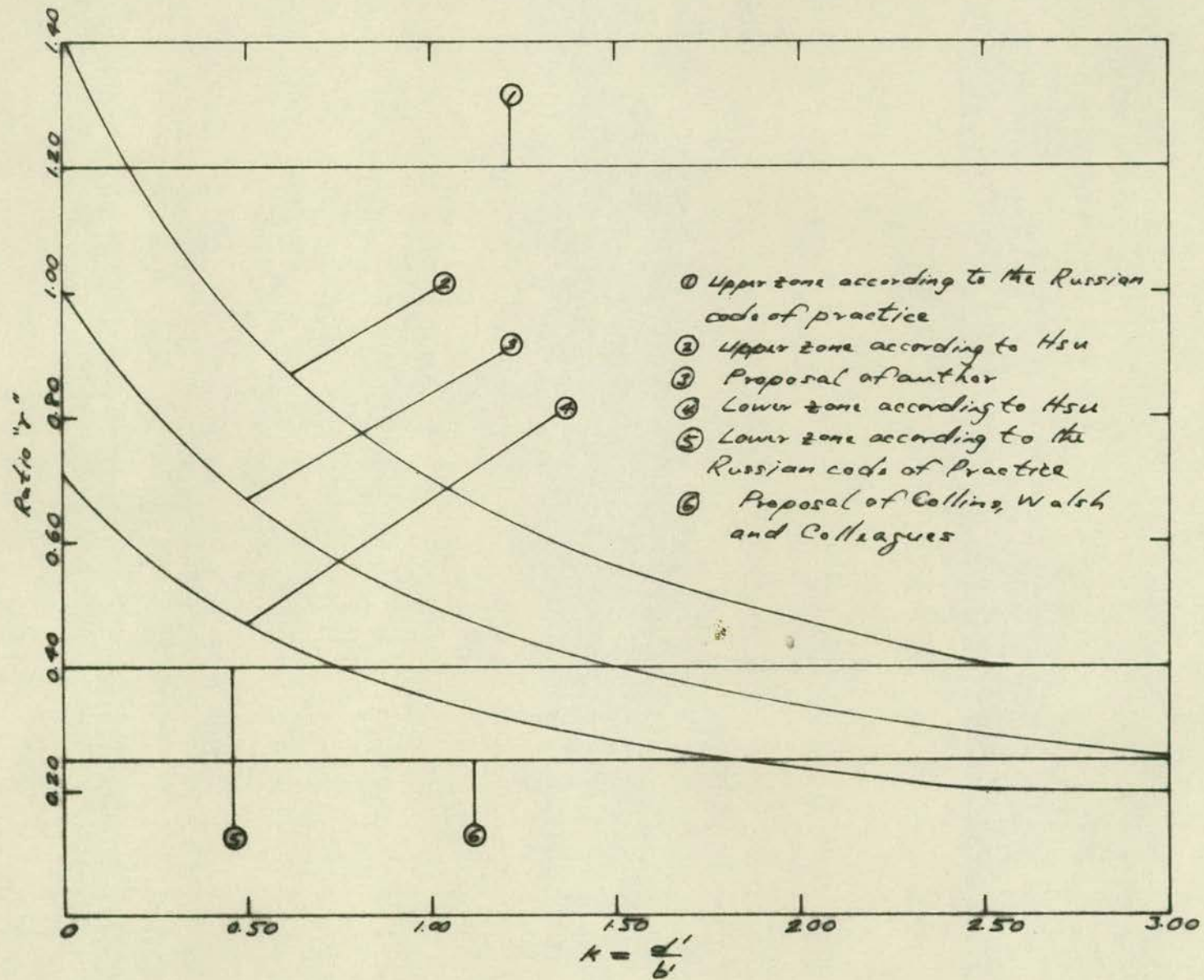


FIG 4.7- Comparison of authors  $r$  value for pure torsion with proposals of others



CHAPTER 5EXPERIMENTAL INVESTIGATION5.1 Introduction

Torsion often exists in a flooring system in conjunction with bending and shear, by the action of loads on secondary beams framing into a primary beam. This type of loading can be simulated in a structural laboratory to study the influence of torsion on the bending capacity of beams. The author has developed a technique for the above investigation and used it to investigate the behaviour and strength of fifteen reinforced concrete beams, subjected to combined bending and torsion. This chapter constitutes the analysis and discussion of the results obtained.

5.2 Object and scope of Investigation

The primary object of the investigation is to verify by experiment the ultimate moment equation developed by the author in chapter three and to study the action of the transverse binders.

The main variables considered are the ratios of bending moment to torque, and the spacing of the transverse binders.

5.3 Description of test specimens

The test programme consisted of tests on fifteen beam specimens grouped in five series as shown in Table 5.1. A typical specimen with dimensions and cross-section is shown in Fig. 5.1. It is in the form of part of a frame, consisting of two transverse arms connected to the longitudinal member which represents a girder with the transverse arms acting as secondary beams. By studying this type of configuration under load, the action of a beam in actual structures

Table 5.1 - Beam properties

Beam No.	$\phi$	Tie spacing ( $\frac{1}{8}$ " diam)	Steel ratio	
			p	r
K16	2.1	6 in. c/c	0.021	0.019
K13	2.1	3 in. c/c	0.021	0.039
K2/266	2.1	2.66 in. c/c	0.021	0.044
K11	2.1	1 in. c/c	0.021	0.116
K16	4.3	6 in. c/c	0.021	0.019
K13	4.3	3 in. c/c	0.021	0.039
K11	4.3	1 in. c/c	0.021	0.116
K16	5.6	6 in. c/c	0.021	0.019
K13	5.6	3 in. c/c	0.021	0.039
K11	5.6	1 in. c/c	0.021	0.116
K16	8.5	6 in. c/c	0.021	0.019
K13	8.5	3 in. c/c	0.021	0.039
K11	8.5	1 in. c/c	0.021	0.116
K2/200	11.8	2 in. c/c	0.021	0.058
K2/150	11.8	1.5 in. c/c	0.021	0.077

\*  $p = A_L/bd$

\*\*  $r = \frac{A_T f_T b'}{A_L f_L s}$

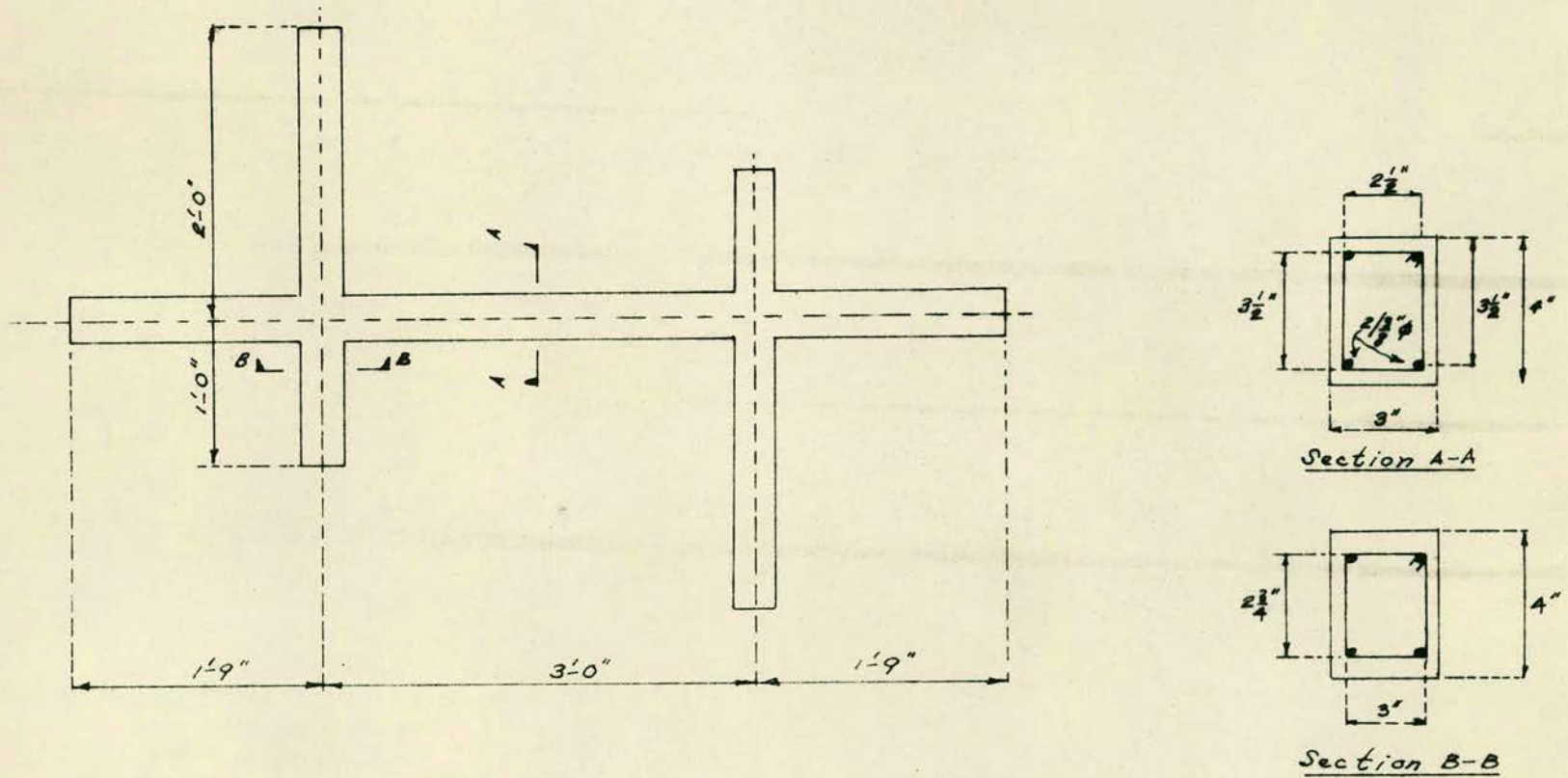


FIG 5.1- Dimensions of beam specimen and cross-sections

may be simulated and a study made of the effects of loading on the joints.

To enable the manufacture of three specimen for each mix, three moulds were designed and constructed. A typical mould is shown in plate 5.1.

The beam specimen contained four longitudinal steel bars placed at each corner of the rectangular beam and transverse binders in the form of closed vertical stirrups. With the exception of the effective length measuring 1'6", the stirrups were closely spaced to prevent any premature failure. The spacing varied from 6 inches to 1 inch, centre to centre, for each series as given in Table 5.1. The beams were denoted as K16, K13, etc., the first number representing the group and the second number the spacing for the binders. The testing of the beams was carried out using five  $\phi$  ratios, so that each  $\phi$  ratio represents a series.

#### 5.4 Description of Torsion bracket

A special feature of the testing programme is the need for placing the beam on the loading frame and simply-supporting it without endangering the end parts of the longitudinal member beyond the joints to the effects of combined bending, shear and torsion. This was done by the use of two specially-designed torsion bracket supports attached rigidly to the longitudinal member, allowing it to rotate both in the

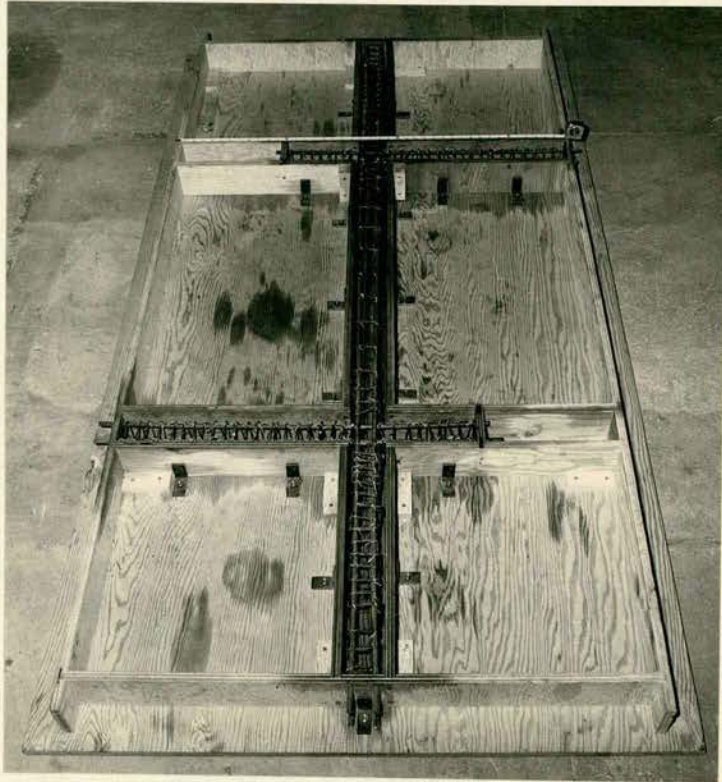


Plate 5.1

longitudinal and transverse directions. A photograph of the torsion bracket is shown in Plate 5.2.

#### 5.5 Materials and Fabrication of specimen

A considerable time was devoted to the sieving and analysis of the aggregate in order to ensure uniformity and consistency of the resulting concrete. The cement used was Ferrocrete and the aggregates consisted of 3/8" Eddlestone.

The graph of McIntosh and Erntroy<sup>(30)</sup> was used for the design of the mix to attain a concrete strength at twenty-eight days of 6000 psi. The concrete was manufactured in a "Cum-flow" type mixer of two cubic feet capacity by mixing for two minutes and then poured and vibrated into the moulds. Three specimen and three control cubes were cast at each concreting. The specimen were then cured by placing them under wet burlap for seven days to simulate actual conditions in practice, while the cubes were transferred to the curing tank where they were kept for twenty-eight days.

In order to ensure failure of the test specimen by yielding of the reinforcement, it is essential for the steel to possess sufficient yield range at constant yield stress. Black mild steel has been found to be suitable for this purpose<sup>(10)</sup>. Unfortunately, at the time of preparing the test specimen, the author could not obtain this type of steel for the longitudinal

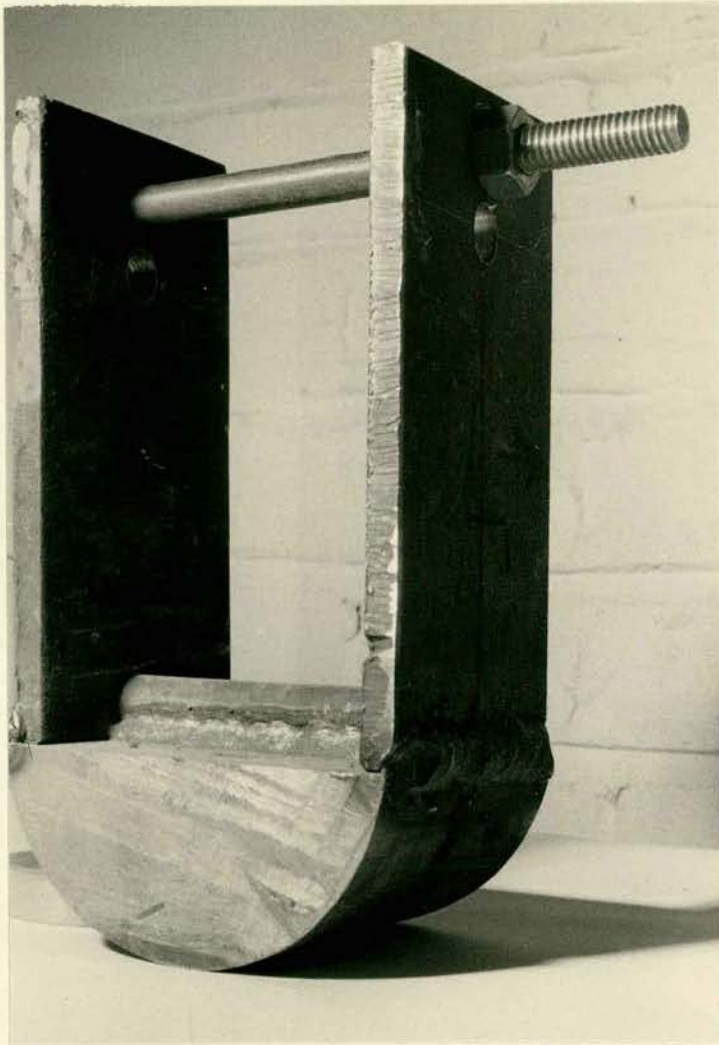


Plate 5.2

bars and cold-worked mild steel had to be used. On testing the sample, the steel was found to possess sufficient yield range for use in the beams. The transverse binders consisted of bright mild steel annealed at 900°C. The yield stresses of the longitudinal and transverse steel were found to be 40,000 psi and 34,000 psi respectively.

It was essential to maintain equal dimensions for the reinforcing cage in order to maintain a constant ratio of k. Therefore, extreme care was taken in bending the stirrups and then tying them to the longitudinal bars with soft wire. The alignment of the reinforcement in the mould was again adjusted before and while concreting.

5.6 Test arrangement and procedure

The loading frame used for testing of the beam specimens is shown in Fig. 5.2 and consisted of two horizontal girders spaced at 6'0" c/c and another girder placed between them for supporting the loading jack.

The configuration of the beam specimen was specially chosen and designed to enable the application of combined bending and torsion within the effective length by a system of spreader beams as shown in Fig. 5.3. It can be seen that by varying the position of the main loading beam resting on the two transverse beams, the ratio of bending moment to torque can be varied. The



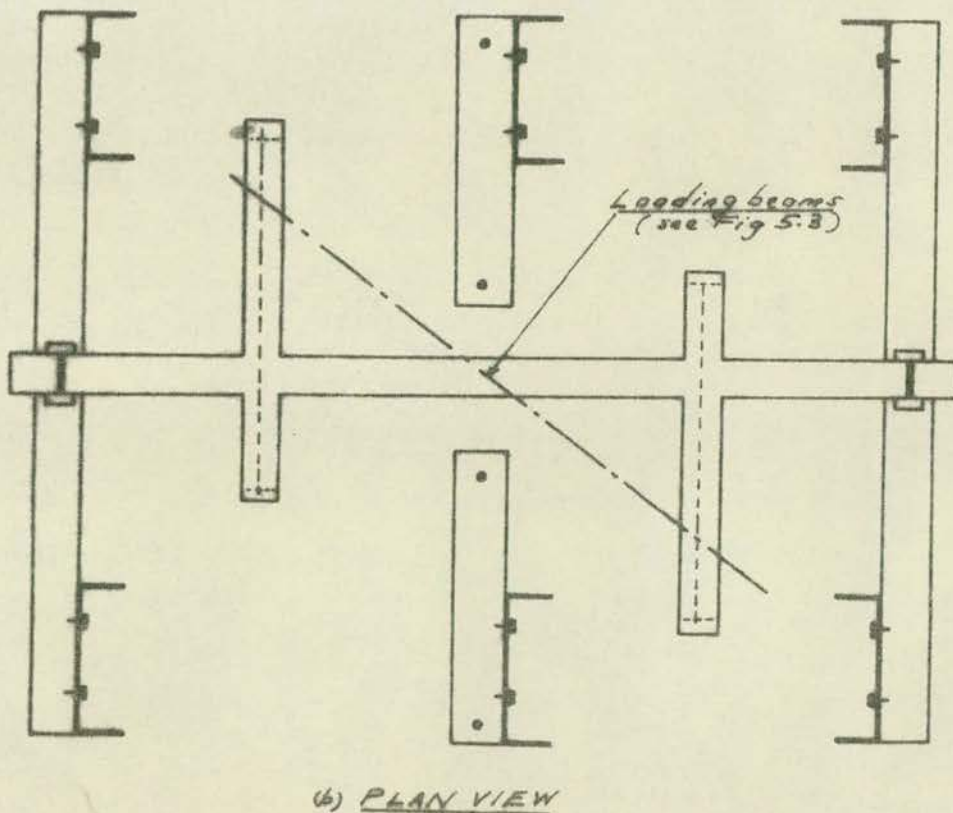
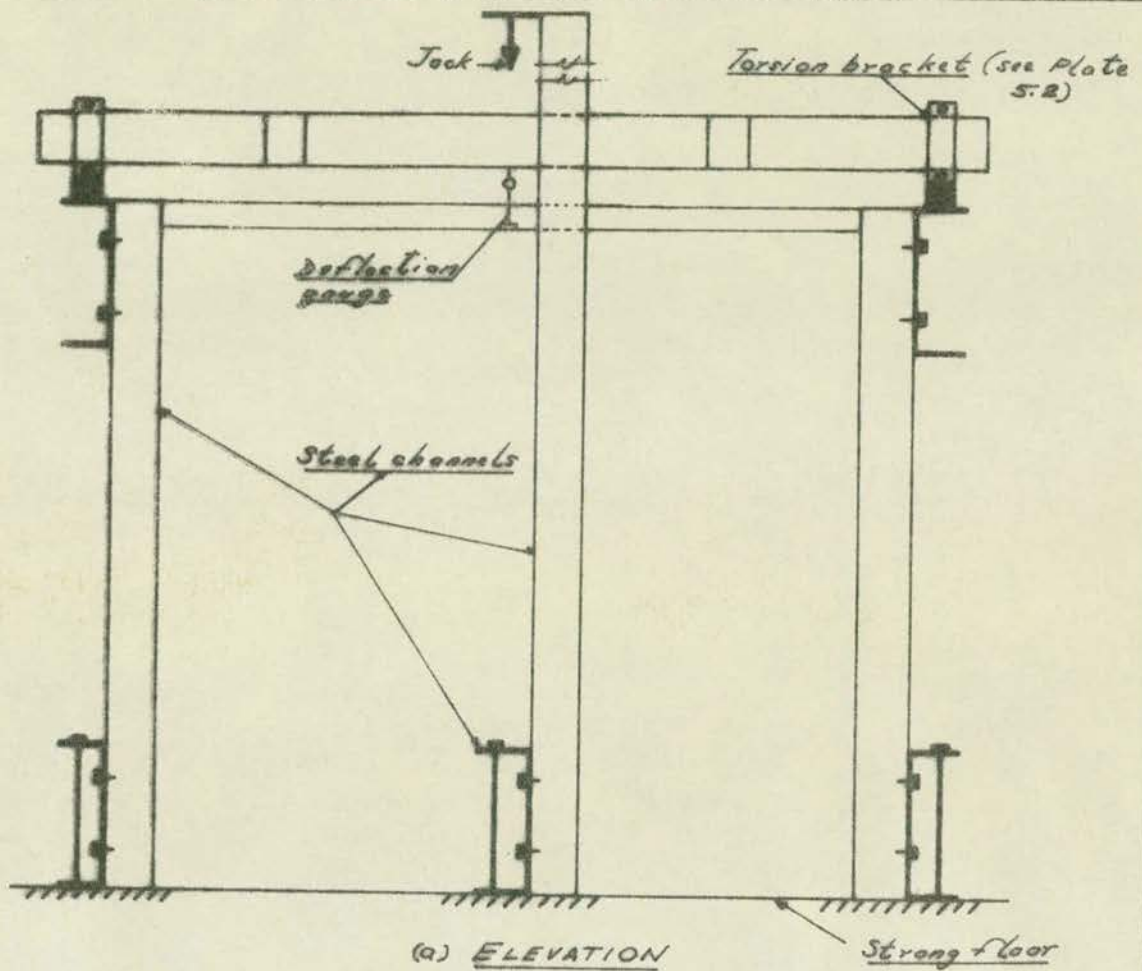


FIG 5.2 - Loading frame

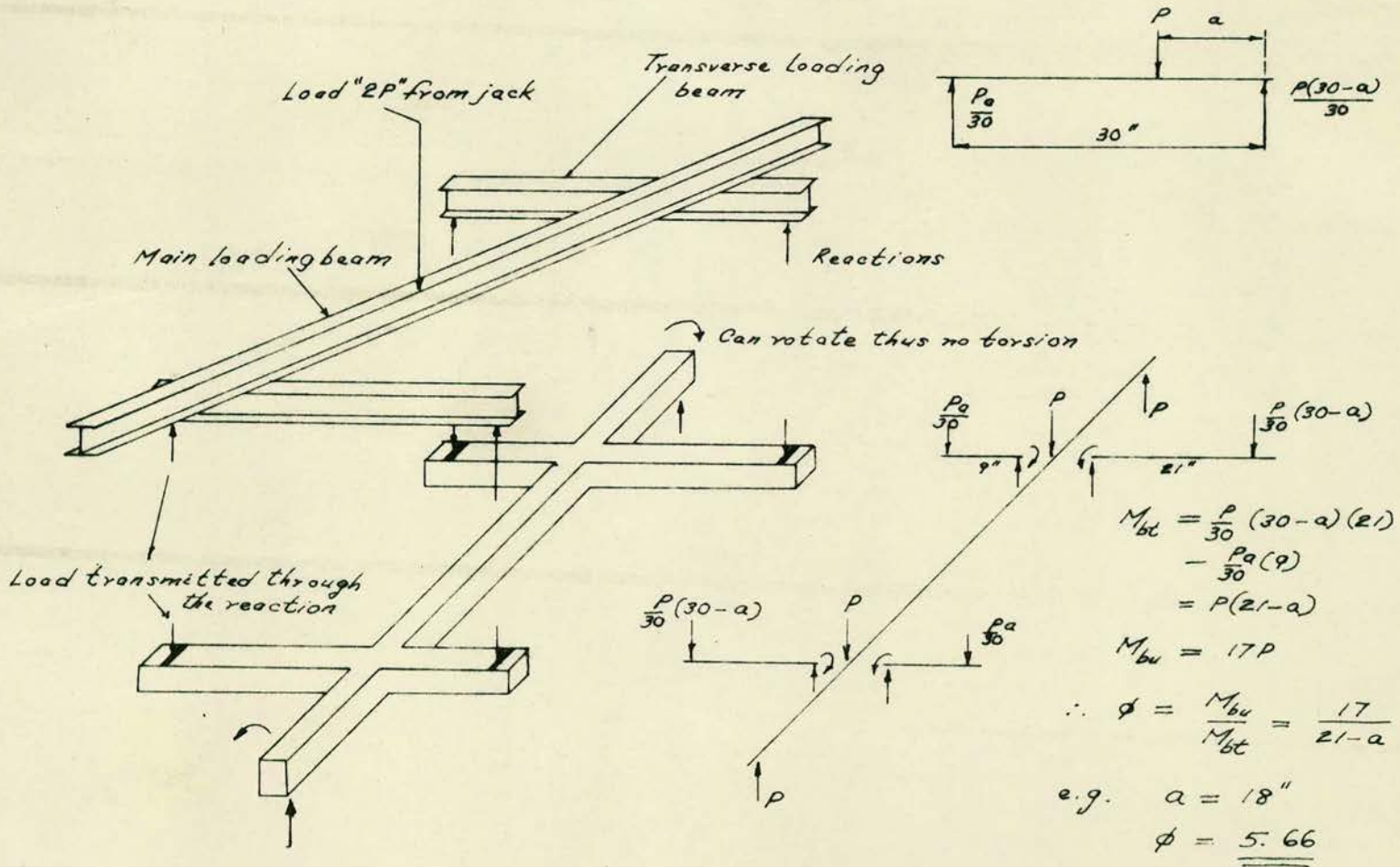


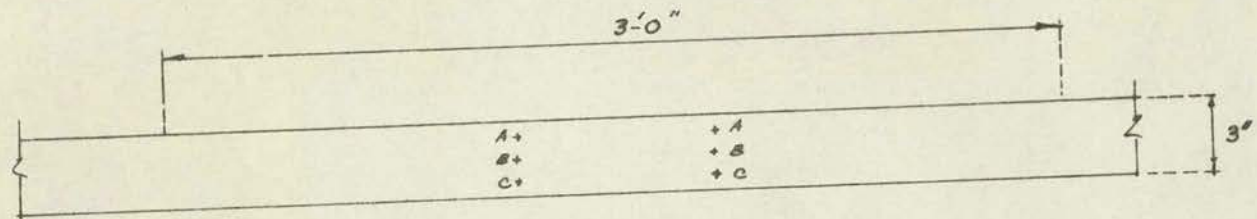
Fig. 5.3 - System of spreader beams

The equation for finding the exact ratio  $\phi$  is given in the Figure.

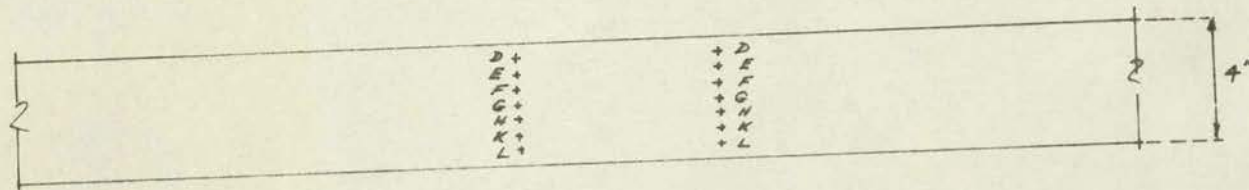
Preparation of the test specimen for testing consisted essentially of the following:- (1) positioning and fixing of the demec points on to the surface of the beams as shown in Fig. 5.4, (2) attaching the torsion bracket supports to the longitudinal member, (3) placing the test specimen on the loading frame, (4) arrangement of the spreader beams on the test beam, and (5) placing the dial gauges for measurement of the deflections.

The load was applied through hydraulic rams connected to a Losenhausenwerk machine and of capacity of 20 tons. In this programme, the loading was adjusted to attain a maximum of five tons. The position of the dial-gauges with a beam in position for testing is shown in Plate 5.3 as well as the location of the loading beams and jack.

The number of load increments in each test varied from 8 to 16, depending on the ratio of bending moment to torque so that the magnitude of each increment varied between 0.10 and 0.15 ton. Load was applied to the beam up to the collapse stage, and after each load stage, readings of dial-gauges and demec points were recorded. The sequence of recording the results consisted generally of, the taking of the dial-gauge readings, then, observing the recording the crack-propagation, then reading the demec



(a) Top face



(b) Front face

FIG 5.4 - Position of demec points

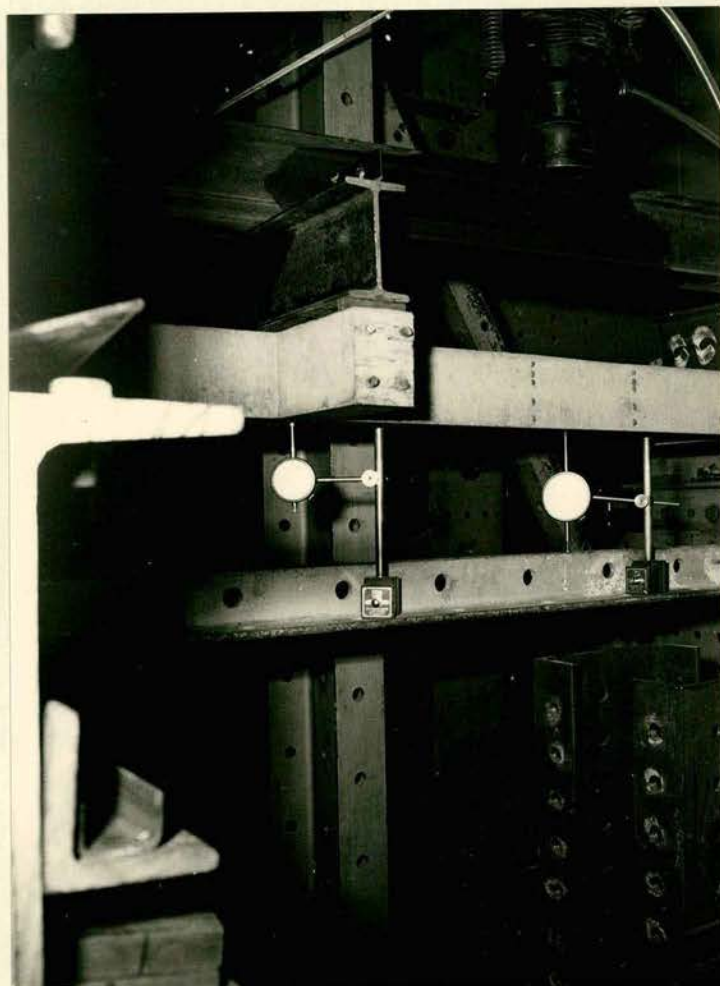


Plate 5.3

points and finally, reading dial-gauges again. The whole process for each load stage generally took from three to five minutes.

### 5.7 Experimental results

The main results of the experiments are listed in Tables 5.2, 5.3, and 5.4.

### 5.8 Analysis and discussion of results

#### 5.8.1 Development of Cracks

As shown in previous investigations<sup>(9,10,12,13,14,15)</sup>, and for all the beams tested in this study, the cracks originated at the bottom edge where flexural tension is a maximum. These cracks widened on further loading, spreading diagonally sideways, both in the horizontal and vertical direction. More cracks then appeared at the bottom, crossing the whole width of the beam, and emerged at the two edges and propagated upwards on the vertical faces.

The inclination of the cracks with respect to the axis of twist was found to be similar on the three faces of the beams tested with similar ratios of  $\phi$ , the magnitude of the angle varying with  $\phi$ . It was found that the angle was close to 45 degrees for low ratios, increasing with  $\phi$  and becoming almost vertical for large ratios. Typical crack patterns for beams tested with different values of  $\phi$  are shown in Plates 5.4, 5.5, 5.6, 5.7 and 5.8 and it can be seen that for low ratios of  $\phi$  the path of cracks traced is essentially a straight line right

Table 5.2 - Ultimate Strength

Beam No.	$\phi$	Cube Strength* (ksi)	Ultimate Moment** (kip-in)	
			$M_{bu}$	$M_{bt}$
K16	2.1	7.03	10.70	5.10
K13	2.1	7.03	13.80	6.57
K2/266	2.1	6.04	16.85	8.02
K11	2.1	7.03	18.00	8.57
K16	4.3	6.99	27.90	6.49
K13	4.3	6.99	24.60	6.19
K11	4.3	6.99	27.40	6.37
K16	5.6	8.12	24.60	4.39
K13	5.6	8.12	25.40	4.54
K11	5.6	8.12	24.50	4.38
K16	8.5	7.23	27.20	3.20
K13	8.5	7.23	25.40	3.00
K11	8.5	7.23	27.20	3.20
K2/200	11.8	6.04	29.90	2.53
K2/150	11.8	6.04	29.90	2.53

\* average of three cubes

\*\* yield values

Table 5.3 Concrete strains measured at the top face

Beam No.	$\phi$	Cube Strength (psi)	Compressive Strain	
			at Yield	Collapse
K16	2.1	7030*	0.0005**	-
K13	2.1	7030	0.0009	-
K2/266	2.1	6040	0.0004	0.0004
K11	2.1	7030	0.0007	0.0007
K16	4.3	6990	0.0008	0.0008
K13	4.3	6990	0.0010	0.0010
K11	4.3	6990	0.0013	0.0013
K16	5.6	8120	0.0010	0.0010
K13	5.6	8120	0.0010	0.0013
K11	5.6	8120	0.0017	0.0017
K16	8.5	7230	0.0015	0.0037
K13	8.5	7230	0.0009	0.0029
K11	8.5	7230	0.0013	0.0058
K2/200	11.8	6040	0.0011	0.0051
K2/150	11.8	6040	0.0011	0.0035

\*average readings at three positions.

\*\* average of strains measured on the compressive side.



Table 5.4 - Principal concrete strains measured at the center\* of beam faces for  $\phi = 2.1$

Beam No.	Horizontal face		Vertical face	
	Tension	Compression	Tension	compression
K16	0.00037*	0.00112	0.00226	0.00057
K13	0.00045	0.00161	0.00069	0.00112
K11	0.00042	0.00114	0.00228	0.00074

\* average readings at three positions.





up to the top edge, while for large values, the path deviates in a curve at about mid-height, with decreasing slope towards the longitudinal axis. Similar observations have been reported by previous investigators<sup>(9,14,15,16,18)</sup>, and in particular, Evans and Sarkar<sup>(9)</sup> assumed the deviated angle as  $45^\circ$ . A possible reason for this crack-behaviour is that there is a position at which the distribution of flexural stresses changes from tension to compression. The neutral axis represents this transition zone so that the flexural stresses at this level are nil and therefore only the torsional stresses are acting hence the tendency for the cracks to deviate at a  $45^\circ$  angle. As the load increases towards the failure stage, the location of the neutral axis also rises and therefore the continuity of the  $45^\circ$  inclination is maintained.

Another interesting observation concerning the crack is the tendency for the cracks to reverse as the failure load is reached. This can be seen in Plates 5.5, 5.9, 5.10, 5.11 and 5.12, resulting in slicing off pyramidal shapes of concrete on the upper face. This process was also observed by Gesund and Boston<sup>(20)</sup>.

The influence of  $\phi$  on the rate of crack propagation

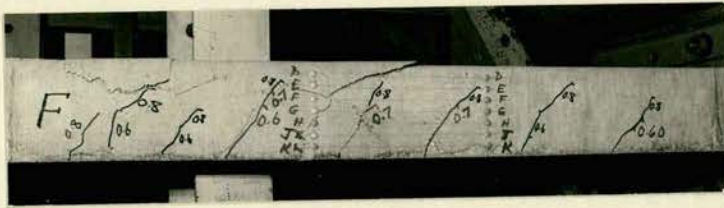


Plate 5.9

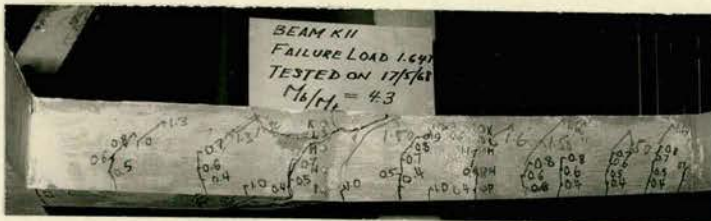


Plate 5.10

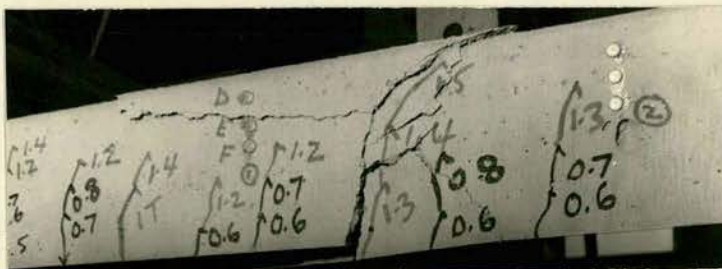


Plate 5.11



was significant. For low ratios, the rate was rapid, for example  $\phi = 2.1$ ; the cracks reached the top face within a few increments beyond the cracking stage. This observation is similar to the report of Chinenkov<sup>(12)</sup> who attributed the phenomena to the rapid rate of stressing and therefore the rapid straining of the reinforcement, resulting in an immediate widening of the cracks. The rate was relatively slow for large values of  $\phi$ , for example,  $\phi = 8.5$ ; for this ratio and higher, the crack movement was not noticeable in some cases, and the cracks tended to remain localized below the top edge even at the collapse stage. The author believes that this is due to the considerable compressive stress of the concrete which restrains or delays the movement. Another possible explanation is that the test beams used in this programme were so under-reinforced that the depth of the compression block was considerable. The beams may have been in compression up to about the mid-point or lower, with the result that the propagation of the cracks in the vertical direction was delayed or slowed down and the torsional stresses are not sufficiently large to crack the beam. The final result is to reduce the slope of the path of cracks from its original straight line to a curve.

The influence of the mechanical properties of the steel, particularly in the yield range is significant. The steel used in this study did not possess sufficient yield plateau to allow inelastic deformation to occur and in the author's opinion, the steel was in the strain-hardening range when failure occurred as suggested by the badly-deflected condition of the beam shown in Plate 5.13.

The general weakness of the reinforcement in the transverse direction influenced the extent of cracking of beams, especially at the lower range of the ratio. For example, beams tested at  $\phi = 2.1$  and  $\phi = 4.3$  failed as a result of extensive cracking. This can be seen from Plates 5.14, 5.15, 5.16 and 5.17 which show the condition of the beams tested at  $\phi = 2.1$ . The weakness of this reinforcement may be discussed from two aspects: first, from the point of view of spacing and second, the cross-sectional area. A possible effect of inadequate spacing of the binders is the development of diagonal cracks between the stirrups precipitating failure to occur as in the case of beam K16 tested at  $\phi = 2.1$  or beam K16 tested at  $\phi = 5.6$  which can be considered a relatively high ratio. The condition of the beam K16 tested at  $\phi = 5.6$  is shown in Plate 5.18. The beam may also fail as a result of the reversed movement of the vertical cracks and splitting of the concrete along







Plate 5.18



Plate 5.19

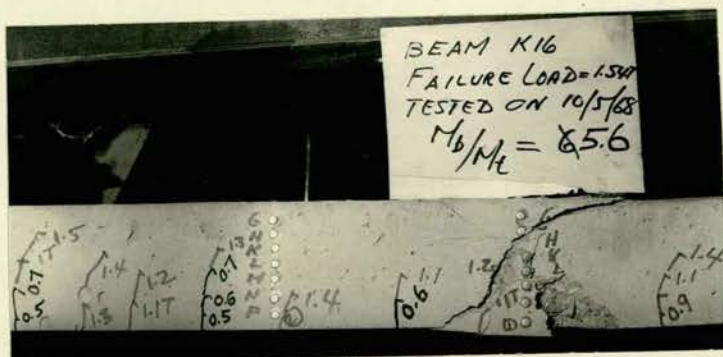


Plate 5.20

the tensile steel at the bottom as shown in Plates 5.16, 5.19 and 5.20. This type of failure is similar to that caused by combined bending and shear as observed by Neville<sup>(19)</sup>.

By the use of closer spacing of the binders, this type of failure can be prevented. The recommendations of Zia<sup>(22)</sup>, Hsu<sup>(23)</sup> and Mattock<sup>(24)</sup> are relevant in limiting the maximum spacing of the binders. On the other hand, the recommendation of the British Code of Practice<sup>(21)</sup> is considered relevant for the behaviour of beams K13 and K2/266 which are shown in Plates 5.9 and 5.15. In the first case, the beam is extensively cracked while the later may be considered comparatively intact. The spacing for the later was limited by the use of the British Code<sup>(21)</sup>. The condition of this beam suggests that the provision in the Code is adequate, but further testing is required to confirm this aspect. The author believes that beam K13 failed due to excessive straining of the binders and the prevention of this condition can be achieved by using binders with larger cross-sectional area, so that the possibility of failure due to inadequate transverse reinforcement is eliminated.

#### 5.8.2 Mechanism of Failure

The basic mechanism of failure for the beams tested in this study consisted of the rotation of the whole beam about the compression hinge on the upper face at the collapse stage.

Typical examples of these compression zones are shown in Plates 5.21, 5.22, 5.23 and 5.24. It can be seen that the compression zone is inclined at an angle to the longitudinal axis in each case.

For all the beams tested, except beams K16 and K13 tested at  $\phi = 2.1$ , failure was always preceded by yielding of the reinforcement. The weakness of the steel in the transverse direction forced yielding to occur in this direction first, followed by yielding of the longitudinal steel. Up to and including the ratio  $\phi = 5.6$ , the beams failed immediately after the longitudinal steel stress reached the yield value, while the failure of beams tested at  $\phi = 8.5$  and higher were gradual and the margin of loads carried beyond the yield range was considerable.

Failure of beams K16 and K13 took place as soon as the vertical cracks reached the top edge. The failure was sudden and crushing of the concrete was observed in both cases. The condition of the top zone is shown in Plates 5.25 and 5.26. The formation of a diagonal crack between the transverse binders and its extension into the compression zone brought about failure of beam K16 so that the longitudinal steel did not reach its yield stress. It is interesting to note in Plate 5.19 that

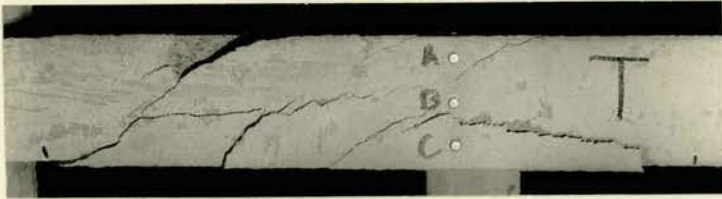


Plate 5.21

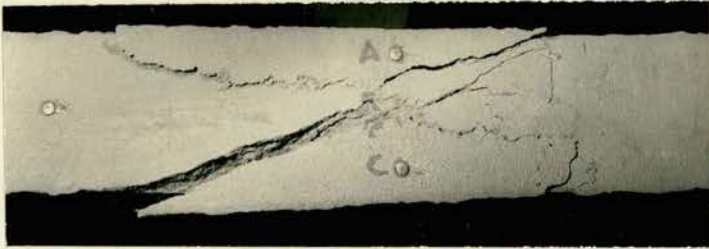


Plate 5.22

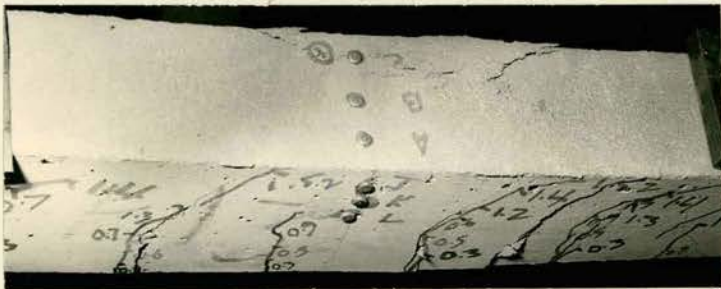


Plate 5.23



Plate 5.24



Plate 5.25



Plate 5.26

rotation took place about the vertical side of the crack surface. This behaviour is thought similar to that observed by Hsu<sup>(25)</sup> for plain concrete beams subjected to pure torsion.

On the other hand, beam K13 failed as the result of inadequate transverse reinforcement. The extensive cracking and widening on the vertical side as shown in Plate 5.15 indicates that the yield stress may have been exhausted. Failure occurred when the potential torsional resistance of the beam was exceeded. There was no sign of yielding of the longitudinal bars.

The mechanism of failure of beams K2/266 and K11 tested at  $\phi = 2.1$  may be considered similar to the three beams tested at  $\phi = 4.3$ . In all cases, the failure took place as soon as the yield stress was attained by the reinforcement and failure was sudden with considerable crushing on the upper face. Typical conditions of this zone are shown in Plates 5.21 and 5.22. The author believes that failure occurred when the reinforcement in both directions reached the yield value, thus imposing excessive compressive and tensile stresses at the compression zone where flexural compression existed as well. The depth of the compression zone is small in this range of  $\phi$ , and thus, the position of the neutral axis plane is near the top edge. The transition from tension below to compression zone is

very small, which means that it is difficult to restrain the vertical cracks from moving up. When the longitudinal steel reaches its yield stress, the short inelastic deformation is sufficient to push the cracks immediately onto the upper face. The maximum compressive stress exceeded the maximum compressive strength of the concrete and failure occurred suddenly. Considerable crushing of the top face can be observed in Plate 5.22. There is an indication of cleavage failure and in the author's opinion this was due to the tensile stress at that point exceeding the tensile strength of the concrete. In addition the evidence shown by McHenry and Karni<sup>(29)</sup> indicates that the presence of combined compression and tension reduces the tensile strength of the concrete. The crack pattern in the compression zone, as shown in Plate 5.22, is similar to that described and obtained by Goode and Helmy<sup>(17)</sup>.

The behaviour and failure mechanism for beams tested at large values of  $\phi$  differ from those tested at low ratios; crushing of the concrete generally takes place at collapse and the orientation of the compression zone is well-defined. A typical example is shown in Plate 5.27. There is distinct evidence of cleavage failure which must have occurred after crushing took place. Due to the short yield range of the longitudinal steel used in these tests, the stress in the steel bar





Plate 5.27



Plate 5.28

is in the ultimate range at the ultimate load and therefore the load taken by the beams tested at  $\phi = 8.5$  and  $\phi = 11.8$  far exceeds the yield load.

A peculiar phenomena was observed in the test of beam K16 at  $\phi = 5.6$ . It was found that at failure the vertical cracks reversed and curved in the direction of the longitudinal steel, splitting the concrete along this direction. This type of splitting can initiate failure and therefore closer spacing of the binders is essential to prevent them.

The beams K2/150 and K2/200 tested at  $\phi = 11.8$  both failed at the joints as shown in Plate 5.28. The failure was caused by the combined action of bending, shear and torsion concentrated at the joint. There is a possibility that this type of failure will occur in actual structures such as at the girder-beam connections. Further investigation is necessary to avoid such failures.

### 5.9 Deformations

Typical load-deflection curves are shown in Figs. 5.5, 5.6, 5.7, 5.8 and 5.9. The first three graphs illustrate the influence of  $\phi$  on the deflection, the fourth graph shows the effect of spacing of binders for beams tested at  $\phi = 2.1$  and the final graph gives a comparison for similar beams tested at

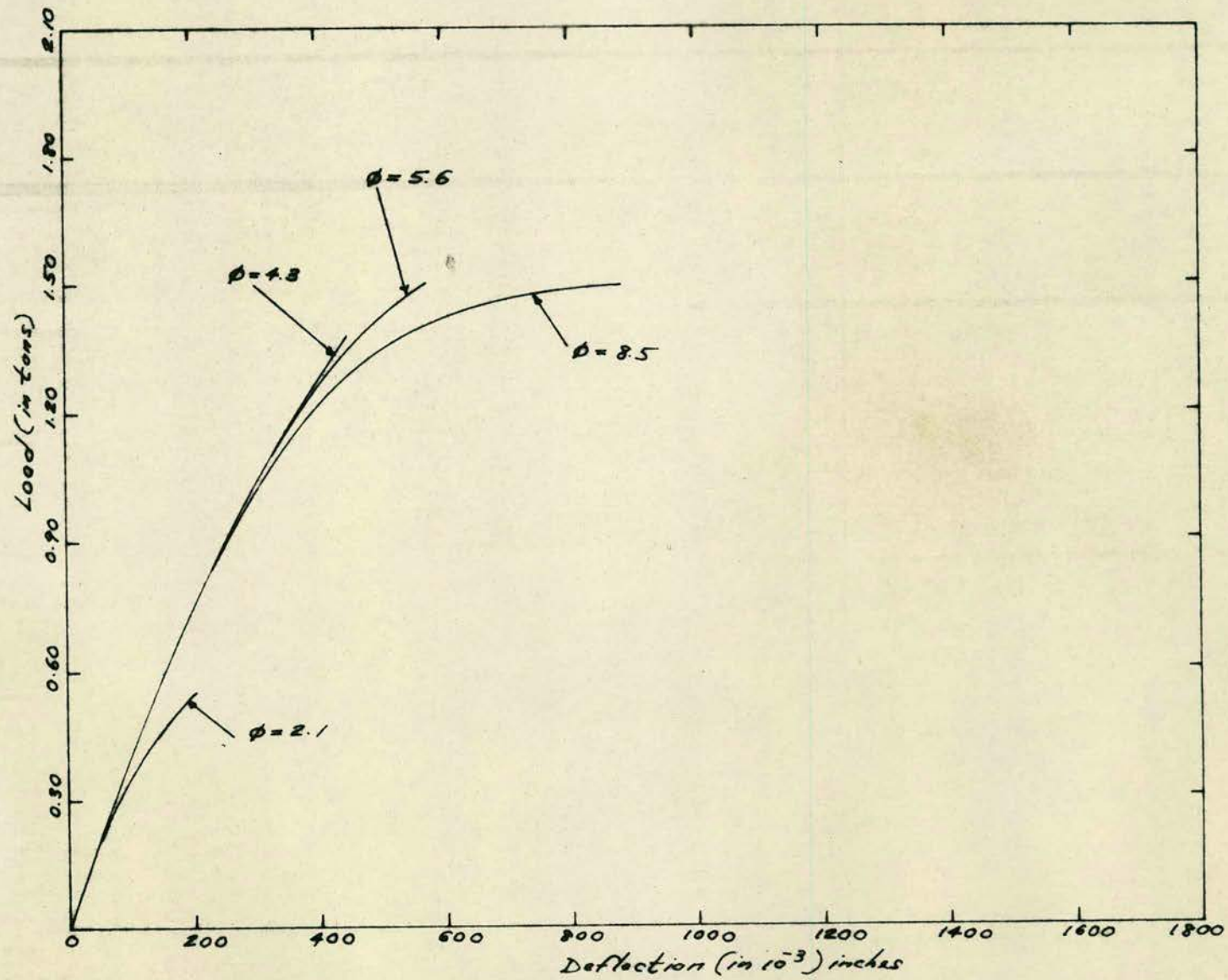


FIG 5.5- Load-deflection curves for beam No. K16 with variation of  $\phi$

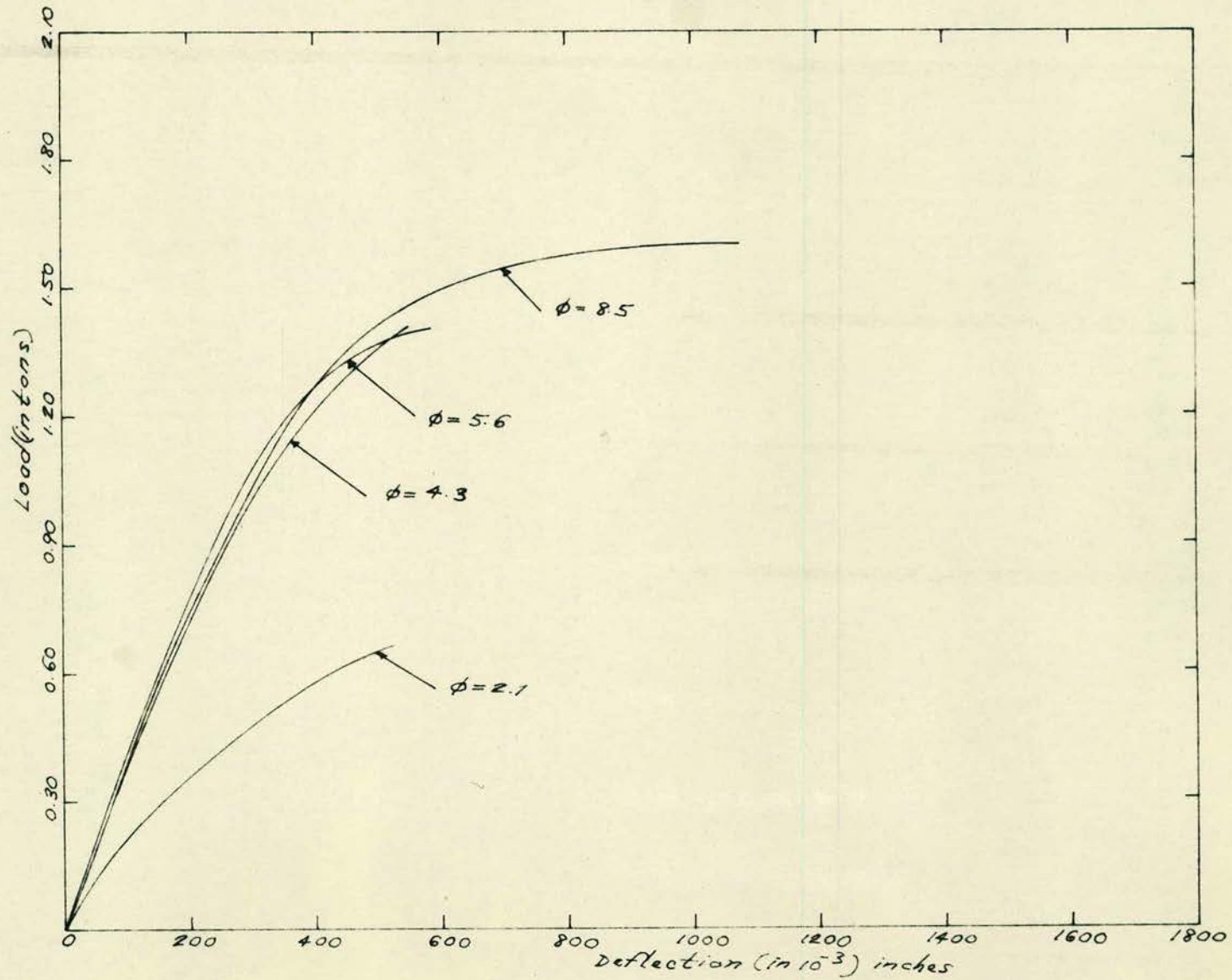


FIG 5.6 - Load-deflection curves for beam No. K13 with variation of  $\phi$

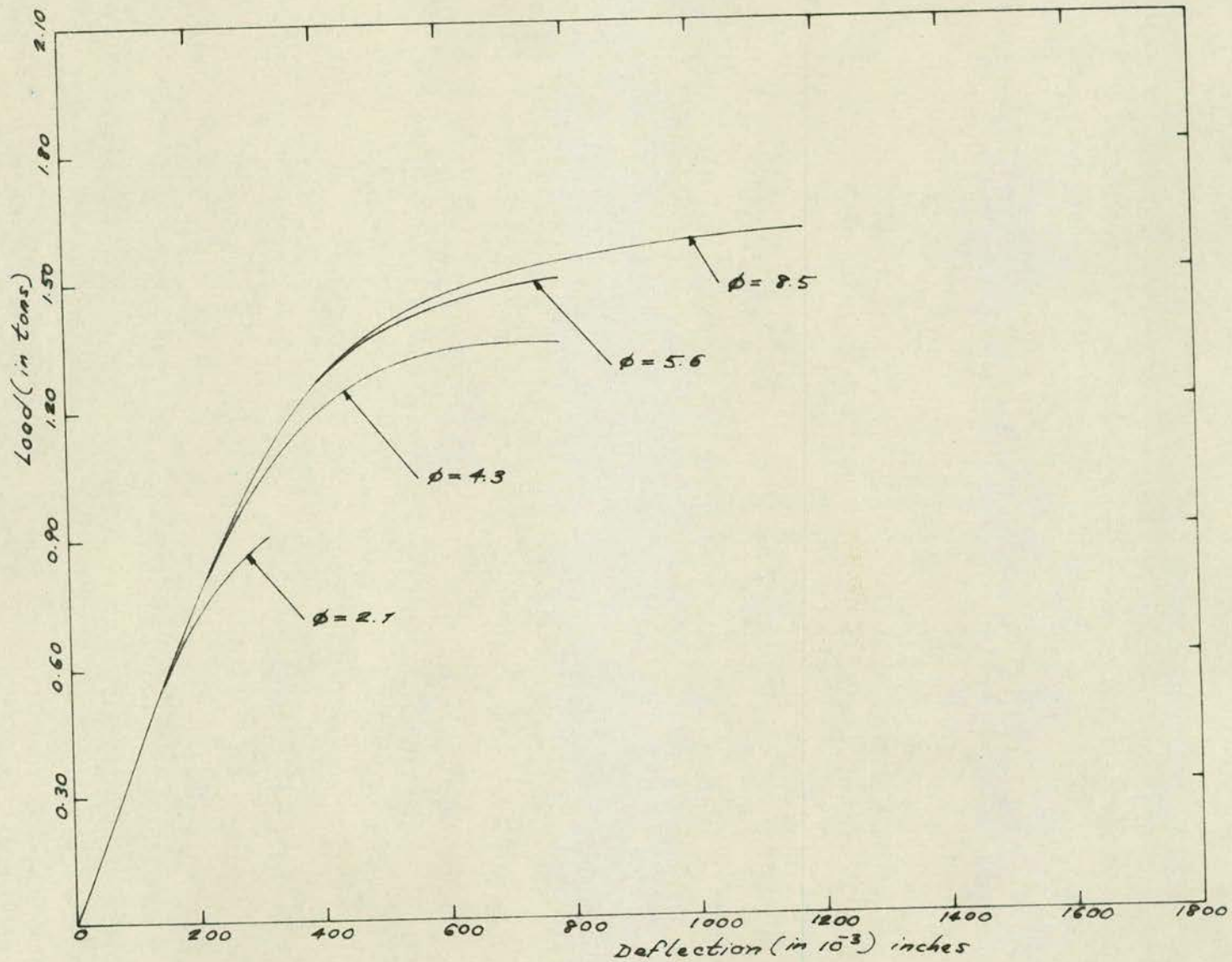


FIG 5.7- Load-deflection curves for beam No. K11 with variation of  $\phi$

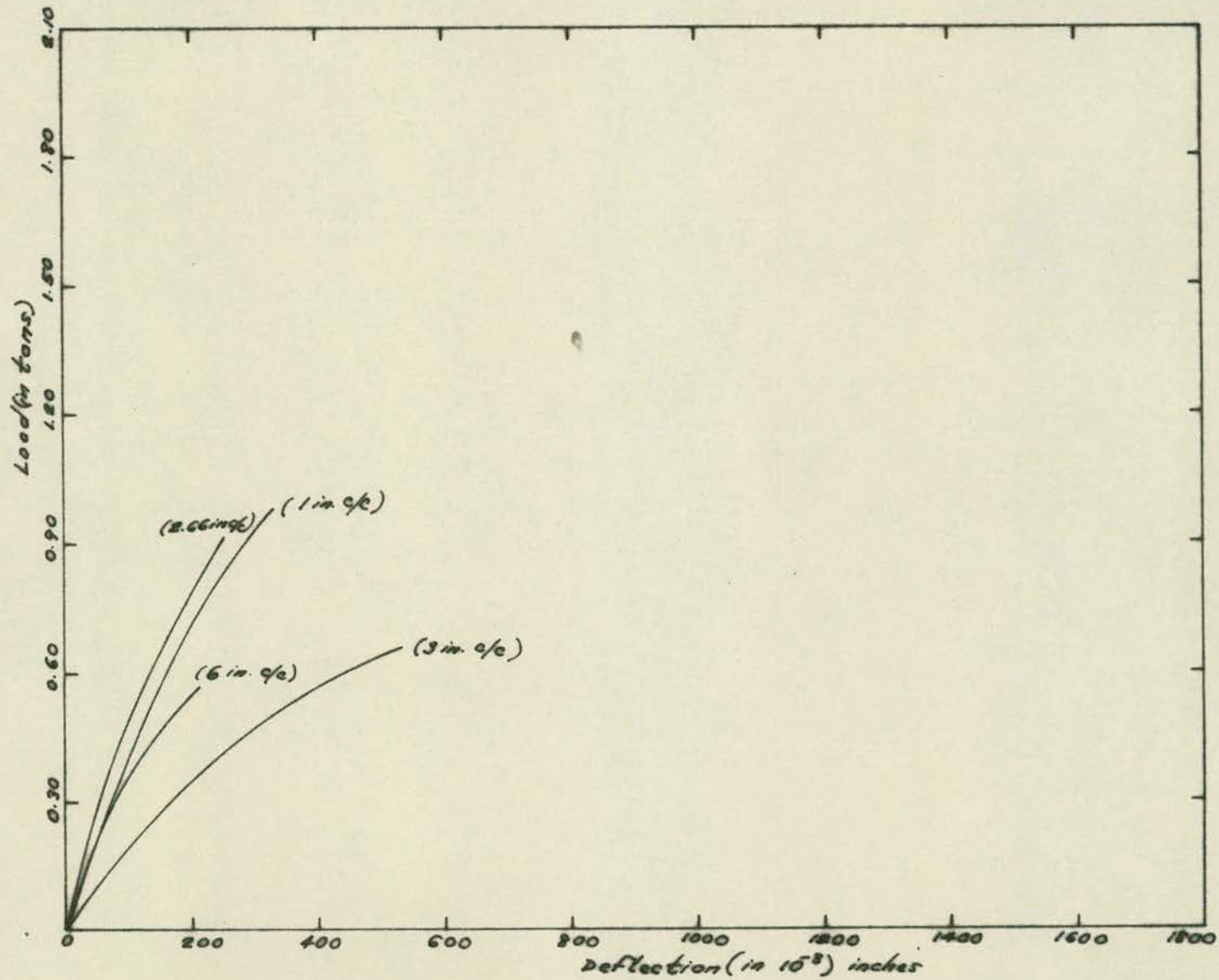


FIG 5.8 - Load-deflection curves with variation of tie spacing for  $\phi = 2.1$

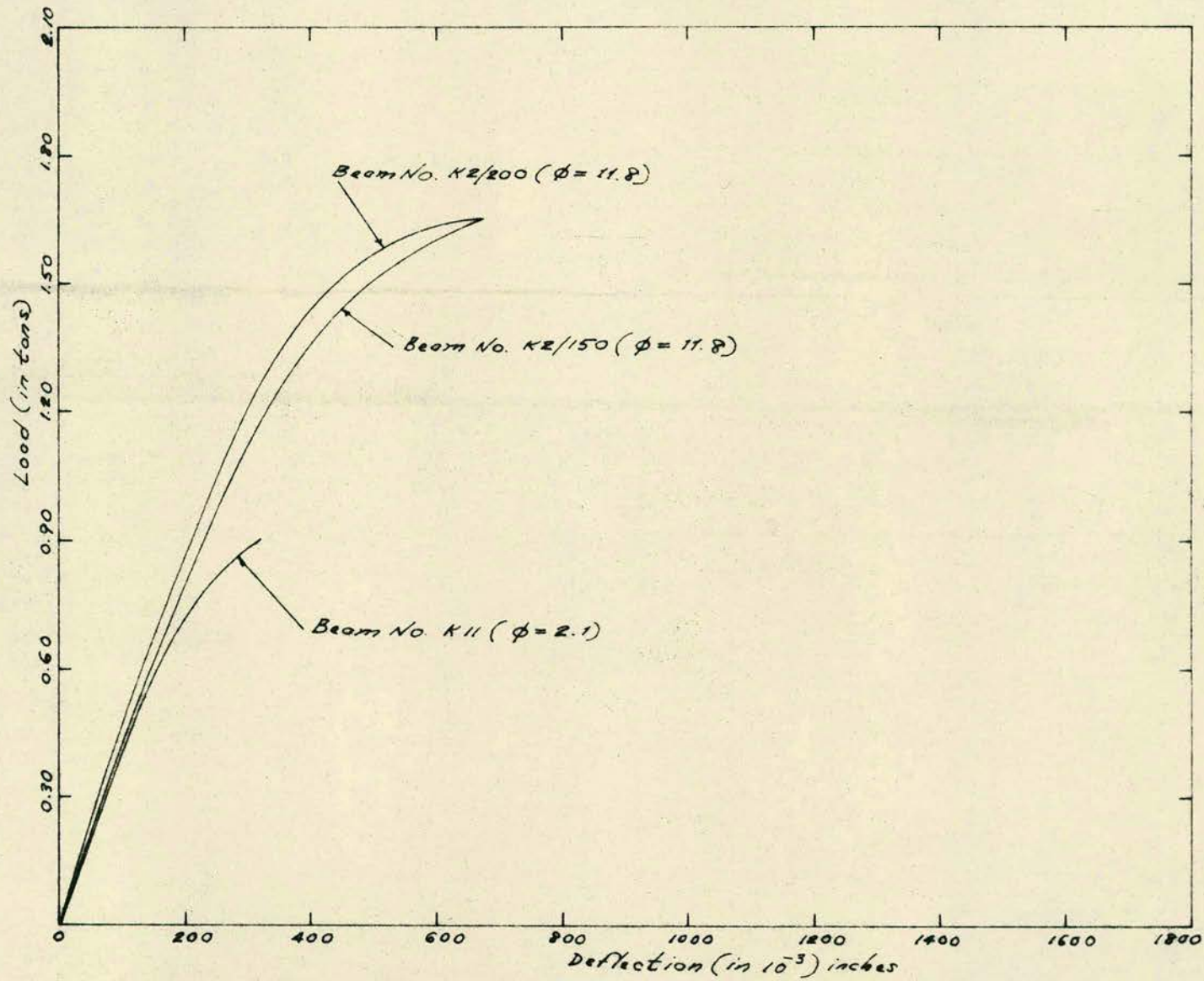


FIG 5.9 - Load-deflection curves showing the influence of the ratio of  $\phi$

extreme values of  $\phi$ , namely beams tested with  $\phi = 11.8$  and  $\phi = 2.1$ .

From Figs. 5.5, 5.6 and 5.8 the abrupt failure of the beams is indicated by the sudden termination of the curves for low  $\phi$  ratios, and from the same graphs, the influence of the spacing of the binders on the ductility of the beams can be deduced. The influence of this spacing is critical at low values of  $\phi$  as illustrated by the load-deflection curves of beams tested at  $\phi = 2.1$  as shown in Fig. 5.8. It is interesting to observe that the behaviour of beams K11 and K2/266 are similar. This suggests that the spacing for the latter is adequate. Fig. 5.9 illustrates the contrast between beams with moderate and high levels of bending moment. It can be seen that the deflection of beams tested in combined bending and torsion is primarily influenced by the level of the bending moment.

Chinenkov<sup>(12)</sup> showed in his experiments that for beams tested with different ratios of  $\phi$ , the deflection for beams with large values of  $\phi$  is higher. This was not observed in the beams tested by the author, except for the extreme case as given in Fig. 5.9. The deflection of beams tested between  $\phi = 4.3$  and  $\phi = 11.8$ , shown in Figs. 5.5, 5.6 and 5.7 indicates that the



magnitudes of the deflections are in the same range and almost the same. This is contrary to Chinenkov's observation. However, since the beams have the same amount of longitudinal steel throughout, the author feels that the deflection cannot be considerably different and any study of the influence of  $\phi$  should be related to the quantity of longitudinal reinforcement. Further, it is believed that the spacing and amount of the transverse binders influence the behaviour of the beams. The results from this study, however, are not sufficient to allow any general conclusion to be made.

The compressive strains measured on the top surface are shown in Table 5.2, while the principal compressive and tensile strains measured at the horizontal and vertical faces for beams tested at  $\phi = 2.1$  are shown in Table 5.3. It is interesting to observe the similarities of values of the principal strains on the horizontal and vertical faces, which seems to support the author's contention that the beams attempted to fail as a torsional failure.

#### 5.10 Ultimate Strength

The ultimate strength of the beams tested was analysed using the equation developed in Chapter 3. The results are tabulated in Table 5.2. For all cases where failure occurred by yielding of the reinforcement, the analysis was made on the

86

assumption of a rectangular stress distribution with an average compressive stress of  $\frac{2}{3}c_u$ . Sample calculations are shown in Appendix A. The ratio  $k$  for the dimensions of the reinforcing cage, was taken as 1.4.

Due to the extensive cracking of the beams tested at  $\phi = 2.1$  and  $\phi = 4.3$ , it was felt that analysis of the beams using the ultimate torque formula would be valid. It was therefore decided to use a combination of the formulae of Nadai<sup>(31)</sup> and Rausch<sup>(32)</sup> with the assumption that the ultimate torque consists of the torque resisted by the concrete and the reinforcement. The validity of this assumption has been shown by Cowan<sup>(33)</sup>, Hsu<sup>(23)</sup> and recently by Pandit and Warwaruk<sup>(18)</sup>. The allowable useful tensile strength of the concrete was taken as  $5(f'_c)^{\frac{1}{2}}$  as given by Hsu<sup>(25)</sup>. The results are shown in Table 5.5. Sample calculations are given in the Appendix B.

The theoretical results and their comparison with the experimental values are listed in Table 5.6. It can be seen that the theory estimates the strength of the beams with fair accuracy. It is therefore concluded on this basis that the ultimate moment equation developed in Chapter 3 can be used with confidence. On the other hand, the results obtained using the ultimate torsion formula of Nadai and Rausch are erratic and unreliable for application to the combined bending and torsion of

Table 5.5 - Comparison of theoretical and experimental  
value (Torque only)

Beam No.	$\phi$	Ultimate Torque		Ratio
		Expt.	Calc.*	Expt./Calc.
(kip-in)				
K16	2.1	5.10	6.40	0.80
K13	2.1	6.57	7.59	0.87
K2/266	2.1	8.02	8.00	1.07
K11	2.1	8.57	12.35	0.86
K16	4.3	6.49	6.39	1.02
K13	4.3	6.19	7.58	0.82
K11	4.3	6.37	12.35	0.52

\*calculated using fully plastic torque equation of Nadai and Rausch's equation for resistance of steel to torque adopting the tensile strength of concrete as  $5(f'_c)^{\frac{1}{2}}$ .

Table 5.6 - Comparison of theoretical and experimental  
value

Beam No.	$\phi$	Ultimate Moment (kip-in)		Ratio
		Expt.	Calc.	$\frac{\text{Expt.}}{\text{Calc.}}$
K16	2.1	10.70	16.61	Shear failure
K13	2.1	13.80	16.90	Shear failure
K2/266	2.1	16.85	16.80	1.00
K11	2.1	18.00	17.40	1.03
K16	4.3	27.90	24.40	1.14
K13	4.3	26.60	24.40	1.07
K11	4.3	27.40	24.60	1.11
K16	5.6	24.60	25.20	0.98
K13	5.6	25.40	25.20	1.01
K11	5.6	24.50	25.30	0.97
K16	8.5	27.20	27.10	1.00
K13	8.5	25.40	27.10	0.94
K11	8.5	27.20	27.20	1.00
K2/200	11.8	29.90	26.90	1.11
K2/150	11.8	29.90	27.70	1.10
Average				1.04

reinforced concrete beams. The results are shown in Table 5.6. An attempt was also made to use the new formula for torsion derived by Hsu<sup>(23,25)</sup> but the reinforcement ratios of beams tested in this experiment did not fulfil the conditions for its validity and thus it was abandoned.

#### 5.11 Summary and Conclusions

The results obtained by testing fifteen beams reinforced in both longitudinal and transverse direction have been analysed in this Chapter. On the basis of the observed mode of failure and the close correlation between the theoretical results and the experimental values, the equation developed in Chapter 3 may be used with confidence.

The mode of failure of the beams are as obtained and described by Lessig<sup>(13)</sup>, Yudin<sup>(27)</sup>, Gesund et al<sup>(15)</sup>, Cowan<sup>(28,33)</sup>, Chinenkov<sup>(12)</sup>, Evans and Sarkar<sup>(9)</sup> and Fairbairn<sup>(10,11)</sup>, but in the case of the inclination of the vertical cracks, there is a tendency for the angle to deviate from its original path towards the longitudinal axis at about the neutral axis. The inclination of the compression zone with respect to the axis of twist is not clear for low values of  $\phi$ .

Thus, using the data obtained from the tests, the following conclusions are drawn:-

- (1) For  $\phi$  less than or equal to 2.00, the transverse binders should be spaced at  $b'$  as suggested by the author in Chapter 3.
- (2) For all values of  $\phi$  larger than 2.00, the minimum shear reinforcement ratio recommended by the British Code of Practice<sup>(21)</sup> appears to be adequate.
- (3) The author's equation may be used with confidence to obtain the ultimate bending moment of beams provided the conditions laid down for its validity regarding the range of transverse reinforcement are fulfilled.
- (4) Until the actual concrete bending stress to be used for combined bending and torsion at the ultimate stage is established, the allowable bending stress for pure bending seems sufficiently accurate.
- (5) The use of closed stirrups in general tends to induce formation of the first mode of failure of beams as enunciated by Lessig<sup>(13)</sup>
- (6) Further research is necessary to investigate the interaction of beams and girders at the beam-girder connections.

## CHAPTER 6

### CONCLUSIONS AND RECOMMENDATIONS

#### 6.1 Conclusions

The main conclusions drawn from the investigation in this thesis are listed as follows:-

- (1) The ultimate moment equation developed in Chapter 3 may be applied with confidence for the analysis and design of under-reinforced rectangular beams reinforced in both longitudinal and transverse directions within the limits of this investigation.
- (2) The ultimate moment consists of the contributions of longitudinal and transverse reinforcement.
- (3) The longitudinal reinforcement in the tension zone contributes to the resistance of torsion thereby reducing the bending capacity of the section.
- (4) The reduction of the bending resistance due to torsion is augmented to a certain extent by the contribution of transverse binders.
- (5) The expression proposed for computing the depth of the compression block is a reliable method of obtaining the position of the neutral axis.
- (6) Provision of longitudinal steel using the balanced ratio for pure torsion ensures yielding of the steel.

- (7) The proposals for proportioning transverse binders may be applied to obtain the optimum transverse binders to ensure yielding of the reinforcement.
- (8) The spacing of transverse binders is critical for low ratios of  $\frac{M_{bu}}{M_{bt}}$  and should be restricted to the width of the reinforcing cage to prevent torsional failure.
- (9) The allowable compressive strength recommended for pure bending by the British Code of Practice may be applied to the case of combined bending and torsion with satisfactory results.
- (10) In designing beam-girder connections, the high moments which occur at this section should be taken into account to proportion the beam sections.

## 6.2 Recommendations for Future Research

In the light of the analytical and experimental works carried out in this study, the following recommendations are considered for future research works:-

- (1) Experimental verification of the proposed balanced longitudinal reinforcement for combined bending and torsion.



- (2) The torsional resistance of the compressed concrete layer.
  - (3) Establishment of the concrete compressive strength for combined bending and torsion.
  - (4) The possibility of establishing the flexural rigidity of the beams under combined moments for analysis of indeterminate structures.
- and (5) Extension of the ultimate equilibrium method to the analysis of combined bending, torsion and shear.



6. H.J. Cowan Reinforced and Prestressed  
Concrete in Torsion, Edward  
Arnold Publications, 1965.

7. H.J. Cowan Philosophy for design of concrete  
structures in torsion, Torsion of  
structural concrete, S.P.18,  
Amer.Conc.Inst., 1968.

8. A.A. Gvozdev Design of Reinforced Concrete  
Structures, P.C.A. Foreign Lit.  
Study No. 398, 1961.

9. R.H. Evans A method of ultimate strength  
S. Sarkar design of reinforced beams in  
combined bending and torsion,  
Struct.Engr., 43, 10, 1965.

10. D.R. Fairbairn "An Experimental and Analytical  
Investigation of the Behaviour of  
Reinforced Concrete Beams Subjected  
to Combined Bending and Torsion,"  
Ph.D. Thesis, University of Edinburgh,  
1967.

11. D.R. Fairbairn Combined bending and torsion in  
S.R. Davies reinforced concrete beams, Struct.  
Engr., 47, 4, 1969.

12. Yu. V. Chinenkov Study of the behaviour of reinforced concrete elements in combined flexure and torsion, P.C.A. Foreign Lit. Study No. 370, 1959.
13. N.N. Lessig Determination of the load-bearing capacity of reinforced concrete elements with rectangular cross-section subjected to flexure and torsion, P.C.A. Foreign Lit. Study No. 371, 1959.
14. S. Sarkar Study of combined bending, shear and torsion on a hollow reinforced concrete section, Ph.D.Thesis, University of Leeds, 1964.
15. H. Gesund  
G.J. Schuette  
G.R. Buchanan  
C.A. Gray Ultimate strength in combined bending and torsion of concrete beams containing both longitudinal and transverse reinforcement, J. Amer. Concr. Inst., 61, 12, 1964.
16. C.D. Goode  
M.A. Helmy Ultimate strength of reinforced concrete beams subjected to combined bending and torsion, Torsion of structural concrete, SP18, Am. Concr. Inst., 1968.

17. C.D. Goode  
M.A. Helmy  
The strength of concrete under combined shear and direct stress, Mag.Conc.Res., 19, 59, 1967.
18. G.S. Pandit  
J. Warwaruk  
Reinforced concrete beams in combined bending and torsion, Torsion of structural concrete, SP18, Am. Conc.Inst., 1968.
19. A.M. Neville  
Some factors in the shear strength of reinforced concrete beams, Struct.Engr., 38, 7, 1960.
20. H. Gesund  
L.A. Boston  
Ultimate strength in combined bending and torsion of concrete beam containing only longitudinal reinforcement, J.Am.Concr.Inst., 61, 11, 1964.
21. --  
B.S. Code of Practice C.P.114(1957),  
The structural use of reinforced concrete in buildings, British Standards Institution, London.
22. P. Zia  
Torsional strength of Prestressed Concrete Members, J. Am.Conc.Inst., 32, 10, 1961.
23. T.T.C. Hsu  
Torsion of structural concrete behaviour of reinforced concrete rectangular members, Torsion of structural concrete, SP18, Am.Conc. Inst. 1968.

24. Allan H. Mattock                      How to design for torsion, Torsion of structural concrete, SP18, Amer.Conc.Inst., 1968.
25. T.T.C. Hsu                              Torsion of structural concrete - plain concrete rectangular sections, Torsion of structural concrete, SP18, Am. Conc. Inst., 1968.
26. G.C. Ernst                              Ultimate Torsional Properties of Rectangular Reinforced Concrete Beams, J. Am. Conc. Inst. 29, 4, 1957.
27. V.K. Yudin                              Determination of the load-bearing capacity of reinforced concrete elements of rectangular cross-section under combined bending and torsion, P.C.A. Foreign Lit. Study No.277,1962.
28. H.J. Cowan                              The strengt. of plain and reinforced concrete under the action of combined stresses with particular reference to combined bending and torsion of rectangular sections, Mag. Concr. Res., 5, 14, 1953.
29. D. McHenry  
    J. Karni                              Strength of concrete under combined tensile and compressive stresses. J. Am. Conc. Inst., 29, 10, 1958.

30. J.D. McIntosh  
H.C. Erntroy  
Design of concrete mixes with aggregate of  $\frac{3}{8}$ " maximum size, Research Report No.4, Cem. and Concr. Assoc., London, 1955.
31. A. Nadai  
Theory of Flow and Fracture of Solids, McGraw-Hill Book Co., New York, 2nd Edition, 1950.
32. E. Rausch  
Design of Reinforced Concrete for Torsion and Shear, J. Springer, Berlin, 1929.
33. H.J. Cowan  
Experiments on the strength of reinforced and prestressed concrete beam and of concrete-encased steel joists in combined bending and torsion, Mag. Concr.Res., 6, 19, 1955.
34. G.C. Ernst  
Reinforced concrete in the plastic range, 3. Torsion, Univ. of Nebraska, Lincoln, 1956.
35. C.D. Goode  
M.A. Helmy  
Design of rectangular beams subjected to combined bending and torsion,
36. I.M. Lyalin  
The ultimate equilibrium method, reinforced and prestressed concrete structures in torsion, Arnold, 1965.

37. B. Bresler  
K.S. Pister  
Strength of concrete under combined stresses, J.Am.Conc.Inst., 30,3, 1958.
38. B. Bresler  
K.S. Pister  
Failure of plain concrete under combined stresses, Proc.Am.Soc. Civ. Engrs., 81, 674, 1955.
39. J.S. Reeves  
Combined bending and torsion of prestressed T-beams, TRA/364, Cem. and Concr. Assoc., London, 1962.
40. L.L. Jones  
Ultimate Load Analysis of Reinforced and Prestressed Concrete Structures, Chatto and Windus Publications, 1961.
41. B. Bresler  
K.S. Pister  
Strength of Concrete under Combined Stresses, University of California, Structures and Materials Research, Series No.100, Issue No.1, 1956.
42. M.P. Collins,  
P.F. Walsh,  
F.E. Archer,  
A.S. Hall  
Ultimate strength of reinforced concrete beams subjected to combined torsion and bending, Torsion of structural concrete, S.P.18, Am. Conc. Inst., 1968.



Appendix ACalculation for beam K11 tested at  $\phi = 2.1$ 

Given data:  $b = 3"$ ,  $h = 4"$ ,  $d = 3.5"$ ,  $b' = 2.5"$ ,  $d' = 3.5"$

$$A_L = 2\frac{2}{3}" \text{ diam. } f_L = 40\text{ksi}$$

$$A_T = \frac{1}{4}" \text{ diam. @ lin c/c, } f_T = 34\text{ksi}$$

$$C_u = 7.03\text{ksi}$$

The calculated reinforcing cage is 2.5" by 3.5"

$$\text{Step (1): } k = \frac{3.5}{2.5} = 1.4$$

$$\text{Step (2): } \text{By formula (3.2), } \cot \alpha = \frac{0.80}{2.1} = 0.38$$

$$\text{Step (3): } \text{By formula (3.12), } C_1 = \frac{2.1}{2.1 + (1 + 2.8)(0.38)} = 0.59$$

$$\text{Step (4): } \text{By formula (3.13), } C_2 = 0.59(1 + 3)(0.38)^2 = 0.34$$

Step (5): Use formula (3.39) to find n:

$$n = \frac{(0.11)(40)(0.59)}{\frac{2}{3}(7.03)(3)} = 0.62"$$

Step (6): Calculate the value of  $M_{bu}$  by expression (3.14)

$$M_{bu} = (0.11)(40)(3.5 - 0.31)$$

$$+ \frac{(0.012)(34)(2.50)}{(0.11)(40)(1)}$$

$$= \underline{17.80\text{kip-in.}} \text{ (answer)}$$

Appendix B

Calculation for  $M_{bt}$  for beam K11 tested at  $\phi = 2.1$

Data given same as above:

Use Raush formula: i.e.  $M_{bt} = \frac{1}{2}b^2 (h - \frac{b}{3})f_t + \frac{1}{2}A_T f_T \frac{b'd'}{s}$

Using Hsu's recommendation for  $f_t$ ,  $f_t = 5(f'_c)^{\frac{1}{2}}$

i.e.  $f'_c = 0.85C_u$ ;  $f_t = 0.44\text{ksi}$

$$\begin{aligned} M_{bt} &= \frac{1}{2}(3)^2(4-1)(0.44) + \frac{1}{2}(0.012)(34) \frac{(2.5)(3.5)}{1} \\ &= 6.00 + 1.80 \\ &= \underline{7.80\text{kip-in}} \end{aligned}$$

The experimental  $M_{bt} = \frac{17.60}{2.1} = \underline{8.50}$  kip-in